LAPPEENRANTA
UNIVERSITY OF TECHNOLOGY

Risto Tiainen

UTILIZATION OF A TIME DOMAIN SIMULATOR IN THE TECHNICAL AND ECONOMIC ANALYSIS OF A WIND TURBINE ELECTRIC DRIVE TRAIN

Thesis for the degree of Doctor of Science (Technology) to be presented with due permission for public examination and criticism in the Auditorium of the Student Union House at Lappeenranta University of Technology, Lappeenranta, Finland, on the 13th of August, 2010, at noon.

Acta Universitatis
Lappeenrantaensis
391

Supervisors	Professor Jero Ahola Lappeenranta University of Technology Finland
	Dr. Tuomo Lindh Lappeenranta University of Technology Finland
Reviewers	Professor Kimmo Kauhaniemi University of Vaasa Finland
	Dr. Jouko Niiranen ABB Drives Finland
Opponents	Professor Kimmo Kauhaniemi University of Vaasa Finland
	Dr. Jouko Niiranen ABB Drives Finland

ISBN 978-952-214-947-3
ISBN 978-952-214-948-0 (PDF)
ISSN 1456-4491

Lappeenrannan teknillinen yliopisto
Digipaino 2010

Abstract

Risto Tiainen

Utilization of a Time Domain Simulator in the Technical and Economic Analysis of a Wind Turbine Electric Drive Train

Dissertation, Lappeenranta University of Technology
109 p.
Lappeenranta 2010
ISBN 978-952-214-947-3, ISBN 978-952-214-948-0 (PDF)
ISSN 1456-4491

The amount of installed wind power has been growing exponentially during the past ten years. As wind turbines have become a significant source of electrical energy, the interactions between the turbines and the electric power network need to be studied more thoroughly than before. Especially, the behavior of the turbines in fault situations is of prime importance; simply disconnecting all wind turbines from the network during a voltage drop is no longer acceptable, since this would contribute to a total network collapse. These requirements have been a contributor to the increased role of simulations in the study and design of the electric drive train of a wind turbine.

When planning a wind power investment, the selection of the site and the turbine are crucial for the economic feasibility of the installation. Economic feasibility, on the other hand, is the factor that determines whether or not investment in wind power will continue, contributing to green electricity production and reduction of emissions. In the selection of the installation site and the turbine (siting and site matching), the properties of the electric drive train of the planned turbine have so far been generally not been taken into account. Additionally, although the loss minimization of some of the individual components of the drive train has been studied, the drive train as a whole has received less attention. Furthermore, as a wind turbine will typically operate at a power level lower than the nominal most of the time, efficiency analysis in the nominal operating point is not sufficient.

This doctoral dissertation attempts to combine the two aforementioned areas of interest by studying the applicability of time domain simulations in the analysis of the economic feasibility of a wind turbine. The utilization of a general-purpose time domain simulator, otherwise applied to the study of network interactions and control systems, in the economic analysis of the wind energy conversion system is studied. The main benefits of the simulation-based method over traditional methods based on analytic calculation of losses include the ability to reuse and recombine existing models, the ability to analyze interactions between the components and subsystems in the electric drive train (something which is impossible when considering different subsystems as independent blocks, as is commonly done in the analytical calculation of efficiencies), the ability to analyze in a rather straightforward manner the effect of selections other than physical components, for example control algorithms, and the ability to verify assumptions of the effects of a particular design change on the efficiency of the whole system.

Based on the work, it can be concluded that differences between two configurations can be seen in the economic performance with only minor modifications to the simulation models used in the network interaction and control method study. This eliminates the need of developing analytic expressions for losses and enables the study of the system as a whole instead of modeling it as series connection of independent blocks with no loss interdependencies. Three example cases (site matching, component selection, control principle selection) are provided to illustrate the usage of the approach and analyze its performance.

Keywords: Wind power, simulation, technical and economic analysis
UDC 621.548:621.311.245:004.94.003

Acknowledgments

The research documented in this thesis was carried out at the Institute of Energy Technology (LUT Energia) at Lappeenranta University of Technology (LUT) during the years 2008–2009. The research was partly funded by the Graduate School of Electrical Engineering (GSEE) and The Switch Ltd.

I would like to thank the people I have had the pleasure of working with at the University. Especially my supervisors, Professor Jero Ahola and Dr. Tuomo Lindh, and my former colleague, Dr. Ville Särkimäki, deserve a big thank you. You have been an inexhaustible source of ideas, comments, and (constructive) criticism over the years.

I would also like to thank the pre-examiners of this thesis, Professor Kimmo Kauhaniemi and Dr. Jouko Niiranen, for their valuable comments and corrections during the preparation of this thesis. Many of your comments gave me new insight on the topics discussed in this book.

Furthermore, the contribution of Dr. Hanna Niemelä, who helped me rid the manuscript of all of those recurring mistakes I tend to make with my English, is sincerely acknowledged.

When working in an academic environment, the work pace is sometimes hectic. More often than not, however, there is time for lengthy coffee breaks. These breaks, if spent with a good coffee-drinking squad, provide an excellent chance to get new ideas and to broaden your thinking. I had the pleasure to take part in many such occasions, and I would like to thank all those colleagues who used to sit around the round table with me.

The financial support by the Walter Ahlström Foundation, the Jenny and Antti Wihuri Foundation, the Lahja and Lauri Hotinen Fund, and the Ulla Tuominen Foundation is greatly appreciated.

Finally, I would like to express my gratitude to my family. Especially I'd like to thank you, Tiina, my dear fiancée, for bearing with me when I was sitting by the computer writing for the most of the day and just acting grumpy for the rest of the day. Or deriving equations in the middle of the night. I wish I could guarantee that this won't happen ever again, but I'm

afraid I can't. But I'm also sure we'll pull through just fine.

Lappeenranta, May 31st, 2010

Risto Tiainen

Contents

List of Symbols and Abbreviations

Roman Letters

A	Area
$\mathbf{A}$	State vector
C_i	Investment cost
C_omr	Operations, maintenance, and repair costs
C_p	Wind turbine power coefficient
c	Weibull distribution scale parameter
D	Diameter
E	Energy
E_ao	Annual energy output (AEO)
$F(v)$	Weibull cumulative distribution function
f_nom	Nominal frequency
J	Income
k	Weibull distribution shape parameter
N	Number of bins
n_nom	Nominal rotation speed (revolutions per minute)
P	Active power
P_e	Electrical power
P_w	Power of wind
$\overline{P}_\mathrm{w}$	Average power of wind
p	Instantaneous power; Interest rate; Number of pole pairs
$p(v)$	Weibull probability density function
Q	Reactive power
r	Radius
S	Scrap value, salvage value
T	Turbine life
$\boldsymbol{T}_\mathrm{e}$	Electrical torque (space vector)
T_pb	Payback time
t	Time
t_0	Initial time index
u	Voltage (instantaneous value)

v, v_{w}	Wind speed (scalar)
$\overline{v}$	Average wind speed (scalar)
$v_{\mathrm{cut-in}}$	Cut-in speed of a wind turbine
$v_{\mathrm{cut-out}}$	Cut-out speed of a wind turbine

Greek Letters

$\Gamma(x)$	The gamma function
η	Efficiency
λ	Tip speed ratio
$\overline{\pi}$	Average price of electricity
ρ	Density of air
$\boldsymbol{\psi}_{\mathrm{s}}$	Stator flux linkage (space vector)
ω	Angular frequency

Subscripts

e	Electrical
m, mech	Mechanical
n, nom	Nominal
opt	Optimal
t	Turbine
w	Wind

Acronyms

AEO	Annual Energy Output
CDF	Cumulative Density Function
COE	Cost of Energy
DD	Direct Drive
DFIG	Doubly Fed Induction Generator
DFT	Discrete Fourier Transform
EMC	Electromagnetic Compatibility
ESR	Equivalent Series Resistance
ESL	Equivalent Series Inductance

FEM	Finite Element Method
FRT	Fault Ride-Through
HAWT	Horizontal-Axis Wind Turbine
HV	High Voltage
IEA	International Energy Agency
IEC	International Electrotechnical Commission
IGBT	Insulated Gate Bipolar Transistor
LV	Low Voltage (<1000 V)
MPPT	Maximum Power Point Tracking
MV	Medium Voltage
OECD	Organization for Economic Co-operation and Development
OMR	Operations, Maintenance, and Repair
PCC	Point of Common Coupling
PDF	Probability Density Function
PM	Permanent Magnet
PMSG	Permanent Magnet Synchronous Generator
RPM	Revolutions per Minute
TSO	Transmission System Operator
VSI	Voltage Source Inverter
WECS	Wind Energy Conversion System
WWEA	World Wind Energy Association

Chapter 1

Introduction

Wind was one of the first sources of energy taken into use by man. It was used as an alternative to human or animal power, for example in grinding grain and pumping water. After the technological advances in the 18th and 19th centuries, however, wind power gave way to more easily controllable and predictable means of power production, such as coal-powered steam engines and hydroelectric generators. Interest in wind energy was renewed in the 1960s and 70s along with an increase in general awareness of environmental protection – and an increase in the price of oil.

Although some (not very successful) megawatt-class turbines were built in the 1970s, early modern wind turbines were typically small in today's terms. In the early 1980s, the nominal power of wind turbines was typically around 50 kW. The applied technology was further developed and upscaled. In the mid-1990s, the nominal power of new wind turbines had already reached the next order of magnitude, being approximately 500–750 kW (Neij, 1999). Since then, upscaling has continued, and modern utility-scale wind turbines have commonly a nominal power of 1 MW or more.

The installed wind power capacity is constantly growing. After the year 2000, the annual increase in total installed wind power capacity[1] has been approximately 25–30 % (WWEA, 2008, REN21, 2008). However, globally, the total electrical energy production from wind is still small compared with many other sources: approximately 1 % of global electricity production comes from wind generators (WWEA, 2008). Potential for further growth exists. Hoogwijk et al. (2004) estimate the global technical potential of on-shore wind energy to be approximately six times the current global electricity consumption. Archer and Jacobson (2005) arrive at similar figures.

The approximately one percent of the world's electricity generation by wind turbines is not the whole picture. This wind energy production is very unevenly distributed over the surface of the planet. 73 % of the installed global wind power capacity was located in Europe in

[1] The sum of the nominal powers of all installed turbines

2004, Germany being the largest single contributor (17 GW, 49 % of the total European capacity) and Denmark being the country with the largest percentage (20 %) of electricity demand covered by wind power production (Hansen and Hansen, 2006). The European coast is one of the most favorable sites for wind power production (Archer and Jacobson, 2005). However, increasing wind power capacity has thus far also necessitated economic incentives. Tariff-based remuneration systems for wind power in otherwise liberalized electricity markets have generally been successful. On the other hand, lack of stable conditions for investment in wind power may be a significant obstacle to major adoption of wind turbines. This has been the case in, for example, the United Kingdom, which is one of the windiest countries in Europe and yet has only a modest amount of wind power capacity (Ibenholt, 2002). This kind of economic supportive measures by the government often also have an impact on the development of wind power industry in a country, as concluded by Lewis and Wiser (2007). The leading wind turbine manufacturers come from countries with significant wind power production; the four manufacturers with the greatest market share were in 2004 Vestas (34 % world market share; Denmark), Gamesa Eolica (17 %; Spain), Enercon (15 %; Germany), and GE Wind (11 %; USA) (Hansen and Hansen, 2006).

Thus, economic factors play a key role in the increase in wind power generation. Traditionally, the feasibility of a planned wind power installation is evaluated by calculating the cost of producing a kilowatt-hour of electricity (see e.g. (Tande and Hunter, 1994)). This figure can then be used to compare the wind power-based system with another power source (for example, a diesel-powered system in Lysen (1983, Section 12)), another wind turbine, or another location for the same turbine. The latter two are called wind turbine site matching and siting, respectively. Studies of this kind have been widely published, for example by Rehman et al. (2003), Rehman and Ahmad (2004), Ucar and Balo (2009b,a), Ahmed Shata and Hanitsch (2008), Jowder (2009). The studies referenced do not go into the details of the wind turbine drive train. Instead, they treat the turbines as ”black boxes”, where the output electrical power of the turbine system equals the mechanical power captured by the turbine. In reality, the efficiency of the electric drive train is not unity and not even constant but a function of the operating point (wind speed).

Regarding the turbine system as a black box, as described above, is often sufficient when selecting the most suitable site for a turbine or selecting the power rating of a planned system. However, this kind of an analysis is of no help to a manufacturer of wind turbine drive train electric components (such as generators and converters) when selecting these components and their parameters, or control algorithms. This kind of an analysis and optimization has been carried out by deriving analytical expressions for the efficiency of subsystem components by, for example, Grauers (1996), Polinder et al. (2006), Li and Chen (2007).

1.1 Motivation of the Research

The economic feasibility of a turbine is, as discussed, of prime importance. Wind power technology is constantly developing, and there are multiple technologies for the conversion of mechanical rotation energy of the turbine into electrical energy. The selection of drive

train components and their parameters involves thus quite a lot of work. Optimally, the configuration selected is the one which provides the lowest cost of energy while meeting all technical requirements. These technical requirements include, for example, fault tolerance (or, fault ride-through, FRT, capability). FRT capabilities of wind turbines are of increasing importance as the level of wind power penetration in power systems increases. In many cases, the fulfillment of FRT requirements is tested and verified using simulations (see (Luukko et al., 2009b)). The fault ride-through capability (especially in full power converter-based drives) can be affected by electrical and control design, and, therefore, there often exists a simulation model of the electric drive train.

Knowing the difficulties related to the analytic calculation of losses and knowing that there often exist simulation models of the electric drive train of a wind turbine system suggest that it might be feasible to combine the economic feasibility study (e.g. siting, site matching) and the technical simulation models into a technical and economic analysis of the feasibility of a proposed wind turbine system. This kind of a system would eliminate the need to develop any additional loss models and yet be able to analyze the feasibility of a given component or subsystem selection compared with others, thereby including the contribution of differing technical selections in the economic analysis. In practice, by adopting this kind of an approach, a wind power manufacturer or a technology integrator with existing simulation models of their technology could with relatively little effort show a potential customer (wind power investor) the effect of alternative technical selections on the economy of the candidate systems in various wind conditions.

Analytical calculation of losses has at least two downsides. First of all, analytical calculation of losses in multiple operating points is far from straightforward even for a single component. Secondly, and perhaps more importantly, considering components of the drive train independently fails to take into account the possible effects of parameter selections in one part of the drive train on the losses of another part of the same drive train. The effects are often such that they demand an iterative solution. For example, changing the components of the generator filter will change the voltages in the generator terminals, which will change the generator stator copper losses, which will change the stator current, which will change the losses in the generator filter, which will change the voltages in the generator terminals, and so on. The efficiency of the series connection of elements is not generally the product of the efficiencies of the individual components measured independently of the series connection. In other words, the efficiency of a single component (or subsystem) is not a constant, but rather a function of the operating point of the component. Furthermore, the operating point can be defined to be determined by the vectors of state variables (currents and voltages) of both the input and the output terminals,

$$\eta_i = f\left(\mathbf{A}_{\mathrm{in},i}, \mathbf{A}_{\mathrm{out},i}\right), \tag{1.1}$$

where η_i is the efficiency of component i, $\mathbf{A}_{\mathrm{in},i}$ is the vector of state variables for the input port of component i, and $\mathbf{A}_{\mathrm{out},i}$ is the vector of state variables for the output port of component i. The dependency of the efficiency of a component of the states of the input and output ports (the function f) can be determined by, for example, laboratory measurements, or simulations.

When multiple components are connected in series (or in parallel), the states of the ports of a component are no longer independent of the other components. The efficiency of the

total system is not generally equal to the product of the efficiencies of individual components determined independently of the whole system. Figure 1.1 illustrates the case.

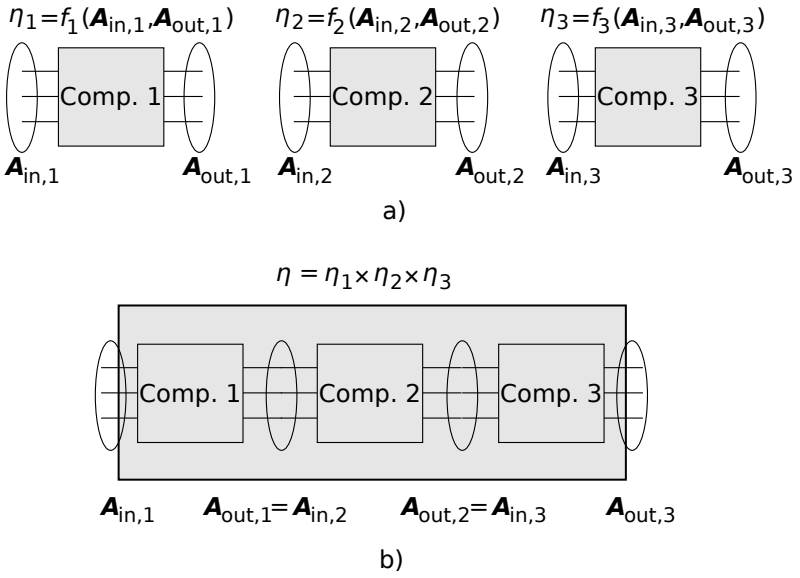

Fig. 1.1. Efficiency of a component is a function of the states of its input and output (a). When connecting components in series (b), each individual component is no longer independent. The total efficiency of the series connection is not generally equal to the product of the efficiencies of individual components measured (or calculated, or simulated) independently of the whole system.

Simulations are a useful tool in the determination of the states of the subsystem interfaces in a complex system, something which is far from straightforward using analytic methods. With simulation models that accurately model all relevant loss mechanisms and component interactions, the total system efficiency can be determined with good accuracy. Thus, a significant benefit of the simulation-based approach over analytic methods is the fact that the states of the inputs and outputs of all components in a system can be determined in a relatively straightforward way. Additionally, determining the efficiency of a component as a function of the states of its input and output can also be more straightforward than using analytic methods. Since a change improving the performance of a component could actually result in degraded performance of the whole system, finding the total economic optimum for the drive is downright impossible without considering the drive train as a whole.

In addition to taking into account some of the interactions between the constituent components of the drive train, the effects of different control principles are more straightforward to analyze with a simulator than by using analytical modeling. For example, the economic performance of different modifications to the standard $i_\mathrm{d} = 0$ control of a permanent magnet generator could be compared. Furthermore, the effects of these modifications to the technical performance (FRT, for example) could be checked with the same simulator. Also, if a selection or change is assumed to have a certain effect on the economic performance of the plant

(assumed improvement of efficiency, for example), the simulator can be used to check and verify the assumption.

A disadvantage of the simulation-based approach compared with analytic calculation could be the required simulation time, which is often several hours, while the values of the analytical expressions can be calculated almost instantaneously. However, the time required to develop the simulation models could be short compared with time needed for developing analytic expressions, especially if simulation models already exist for purposes other than efficiency analysis. Furthermore, multiple simulations can be calculated in parallel (on multiple computers), and the calculation requires no human intervention thereby enabling the designer to do other work while the analyses are being calculated. Tools developed during this project are specifically designed so that they require no user intervention during the simulation process (for example starting the simulation for multiple operating points, storing the results).

The traditional cost of energy (COE) based comparison metric of alternative configurations is very illustrative in many cases (for example, when comparing a wind turbine with a diesel generator). However, in the analysis of the electric drive train, there might arise situations in which this metric is not very descriptive. An example could be the selection of a filter core material; one of them has lower iron losses than the other, but is also more expensive. The designer can analyze both configurations in some wind conditions and get the COE of both configurations and select the more feasible one. However, if the question is instead formulated ”How much more can the better core cost in order to still be more feasible in these wind conditions?”, then the COE does not give a direct answer. Therefore, in this work, an alternative method for assessing and comparing wind turbine systems was developed.

The use of a simulator enables various different types of technical and economic analyses to be performed that are not possible by an analytical approach. The cost of the method is the need for simulation models. However, the models might already exist for other purposes. The improvement and even optimization of the economic efficiency of wind energy production would presumably make the investment in wind power more feasible, thus contributing to an increase in renewable energy production. This work attempts to test the applicability of the simulation-based approach in the technical and economic analysis of wind power and to find its benefits and limitations. To the best of the author's knowledge, the use of a simulation-based approach in the technical and economic analysis has not been proposed before.

Figure 1.2 presents the position of the work at hand in relation to siting and COE-related analyses, and the simulations used for FRT capability development. The simulator is a tool that can be used in both the technical and the economic analysis and to analyze interconnection between the two worlds.

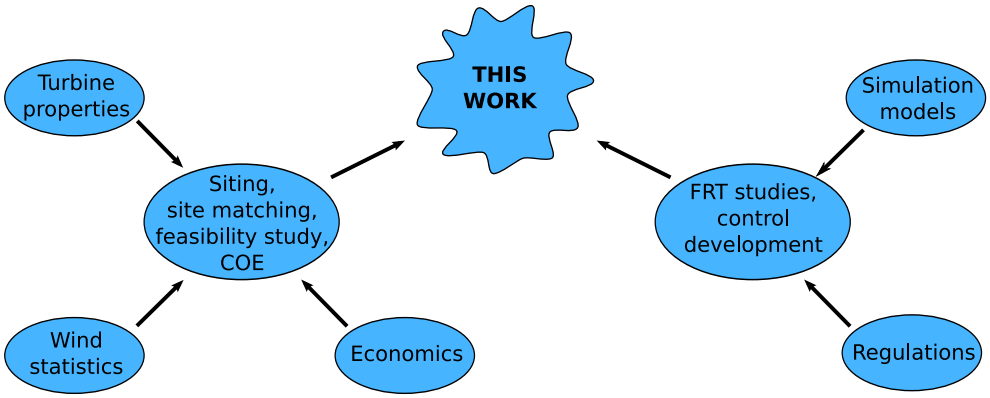

Fig. 1.2. This work combines traditional siting and COE (cost of energy) analysis with simulations used in FRT (fault ride-through) studies.

1.2 Objective of the Research

The objective of the study was to analyze the usability of a time domain simulator in the technical and economic analysis of a wind turbine electric drive train. In addition to siting and site matching, the simulation-based method was expected to be applicable to the selection of the components and parameters of the electric drive train of the turbine, something which is not straightforward using the more conventional analytical calculation based on models of the individual subsystems. In the work, the utilization of the simulator is studied at a general level and with the help of example cases.

1.3 Outline of the Thesis

The remaining parts of this doctoral dissertation are organized to chapters as follows.

Chapter 2 introduces the boundary conditions inside which the wind turbine designer operates. First, the power of wind and wind statistics are introduced. Second, the calculation of the annual energy output (AEO) is discussed. Regulations and standards are briefly overviewed. Finally, basics of investment analysis are presented. An analysis method is proposed. Sensitivity of the proposed metric to changes in input parameters is analyzed.

Chapter 3 discusses the application of simulations to calculate the efficiency of the electric drive train. Calculation of electric efficiency is presented. The chapter attempts to find

the benefits and shortcomings of the simulation-based analysis method using three example cases: component selection, site matching, and control principle selection.

Chapter 4 concludes the work, presents the results obtained, and gives suggestions for further applications of the proposed method.

1.4 Scientific Contribution of the Thesis

The main scientific contribution of the thesis is the analysis of the applicability of time domain simulations in the technical and economic analysis of a wind energy conversion system. The benefits and disadvantages of the simulation-based approach compared with analytical calculations are studied. The economic analysis method itself is not new, but simulations have not been used to provide the efficiency information required. The simulation-based approach is expected to enable an analysis of the whole drive train (including interactions between the constituent components and the effect of control algorithms), something which is very difficult using analytical calculation.

The author created all the simulation models presented in the case examples as well as the required analysis tools. Furthermore, the author developed the power and loss calculation blocks for the simulation environment. However, most of the simulation models of the individual components were developed by others. The simulation environment and the efficiency analysis tools have been documented in (Luukko et al., 2009a) and (Luukko et al., 2009b).

Chapter 2

Development of the Analysis Method

The objective of this chapter is to formulate a technical and economic analysis method to compare alternative wind turbine electric drive train configurations. As a first step towards that goal, the calculation of the annual energy output (AEO) of a wind turbine is discussed. For the AEO calculation, the properties of the wind as well as those of the turbine are needed. Therefore, this chapter begins with discussion of the power of wind, wind statistics, and AEO calculation methods. After the AEO calculation, some of the regulations relevant to wind turbine design are reviewed to give an idea of the legal boundary conditions that need to be taken into account in the design. Finally, a technical and economic analysis method based on the difference of the present value of the generated electricity for the compared configurations is developed. This method will be used in conjuction with simulations, described in the next chapter.

2.1 Introduction to Wind Power

The concept on wind energy has been known for centuries. Windmills were used for numerous tasks, such as pumping water and grinding grain (Carlin et al., 2001, Johnson, 2001). The first windmills on record were built by the Persians in approximately 900 CE (Manwell et al., 2002), but the technology is older, possibly over 3000 years (Burton et al., 2001). Wind remained an important source of usable energy up until the invention of the steam engine and other fossil fuel-based energy conversion systems. The main attributes contributing to the demise of wind mills were the non-transportability and the non-dispatchability of wind energy. In other words, the energy could not be used where and when it was desired. Hydropower, another form of energy widely used before the age of steam engines, is to some extent transportable (using canals) and dispatchable (when stored in a pool) (Manwell et al.,

2002). Thus, hydropower remained in use through the period of industrialization and remains in use today.

The use of windmills (wind turbines) to generate electricity originated in the 19th century in the USA (by Charles F. Brush) and Denmark (by Poul la Cour) (Burton et al., 2001). The interest in wind energy generation remained fairly marginal, however, until the end of the 1960s. It was then that people became increasingly aware of the environmental consequences of industrial development and fossil fuels in particular. The Oil Crises of the 1970s further elevated interest in renewable energy sources (Manwell et al., 2002).

At present, the contribution of wind energy to all globally generated electricity is only about 1 % (WWEA, 2008). The total installed capacity was (at the end of 2007) approximately 95 MW (REN21, 2008). However, the capacity is steadily increasing: after the year 2000, the annual increase in total installed capacity has remained around 25–30 % (WWEA, 2008, REN21, 2008). It has been estimated by Hoogwijk et al. (2004) that the global technical potential of on-shore wind energy is approximately six times the current global electricity consumption. Realizing this technical potential would, however, require a land area of roughly the size of China (assuming a power density of 4 $\mathrm{MW/km^2}$).

Thus, there is huge potential for new wind turbine installations. However, not all technical potential is economically feasible. The economic feasibility of wind power is heavily dependent on the site of the installation. Local topology has an effect on the wind conditions in a given site. If the best locations are assumed to be taken into use first, the total amount of installed wind power capacity has an effect on the economic feasibility. For example, Hoogwijk et al. (2004) estimate a kilowatt-hour of wind-generated electricity to cost approximately 0.06 US$ in both the USA and OECD Europe if the utilized technical potential is $\lesssim 1$ PWh/a. However, if the utilized technical potential is increased to 5 PWh/a, the cost-per-kWh is estimated to rise to 0.07 US$ in the USA, whereas in OECD Europe it would be off the scale used in (Hoogwijk et al., 2004, Fig. 9) (> 0.2 US$). A major factor in the wind energy potential utilizable in an economically feasible manner is thus the natural wind conditions of the area. However, also the costs of the wind turbine technology have an effect. It has been observed in many cases that the cost of a product decreases as the cumulative output increases. This effect is commonly called the learning curve, and it has been analyzed for wind power by numerous authors, for example Ibenholt (2002), Junginger et al. (2005), Neij (2008). It can thus be expected that the prices of wind turbine technology will continue to decrease as the installed capacity increases.

The cost of produced energy discussed above arises from the costs of the wind turbine and the yield of the turbine. In the case of wind power, the costs mainly consist of investment costs (including the turbine, the required land, permits, installation work, and so on) and maintenance costs. Since there are no fuel costs, the optimal operation is to always run with maximum attainable power (assuming that the generating turbine is a price taker, i.e., does not affect the price of energy by its operation, which, in the case of a wind turbine or even a wind park, is a justifiable assumption). The feasibility, then, is defined by the installation costs and the generated revenue over the life of the turbine. A technical and economic analysis is a means to quantify the feasibility of a given turbine with particular wind conditions.

Design of a wind turbine system involves, among other things, design of the control algorithms and analysis of the interactions between the turbine and the electric network. As already mentioned in the previous chapter, especially the performance of a wind power plant during a network disturbance is of interest. Simulations are a useful tool when performing these tasks (see, e.g., (Luukko et al., 2009b)). In this work, the utilization of these simulations in the feasibility analysis of a wind turbine is studied. The treatment of the subject is divided into two chapters. In this chapter, a technical and economic analysis method is formulated. The utilization of simulations in the analysis is discussed in the next chapter.

This chapter begins with an introduction to the fundamental physics of wind power production, properties of wind turbines, and the wind itself. Regulations-induced boundary condition (standards, transmission system operation requirements) are discussed in brief. Finally, the costs of produced wind energy are analyzed and a method for economic comparison of the performance of alternative wind turbine configurations is proposed.

2.2 Wind Turbine Annual Energy Output

2.2.1 Power of Wind

The power of wind is the kinetic energy of the air flow per unit time,

$$P_\mathrm{w} = \frac{1}{2}\frac{\mathrm{d}m}{\mathrm{d}t}v_\mathrm{w}^2, \tag{2.1}$$

where P_w is the power of the wind, $\frac{\mathrm{d}m}{\mathrm{d}t}$ is the mass flow, and v_w is the speed of the wind relative to the ground (and the turbine). This can be shown to be

$$P_\mathrm{w} = \frac{1}{2}\rho A v_\mathrm{w}^3, \tag{2.2}$$

where ρ is the density of air. It can be seen that the power attainable from wind is directly proportional to the density of air, the area of energy capture (rotor area A) and, importantly, the cube of the velocity of air. All of this power cannot be, however, captured. The power captured by the turbine is

$$P_\mathrm{t} = \frac{1}{2}\rho A C_\mathrm{p} v_\mathrm{w}^3, \tag{2.3}$$

where C_p is the power coefficient. C_p is generally a function of blade angle β and tip-speed ratio λ, which is the ratio of the speed of the blade tip and the wind speed,

$$\lambda = \frac{\omega_\mathrm{t} r_\mathrm{t}}{v_\mathrm{w}}, \tag{2.4}$$

where ω_t is the angular velocity of the turbine rotor and r_t is the radius of the rotor. For a given wind velocity, there exists an optimal tip-speed ratio λ_opt that will maximize the value of the power coefficient. Maximizing the value of the power coefficient for different wind speeds requires thus turbine speed control.

There is a theoretical upper limit for the power coefficient C_p, called the Betz limit, which has a value $C_\mathrm{p,Betz} = \frac{16}{27} \approx 0.6$ (Manwell et al., 2002). This theoretical upper limit arises from the fact that if all kinetic energy were harvested from the air flow, the air would have zero velocity after the turbine. This cannot be the case. Furthermore, other effects (according to Manwell et al. (2002), rotation of the propeller wake, a finite number of blades, and non-zero aerodynamic drag) decrease the value of C_p from the theoretical maximum, and the actual achievable value depends on the particular turbine. For example, Gorban' et al. (2001) calculated the maximal efficiency of a plane propeller turbine in free flow (such as wind) to be approximately 0.3. In practice, turbine manufacturers give the nominal output power (and the nominal wind speed) as well as the dimensions of the turbine, which enables the calculation of the nominal power coefficient, if required.

2.2.2 Wind Turbine Output Power

Generally stated, a turbine is a device delivering rotational shaft power on the basis of some other type of mechanical energy (Sørensen, 2007). A wind turbine, then, is a machine that converts the kinetic energy of the motion of air – wind – to rotation energy and further into electrical energy. The most commonly used turbine type is the horizontal-axis wind turbine (HAWT) (Manwell et al., 2002), illustrated in Figure 2.1. The axis of turbine rotation is horizontal, that is, parallel to the ground. Furthermore, the turbine depicted below is of upwind type – the rotor is facing the wind.

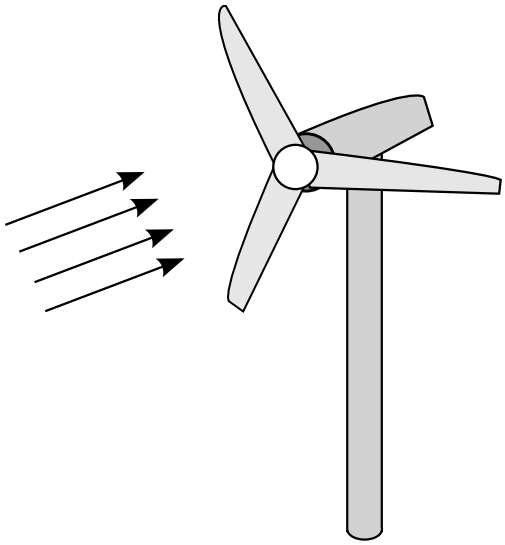

Fig. 2.1. Principle of the most commonly used wind turbine type, the upwind horizontal-axis wind turbine (HAWT). The arrows denote wind direction.

There are numerous variants of the basic HAWT-type turbine. Figure 2.2 presents a block diagram of one possibile configuration, showing the main parts. The blades can have a fixed blade angle, or the angle can be controllable. If the angle is fixed, the rotor is designed such that it will stall above a certain wind speed (Manwell et al., 2002). The rotation speed of the turbine rotor is typically tens of RPM. If the rotation speed of the generator is higher, a gear box is needed. In the case of the system shown in the figure, the generator is fed with a full-power (four quadrant) frequency converter. Alternatively, the generator could be connected directly to the network, or a doubly fed generator with a partial power converter in the rotor circuit could be used. The advantage of a power converter is the ability to allow variations in the rotation speed of the generator (and the turbine), which is required to keep the tip speed ratio constant with varying wind speeds. In the figure, the converter is located at the base of the tower, but it could also be located up in the nacelle. The nacelle is turned by the yaw system so that the rotor faces the wind when the turbine is operating. The yaw system is usually active, that is, there are motors turning the nacelle. The yaw system is controlled by the high-level control system, which measures the wind speed and direction and controls the yaw and the rotation speed of the generator. The control system is not shown in the figure. The turbine is connected to the power network through a transformer. In the case of a converter-based system, an output filter (and possibly a generator filter) would be required. These are not shown in the figure, however. For a more thorough treatment of different wind power generation concepts, see for instance (Hansen et al., 2001, Baroudi et al., 2007).

As discussed in the previous section, the power of wind is generally a function of the cube of wind speed, and the power captured from the wind depends on the power coefficient C_p, which is a function of blade angle and tip-speed ratio. Practical turbines have, however, additional limitations. First of all, there is a wind speed below which the turbine will not operate. This is called the cut-in wind speed of the turbine. Above the cut-in and below the nominal wind speed of the turbine, the turbine output power will follow the cubic curve described by Equation 2.3. This requires the power coefficient to be kept optimal at all wind speeds (which is the case if the turbine is speed-controlled). Keeping the power coefficient optimal is called maximum power point tracking (MPPT). This simple approach does not take into account the losses in the electric drive train. Owing to these losses and their being a function of operating point, the maximum electric power might not be generated in the point where the maximum turbine output is achieved. The effect of the electric drive train can be taken into account in the MPPT algorithm, as discussed by Tan et al. (2005).

Above the nominal wind speed (which, according to Söder and Ackermann (2005), is usually in the range of 12–16 m/s), the output power is limited to the nominal value. There are two power limitation methods in use: pitch control and stall control. In pitch-controlled turbines, the blade angle of the turbine is actively controlled to control C_p, whereas in stall-regulated turbines the aerodynamic design of the turbine is such that it will make the turbine stall above the nominal point, limiting the power capture. Stall regulation was the traditional method of limiting the mechanical power because it is simple to implement. However, its drawbacks include rather unsteady and unpredictable behavior in the stall range (see, for example, (Burton et al., 2001)). Pitch regulation provides a power curve more closely resembling the ideal case (constant power above nominal wind speed), at the expense of having to implement a blade angle control system.

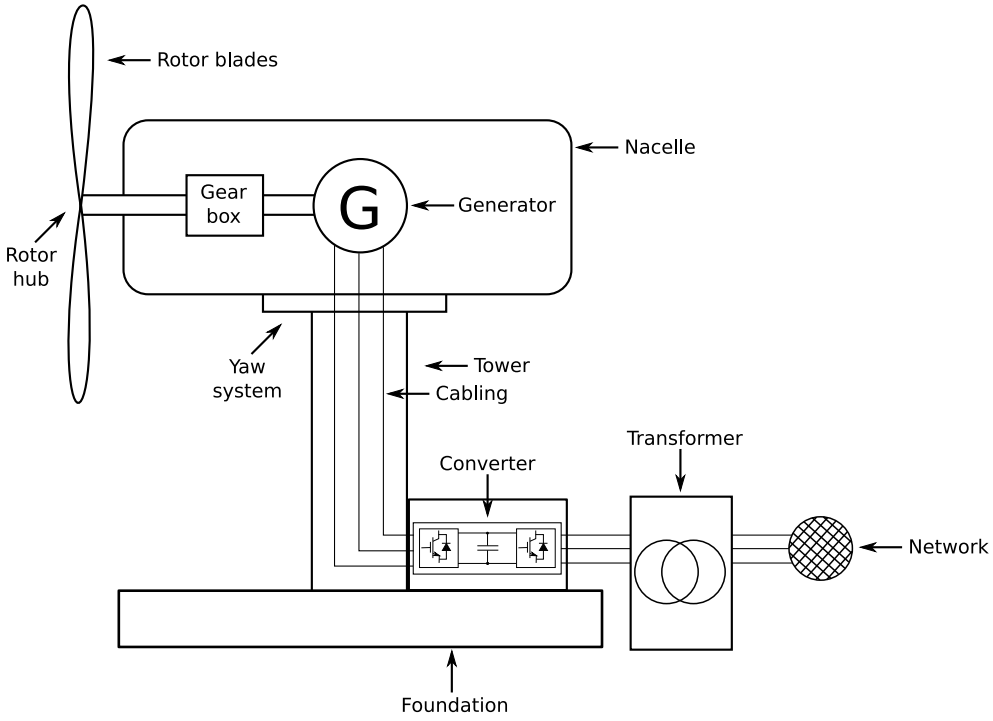

Fig. 2.2. Block diagram of the main parts of a wind turbine. The turbine in the figure is based on a full-power converter and a medium or high speed generator (compared to the turbine; hence the gearbox). Filters, protective devices, auxiliary devices (such as anemometers), or turbine control systems not shown.

Finally, there is a wind speed value above which the turbine is shut down in order to prevent mechanical damage. This is called the cut-out wind speed. A typical range for the cut-out speed is 20–25 m/s (Söder and Ackermann, 2005). There is often hysteresis in the cut-out: the cut-out speed is different depending on the direction of approach. In other words, when the wind speed increases, the turbine is stopped at the wind speed $v_{\mathrm{cut-out}}$, and when the wind speed then decreases, the turbine is restarted at a wind speed $\tilde{v}_{\mathrm{cut-out}}$ such that $v_{\mathrm{cut-out}} > \tilde{v}_{\mathrm{cut-out}}$. Figure 2.3 illustrates the different areas of operation of a wind turbine (the hysteresis effect not shown). The figure depicts merely the principle; numerical values are not based on any existing turbine. Some pitch-regulated wind turbines implement, instead of the sudden shutdown depicted in Figure 2.3, a smoother power reduction from the maximum power level to zero. This will mitigate the problems caused to the power system by a sudden shutdown of many wind turbines resulting for instance from a passing storm (Söder and Ackermann, 2005).

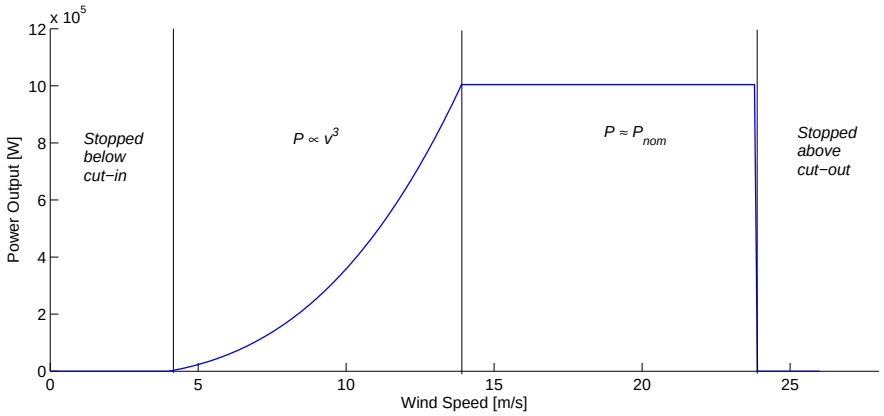

Fig. 2.3. Example of a speed-power curve for a wind turbine (principle; not based on a real turbine). Below the cut-in speed the turbine is stopped. Between the cut-in and nominal speed, the power has a cubic relationship to wind speed. Between the nominal and cut-out speed, the power is constant. With wind speeds higher than cut-out, the turbine is stopped.

2.2.3 Wind Statistics

Wind speed is highly variable, both as a function of time and of place. Globally, wind is caused by the uneven heating of the earth's surface and the resulting atmospheric pressure differences. Geographically, wind variations span over a wide range of scales. On the largest scale, earth has many climatic regions – some of them generally windier than others – defined mainly by the region's latitude. Regional geographic features, such as the proportion of land and sea or the elevation, further divide these regions into smaller ones that differ from each other. Locally, topology (hills and mountains etc.) has an effect on the wind conditions, and, still more locally, buildings and trees and other obstacles significantly reduce wind speeds (Burton et al., 2001) .

Temporal variations of wind speed are commonly divided into three different types based on their time scales (or frequencies). These are represented in the wind speed power spectrum by three peaks: the synoptic peak, the diurnal peak, and the turbulent peak (van der Hoven, 1956, Burton et al., 2001, Söder and Ackermann, 2005). Synoptic variations (peak typically $1/f$ a few days) are due to passing weather systems. Diurnal variations, as the name implies, are variations that occur within a 24-hour time window and are caused by the typically differing weather conditions during day and night. The turbulent peak represents very short-time variations (minutes down to seconds) in the wind speed – turbulences and gusts. They have an impact on the mechanical design of the turbines, and may have an effect on the power quality (Burton et al., 2001, Manwell et al., 2002). Diurnal and synoptic peaks, on the other hand, have an effect on the long-term balancing of the power system (Söder and Ackermann, 2005). Furthermore, the mean wind speed varies from year to year (inter-annual changes). These changes are difficult to predict: meteorologists generally conclude that it takes at least five years to get a reliable approximation for the average annual wind speed for a given location (Manwell et al., 2002). A rule of thumb presented by Aspliden et al. (1986) says that one year of wind speed data is sufficient for predicting a long-term seasonal average wind speeds with ± 10 % accuracy (confidence level 90 %). Also, according to Söder and Ackermann (2005), the estimated variation of the yearly mean power from one 20-year period to the next has a standard deviation of ≤ 10 %. Thus, over the life of a turbine, the uncertainty of the wind resource is not large compared for instance with the uncertainty of the availability of water in hydropower generation in some parts of the world. However, it should be noted at this stage that early years of operation have the greatest weight in the technical and economic analysis, and the wind speed uncertainty might have to be accounted for in the analysis. This will be discussed later in this chapter.

Yearly mean wind statistics for various locations are available in national and regional wind atlases, such as (Troen and Petersen, 1989, Tammelin, 1991). These atlases commonly provide wind speed distribution information in the form of Weibull distribution coefficients. The two-parameter (origin at zero) Weibull probability density function (PDF) is

$$p(V) = \frac{k}{c}\left(\frac{V}{c}\right)^{k-1} \exp\left(-\left(\frac{V}{c}\right)^{k}\right), \tag{2.5}$$

where V is the random variable (wind speed), c is the scale parameter (same units as V), and k is the shape parameter (dimensionless). Figure 2.4 presents the PDF for different parameter values. Keeping the shape parameter constant (Figure 2.4a), one can note that increasing the value of the scale parameter shifts the peak of the distribution to the right and makes the distribution wider (increases the variance). Similarly, keeping the scale parameter constant (Figure 2.4b), it can be seen that increasing the shape parameter generally makes the PDF narrower.

Initially, the Weibull distribution was used to describe statistical wind conditions because it in many cases seemed to give a good fit to the observations and was easier to work with than the more general bivariate normal distribution (which requires five parameters) yet more flexible than the Rayleigh distribution (which is the Weibull distribution with $k = 2$) (Justus et al., 1978). Tuller and Brett (1984) analyzed the distribution and concluded that the Weibull distribution is a logical distribution to represent a wind speed distribution, provided that

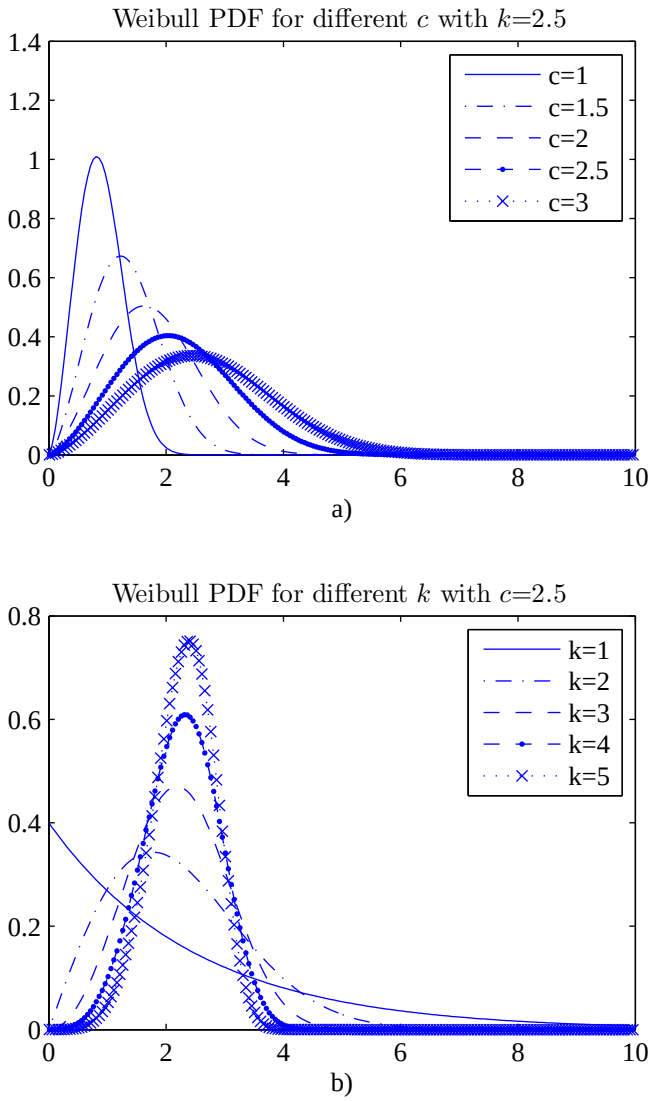

Fig. 2.4. Weibull probability density functions with different values for the parameters c (scale, a)) and k (shape, b)).

a) the orthogonal components of the wind velocity (transformed by raising to the power $k/2$) are normally distributed;
b) the transformed orthogonal components have equal variances and zero means; and
c) the transformed orthogonal components are uncorrelated.

The orthogonal components can be, for example, the directions north–south and east–west. From the conditions it can be concluded that if the transformed wind velocity is circular normal, then the Weibull distribution will give a perfect fit. The special case ($k = 2$) corresponds to the situation where untransformed wind velocity is circular normal, and the Rayleigh distribution will give a perfect fit (Tuller and Brett, 1984).

From the preceding, it can be concluded that in locations where the wind direction pattern is very asymmetric (asymmetry resulting e.g. from local topography), the Weibull distribution will not generally give a good fit. Furthermore, it can be seen (e.g. from Figure 2.4) that $P(v = 0) = 0$ for all parameter values. In reality, however, calms are recorded. The problem can be alleviated by modifying the distribution appropriately (see (Tuller and Brett, 1984)). However, usually wind atlases give the unmodified two-parameter Weibull distribution parameters and the duration of calms separately.

2.2.4 Calculating the AEO

An estimate of the annual energy output (AEO) of a wind turbine can be calculated if the (average) annual wind speed frequency distribution and the properties of the turbine are known. Furthermore, the effect of the mechanical to electric energy conversion can be taken into account if the efficiency of the electric drive train as a function of operating point (the wind speed) can be estimated. Figure 2.5 illustrates the principle of the calculation.

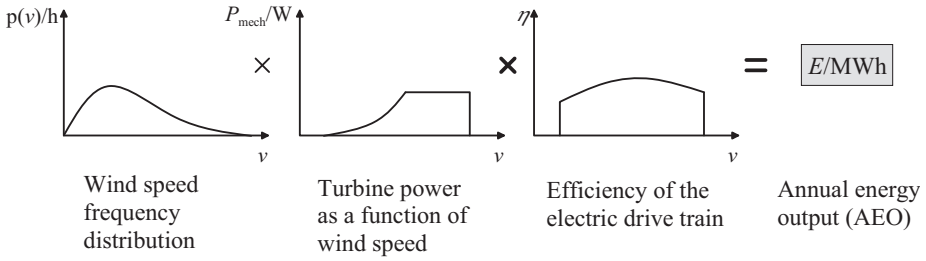

Fig. 2.5. Principle of the AEO calculation.

In many cases, only the two first curves are taken into account and the third is assumed constant (or even unity). This accuracy could be sufficient in determining the size of the turbine or performing rough feasible/not feasible analyses. However, without the third curve, component selections cannot be compared economy-wise. If the profit margin is small, already very small changes in the efficiency cause significant changes in profits, as seen (for hydropower)

for instance in (Tiainen et al., 2008, Lindh et al., 2008). For example, if the profit margin is 10 %, and a change causes an efficiency improvement of 0.5 %-units, the profits will increase by 5 %. If the payback time associated with the change is small, the change may very well be feasible. The economic analysis will be discussed later in this chapter.

The selection of the most convenient method of the actual calculation is largely influenced by the type of wind data available. The two main cases are data in time-series form and data as a wind speed frequency distribution. If the wind speed distribution is available, and the wind speed probability density function $p(V)$ is available, the annual average power can be expressed as (Manwell et al., 2002)

$$\overline{P}_{\mathrm{w}} = \int_0^\infty P_{\mathrm{w}}(v)p(v)\,dv, \tag{2.6}$$

where $\overline{P}_{\mathrm{w}}$ is the annual average power, $P_{\mathrm{w}}(v)$ is the output power of the turbine as a function of wind speed v, and $p(v)$ is the probability density function of the wind speed. Multiplying this average power with the number of hours in a year (8760) yields the annual energy output. The expression can be further developed for different probability density functions. Carlin (1997) calculated the average output power of an ideal turbine (power coefficient equal to the Betz limit $C_{\mathrm{p}} = \frac{16}{27}$), ideal electric power train (efficiency $\eta = 1$) and Rayleigh (Weibull with $k = 2$) wind speed frequency distribution,

$$\overline{P}_{\mathrm{w}} = \rho \left(\frac{2}{3}D\right)^2 \overline{v}^3, \tag{2.7}$$

where ρ is the density of air, D is the turbine diameter, and $\overline{v}$ is the average wind speed. Carlin (1997) calls this the Rayleigh-Betz machine and Equation 2.7 the "one-two-three" equation (exponents being 1, 2, and 3). Again, multiplying the average power by the number of hours per year yields the AEO. The Rayleigh-Betz machine can be considered an upper bound for the AEO of a wind turbine with a diameter D in a given wind regime.

An approach not involving a wind speed distribution is the direct use of measurement data (time series) (Manwell et al., 2002). Wind speed measurements, each averaged over some time interval ΔT, can be used to calculate an estimate for the AEO. Alternatively, wind speed data can be arranged as bins, that is, wind speed intervals and their durations. The average wind speed can be calculated from the bin midpoint values, assuming equal bin widths,

$$\overline{v} = \frac{1}{\mathrm{N}} \sum_{i=0}^{\mathrm{N}-1} v_i, \tag{2.8}$$

where N is the number of bins and v_i are the bin midpoints. Substituting this to Equation 2.3 gives the average turbine output power

$$\overline{P}_{\mathrm{t}} = \frac{1}{2\mathrm{N}} \rho A C_{\mathrm{p}} \sum_{i=0}^{\mathrm{N}-1} v_i^3, \tag{2.9}$$

which can be used to calculate the turbine AEO.

Equations presented so far do not take into account the efficiency of the electric drive train, which is a function of wind speed. If the efficiency of the drive train as a function of wind speed is $\eta(v)$, the turbine output power as a function of wind speed is $P_\mathrm{t}(v)$, and the wind speed distribution is given as N bins with durations T_i and bin midpoints v_i, the annual energy output of the turbine is

$$E_\mathrm{ao} = \sum_{i=0}^{\mathrm{N}-1} \eta(v_i) P(v_i) T_i. \tag{2.10}$$

Using this formulation, the bins need not necessarily be of equal width; constant power wind speed ranges, $[0, v_\mathrm{nom}]$ and $[v_\mathrm{nom}, v_\mathrm{cut-out}]$, can, for example, constitute a single bin each while dividing the cubic part of the output power curve, $[v_\mathrm{cut-in}, v_\mathrm{nom}]$, into narrower bins.

If the wind speed statistics are available as a probability density function, the bins can be generated from the probability density function. This approach was utilized in this work. The approach is convenient because wind speed data are commonly available as Weibull coefficients, yet the electrical efficiency of the drive is calculated in a set of points. A discrete set of points (bin midpoints) is often easier to work with on a computer than a continuous PDF and an interpolated efficiency curve.

The bin width has an effect on the accuracy of the AEO calculation. With only one bin, the AEO is the electrical output power at the bin midpoint multiplied by the number of hours the turbine is running per year. Clearly, this does not produce accurate results. Correspondingly, when $n \to \infty$, the sum in Equation 2.10 becomes an integral and a formulation similar to Equation 2.6 is obtained. A bin width somewhere between these two extremes must be selected. For example, the IEC standard 61400-12-1 (IEC, 2005) states that in the bin-based AEO[1] calculation, a bin width of 0.5 m/s is used. Figure 2.6 illustrates an example of a Weibull PDF (weighed with the number of hours per year) and the corresponding bins with a bin width of 1.0 m/s.

The amount of error in the AEO calculation caused by approximating the PDF with a staircase-like set of bins can be estimated by calculating the AEO for an idealized turbine ($C_\mathrm{p} = \text{constant}, \eta = 1$) with both the bin method and directly from the distribution and comparing the results for different number of bins. The average power of a wind turbine (rotor area A, power coefficient C_p) in wind (air density ρ) regime described by a Weibull distribution with parameters c and k is

$$\overline{P} = \frac{1}{2}\rho A C_\mathrm{p} c^3 \Gamma\left(1 + \frac{3}{k}\right), \tag{2.11}$$

where Γ is the gamma function (Tammelin, 1991). As an example, the AEO of a wind turbine with a turbine diameter $D = 70.5$ m and a power coefficient $C_\mathrm{p} = 0.38$ was calculated using Equation 2.11 and using the bin method with the wind speed range 0–30 m/s and different number of bins. The cut-in speed was thought to be zero and the nominal speed infinity (i.e., 38 % of the power of the wind was thought to be always captured). The AEO calculated from the distribution using Equation 2.11 was 6689 MWh. The results for different number of bins are given in Table 2.1. It can be seen that the error of the bin method compared with

[1] called the *annual energy production*, AEP, in the standard

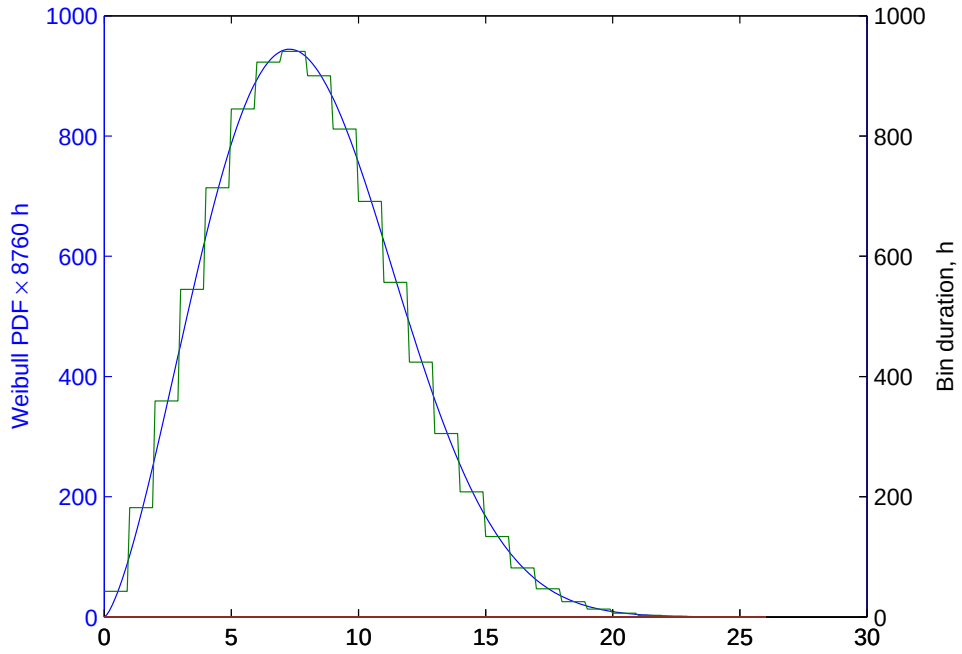

Fig. 2.6. Example of bins (staircase) created based on a Weibull PDF ($c = 9.10, k = 2.41$). The bin width is 1.0 m/s, and the PDF is weighed with the number of hours in a year.

Table 2.1. Effect of the number of bins on the accuracy of the bin-based AEO calculation, example.

Number of bins	Bin width, m/s	AEO, MWh	Error, MWh	Error, %
1	30	26 520	19 831	296.5
2	15	6 385	-304	-4.6
3	10	4 447	-2 242	-33.5
4	7.5	7 626	937	14.0
5	6	7 265	576	8.6
10	3	6 832	143	2.1
15	2	6 752	64	0.9
30	1	6 705	16	0.2
60	0.5	6 693	4	0.1
120	0.25	6 689	1	0.0

the integration method approaches zero when the number of bins is increased. In this case, the 0.5 m/s-bin used in IEC 61400-12-1 gives an error of approximately 0.1 %. Thus, the bin-based calculation in itself does not cause a significant error. In the remainder of the book, bin width of 0.5 m/s was used in all calculations, unless explicitly stated otherwise.

Next, let us consider the error between the estimated wind conditions and the actual wind conditions by analyzing the sensitivity of the AEO calculation to changes in the Weibull parameters. The cumulative density function (CDF) of the Weibull distribution with parameters c and k is

$$F(v) = 1 - \exp\left[-\left(\frac{v}{c}\right)^k\right]. \tag{2.12}$$

Using the CDF, the AEO of a turbine can be expressed as

$$E_{\mathrm{ao}} = T \sum_{i=0}^{\mathrm{N}-1} \left[F\left(v_{i,\mathrm{h}}\right) - F\left(v_{i,\mathrm{l}}\right)\right] P_{\mathrm{e},i}, \tag{2.13}$$

where T is the total number of hours in the analyzed period (8 760 h for a period of one year), $v_{i,\mathrm{h}}$ is the upper limit of the bin, and $v_{i,\mathrm{l}}$ is the lower limit of bin i. Substituting Equation 2.12 yields

$$E_{\mathrm{ao}} = T \sum_{i=0}^{\mathrm{N}-1} \left[\exp\left(-\left(\frac{v_{i,\mathrm{l}}}{c}\right)^k\right) - \exp\left(-\left(\frac{v_{i,\mathrm{h}}}{c}\right)^k\right)\right] P_{\mathrm{e,i}}. \tag{2.14}$$

This form can be used to calculate partial derivatives with respect to c and k to analyze the sensitivity of the AEO to changes in the wind conditions. The partial derivatives are

$$\frac{\partial E_{\mathrm{ao}}}{\partial c} = T\frac{k}{c} \sum_{i=0}^{\mathrm{N}-1} \left[\left(\frac{v_{i,\mathrm{l}}}{c}\right)^k \exp\left(-\left(\frac{v_{i,\mathrm{l}}}{c}\right)^k\right) - \left(\frac{v_{i,\mathrm{h}}}{c}\right)^k \exp\left(-\left(\frac{v_{i,\mathrm{h}}}{c}\right)^k\right)\right] P_{\mathrm{e},i}, \tag{2.15}$$

$$\frac{\partial E_{\mathrm{ao}}}{\partial k} = T\frac{k}{c} \sum_{i=0}^{\mathrm{N}-1} \left[\left(\frac{v_{i,\mathrm{h}}}{c}\right)^k \exp\left(-\left(\frac{v_{i,\mathrm{h}}}{c}\right)^k\right) \ln\left(\frac{v_{i,\mathrm{h}}}{c}\right) - \left(\frac{v_{i,\mathrm{l}}}{c}\right)^k \exp\left(-\left(\frac{v_{i,\mathrm{l}}}{c}\right)^k\right) \ln\left(\frac{v_{i,\mathrm{h}}}{c}\right)\right] P_{\mathrm{e},i}. \tag{2.16}$$

It should be noted that since Equation 2.14 is nonlinear with respect to both c and k, the corresponding partial derivatives depend on the point where they are taken. Furthermore, the logarithm $\ln(x)$ is not defined for argument $x = 0$. If the lower limit of the first bin is zero, the first bin must be treated separately in Equation 2.14 by replacing the calculation of the CDF for argument zero with its value, $F(0) = 0$. This is not usually needed, however, since, as discussed, a wind turbine has a cut-in wind speed $v_{\mathrm{cut-in}} > 0$ m/s below which it will not produce power and, therefore, contribute to the AEO.

As an example, the AEO of a 1.55-megawatt turbine with a nominal speed of 12 m/s, a cut-in speed of 3 m/s, and a cut-out speed of 25 m/s in the same wind conditions as in the previous example ($c = 9.1$ m/s, $k = 2.41$) was calculated. The efficiency of the electric drive train was set unity. The AEO, calculated using 0.5 m/s-bins, was 5 324 MWh. The partial derivatives are $\partial E_{\mathrm{ao}} = 1\ 119$ MWh$/(\mathrm{ms}^{-1})\partial c$ and $\partial E_{\mathrm{ao}} = 4$ MWh∂k. According to these estimates, changing the shape parameter k has in this case an insignificant effect on the AEO, whereas changing the scale parameter c by one m/s should result in a change of approximately 1 000 MWh in the AEO. Indeed, for $c = 10.1$ m/s and $k = 2.41$, the resulting AEO is 6 393 MWh (increase 1069 MWh), and for $c = 8.1$ m/s and $k = 2.41$, the AEO is 4174 MWh (decrease 1150 MWh).

Errors in Weibull parameters can be caused by the data and methods used to form the PDF estimate. Ramírez and Carta (2005) analyzed the effect of the sampling on the standard errors of the Weibull parameters for an example case (Canary Islands). Depending on the sampling, the errors of both of the parameters were somewhere in the range of 0.3 %–3 %. Celik (2003) compared the Weibull method and time-series method in the estimation of monthly wind conditions (and energy output) in various locations over a period of 96 months. The overall error in the monthly energy outputs estimated using the Weibull fit compared with the time series calculations was 2.8 %. Coelingh et al. (1996) analyzed the wind conditions in the North Sea (offshore) over the period of 1985–1992. According to their analysis, during this period, the mean wind speeds had a maximum variation of approximately 10 %. Generally, it would thus be reasonable to assume that the yearly variation in the wind conditions for a given location can be approximately 10 % or less. However, this is dependent on both the quality of the data available and the location itself.

2.3 Regulations Relevant to Wind Power

Constructing and operating a wind power plant is a very multi-disciplined task including, among others, mechanical design, electrical design as well as safety and environmental considerations. Therefore, border conditions to the design parameters and technology selections are set by standards and other regulations. The compared configurations must be such that they conform to their requirements. Some of the standards and requirements are briefly reviewed here in order to give the reader an idea of their contents.

2.3.1 International and European Standards

For the scope of this work, standards published by the IEC (International Electrotechnical Commission) are of most relevance. Wind power is the specific focus of the IEC 61400 family of standards. This includes general design requirements, noise measurements, power performance testing and measurements, and information exchange in plants, among others. Additionally, the IEC 61000 family concerning electromagnetic compatibility (EMC) is often referenced in the 61400 standards.

IEC 61000-4-7 defines general concepts of harmonics and interharmonics as used in the IEC standards (IEC, 2002). The standard also deals with the measurement and calculation of said parameters. The standard is valid for measuring spectral components in the frequency range of $f < 9$ kHz with the fundamental frequency at 50/60 Hz. The standard defines the window length in the discrete Fourier transform (DFT) to be 10 fundamental periods in a 50-Hz network and 12 in a 60-Hz network yielding a window length of 200 ms. The measurement shall be synchronized to the fundamental, and the weighting window used shall be rectangular. The standard further defines the harmonic (and interharmonic) groups to be used in the analysis. In the case of a 50-Hz network, the square of the magnitude of a harmonic group is the sum of the squares of the amplitudes of the harmonic and five adjacent spectral lines on each side of the harmonic frequency itself (with the extreme lines weighted by $1/2$). The spectral lines are 5 Hz from each other (5 Hz $= 1/200$ ms). The standard does not define limits for harmonic emissions, nor does it define the power levels at which the measurements should be carried out. Requirements for the measurement equipment are also laid down in this standard. They are not, however, important in simulations.

IEC 61400-12-1 defines the power performance measurements of a wind turbine, replacing the earlier standard IEC 61400-12 (IEC, 2005). 'Power performance' itself is defined in the standard as "measure of the capability of a wind turbine to produce electric power and energy". The standard begins with a prescription of the measurement setup (location of the meteorological mast etc.). Second, the measurement equipment is specified. Electric power shall be measured by measuring the voltage and current for each phase. The power performance is presented as a function of wind speed. The wind speed axis is divided into bins. Quantities for each bin are set as their mean over the range of the bin. In the standard, the width of each bin is defined as 0.5 m/s centered on multiples of 0.5 m/s. Similar bin-based calculation is, as discussed, extensively utilized in the present work and the bin width of 0.5 m/s is used unless stated otherwise. In the standard, the annual energy output is calculated by using the Rayleigh distribution as the reference wind speed frequency distribution for average wind speeds of 4, 5, 6, 7, 8, 9, 10, and 11 m/s. The remainder of the standard mostly deals with details of the measurement setup, reporting, and error estimation.

IEC 61400-21 deals with the power quality of grid-connected wind turbines (IEC, 2008). The standard is valid for all wind turbines, although only those wind turbine types that

are intended for the point of common coupling (PCC) at medium or high voltage (that is, $U_\mathrm{n} > 1$ kV) are required to be tested and characterized as per the standard. Current harmonics and interharmonics shall be, according to the standard, specified in the power bins 0,10,...,90,100 % of the nominal real power P_n, reactive power being set as close to zero as possible. Individual harmonics shall be specified as subgrouped values for frequencies up to $50 \cdot f_\mathrm{n}$, interharmonics up to 2 kHz, and higher frequencies between 2 kHz and 9 kHz as specified in IEC 61000-4-7. The standard further defines tests for voltage drops, as well as set-point control tests for both active and reactive power.

2.3.2 Transmission System Operator Requirements

Aside from the standards, the requirements set forth by the transmission system operator (TSO) whose network the wind turbine is intended to be connected to have to be taken into account. These requirements are commonly called the "grid code". The purpose of the requirements is to ensure user co-operation and network stability in as many situations as possible. The amount of wind power has increased significantly during the past two decades, and it is becoming increasingly important that wind turbines, too, participate in the stabilization of the network. The grid code has to be considered in the design phase of the wind turbine including the electrical sizing and the control method development. Therefore, the general contents of grid codes are briefly summarized in this section.

The requirements can be divided into three basic categories: frequency control (active power control), voltage control (reactive power control), and fault tolerance.

Frequency Control. For a typical network, the frequency of the network is controlled by controlling the active power exchange; active power surplus tends to increase the system frequency, whereas active power shortage decreases it. To keep the frequency constant, the consumption (including transmission losses) must equal the production at all instants. Thus, the power generation must be able to be varied following the variations in the consumption. If, at a given instant, the output of a power plant must be able to be increased, then the plant must have a spinning reserve, that is, the output of the plant must be lower than the total on-line capacity of the plant. The spinning reserve is often in the range of 1.5–3 % of the peak demand (de Alegría et al., 2007). In addition to the spinning reserve, there must be supplementary reserve for responding to slower changes in power demand.

As an example, let us briefly study the grid code of E.ON Netz (ENE), one of the four German grid operators. The frequency range of "normal operation" is defined as $f = 49.5 \ldots 50.5$ Hz (E.ON Netz GmbH, 2006). The code also defines a frequency envelope, above which the generating unit must not limit its active power output. The envelope consists of a linear frequency drop from 49.9 Hz to 49.0 Hz over 10 seconds, the frequency remaining at 49.0 Hz until 25 seconds, and rising linearly so that 49.8 Hz is reached at 60 seconds. Furthermore, the specification also defines areas in a frequency-voltage plane in which the generating plant must be able to operate for the duration of a given time (or continuously) at a given active

power (function of frequency). The code states further that any generating plant with a capacity $\geq$ 100 MW must be capable of supplying control power with control band of at least ± 2 % of the rated power. Generating plants with a rated capacity $<$ 100 MW can also, by agreement with the network operator, be used to supply control power.

Network operators in other countries (Eltra and Elkraft System in Denmark, Svenska Kraftnät in Sweden etc.) have similar requirements in their grid codes. An overview is given for instance by Matevosyan et al. (2004).

Voltage Control. In a typical network, the voltage level is controlled by controlling the reactive power. Wind turbines with directly grid-connected induction generators cannot be used for reactive power control, since they draw the required magnetizing current from the network and are not able to produce reactive power. This is usually compensated by using capacitors in parallel with the generator. If there are multiple capacitors, the voltage can be stepwise controlled by connecting and disconnecting some of them (Söder and Ackermann, 2005), but generally, directly network-connected induction generators have very limited voltage control capabilities. Since in the early days of wind power (until the end of 20^{th} century) this was the dominant installed wind turbine type (Hansen and Hansen, 2006), there were usually no requirements for reactive power production in wind turbines. The regulations of the Swedish grid operator Svenska Kraftnät (SvK), for example, have less stringent requirements for reactive power exchange in wind farms than in other types of power producers. In the SvK grid code, it is stated that wind farms with a total output $\geq 25\,MW$ shall be equipped with an automatic voltage controller with adjustable voltage reference at ± 5 % of the nominal voltage level, and that the reactive power must be able to be adjusted to zero (i.e. $\cos(\varphi)$=0) (Affärsverket Svenska Kraftnät, 2005). Other operators, such as ENE, define a power factor range that the attached power plant must be able to operate in (E.ON Netz GmbH, 2006, Matevosyan et al., 2004).

Grid codes may also state requirements for the power quality at the point of connection. The grid code of Eltra and Elkraft System (the two Danish network operators), for example, defines limits for flicker as well as harmonic and interharmonic voltages (referencing appropriate IEC standards).

Fault Tolerance. A fault somewhere in the electricity network will cause voltage deviation (drop) from the nominal. The voltage disturbance could trigger some generating units to disconnect themselves from the network to protect themselves, which would make the effects of the fault spread further possibly initiating a chain reaction leading to a network collapse. Therefore grid codes define minimum fault ride-through (FRT) capabilities of the connected generating units by defining a voltage dip curve above which there may not be a disconnection of the generating unit. In the case of ENE, for example, the worst-case voltage drop is defined such that the voltage (scaled to the nominal voltage) drops from 100 % to 0 and remains there for 150 ms, remains above 70 % up to time 700 ms from the onset of the fault, and then rises linearly to the lowest value of normal voltage band reaching it at 1500 ms (E.ON Netz GmbH, 2006). This example is an envelope, it represents the worst case conditions, and the

actual voltages may be anything above the envelope and the nominal during the dip.

2.4 Investment Analysis

2.4.1 Components of the Analysis

The economic feasibility of a planned wind turbine installation is determined by investment analysis. In the analysis, the costs and income of a wind turbine (during its planned life) are calculated and the decisions are made based on these calculations. In a general case, the quantities that need to be quantitatively presented are

- initial investment cost,
- (annual) return,
- (annual) overhead expenses,
- interest rate,
- lifetime of the investment, and
- scrap value (or salvage value).

In the case of a wind turbine, the initial investment cost consists of the costs of material, manufacturing, and installation (including planning, foundation, licensing etc.) (Rehman et al., 2003, Grauers, 1996). The overhead expenses are those expenses that are distributed over the life of the turbine. These include costs such as maintenance and repair work as well as the revenue not generated during maintenance shutdowns. As noted by Grauers (1996), these costs can also be said to include the cost of undelivered energy resulting from losses in the electric drive train.

The annual return or generated revenue depends on the delivered electrical energy (AEO, as discussed above) and the price of electricity. The price of electricity in liberalized electricity markets is a function of time. Price prediction in connection with renewable generation investments has been discussed by Fleten et al. (2007). However, to eliminate price uncertainty and thus encourage investments in renewable generation, some countries and subnational entities have introduced feed-in tariffs for renewables, in this case wind power. If such a tariff is in use and guarantees a minimum price of electricity for wind power producers, the uncertainty of the electricity price is eliminated (or reduced, if the exact duration of the tariff is not known). For an overview of policies encouraging renewable energy production in the countries of the European Union, see for instance Reiche and Bechberger (2004), Ringel (2005), Fouquet and Johansson (2008).

The interest rate may be adjusted to take into account the effect of inflation, or the interest rate may be the nominal interest rate, in which case the effect of inflation must be taken into account with a separate term. In the present study, unless otherwise noted, all of the sums are nominal with inflation included in the interest rate term. Furthermore, in the investment analysis, the interest rate may be selected somewhat higher than the expected price of money

in order to get a security margin.

The scrap value of an investment is the value that the investment has at the end of its life. In the case of a wind turbine, a major contributor is the value of the metals used in the construction of the tower, generator, and the like. Sometimes (e.g. (Tande and Hunter, 1994)), the term is used to refer to the value of the installation (before decommissioning), and the term 'salvage value' is used to refer to the difference of the scrap value and the decommissioning cost. In this work, however, the term 'scrap value' is used for the amount of money obtained from selling the turbine at the end of its life with the decommissioning costs subtracted.

2.4.2 Common Analysis Methods

The value of the produced energy over the life of the turbine cannot be calculated by simply multiplying the average output power with the life of the turbine and the (assumed or known) average electricity price, but the time-value of money must be taken into account. The time-value of money arises from the fact that a sum of money now is worth more than the same sum at some later time. In a wind power investment, the investment cost is to be paid at the beginning of the life of the turbine, whereas the returns are evenly distributed over the turbine life. There are several well-known concepts related to making sums of money spent or returned at different instances in time comparable. These include

a) the present value method,
b) the annuity method,
c) the internal rate of return method, and
d) the payback time method.

Present value. In the present value method, the present value of all income (and costs) over the life of an investment (a wind turbine, in this case) are discounted back to the time of investment. The present value V_p of a sum of money with the future value V_f obtained after n years with an annual interest rate p is

$$V_\mathrm{p} = \frac{V_\mathrm{f}}{(1+p)^n}. \tag{2.17}$$

The n periods need not necessarily be years, in which case p is not the annual interest rate but the interest rate of one period.

Annuity. The annuity method could be described as an inverse of the present value method. In the method, the initial investment is distributed as fixed-size annual payments over the life of the turbine. This method is applicable, if the annual returns do not vary much.

Internal rate of return. This method aims at calculating the interest rate with which the present value of the investment (present value of all returns + present value of the scrap value - present values of all costs including initial investment) is zero. This internal rate of return is the lowest interest rate with which the investment is profitable.

Payback time. The time it takes for the combined net return of the investment to exceed the initial investment cost is calculated. Sometimes, the effect of time-value is ignored, but it can be taken into account by using a similar discounting factor as in the present value method.

2.4.3 Analysis Using the Present Value Method

Often, when considering an investment in wind power, a choice between two or more alternatives must be made. Examples of such choices are selection of the most suitable wind turbine for a specific site or the most suitable site for a specific turbine (Tande and Hunter, 1994). All of the above-described methods could be used in the comparison of the candidates. However, the use of the annuity method is limited to the comparison of two alternatives with equal expected life. The present value method has been widely applied to wind turbine investment analysis. Lysen (1983) presented an equation to calculate the present value of costs of a wind turbine,

$$PVC = C_{\mathrm{i}} + C_{\mathrm{omr}} \left(\frac{1+i}{r-i} \right) \left[1 - \left(\frac{1+i}{1+r} \right)^{L} \right] - S \left(\frac{1+i}{1+r} \right)^{L}, \tag{2.18}$$

where PVC is the present value of costs, C_{i} are the investment costs, C_{omr} are the annual operation, maintenance, and repair costs, i is the inflation rate, r is the interest rate, S is the scrap value, and L is the life of the turbine. The calculated present value of costs is used to calculate the cost of energy over the life of the turbine. The method has subsequently been utilized by, for instance, Rehman et al. (2003), Ucar and Balo (2009b). This "cost-per-kWh" method is useful in many cases. However, there are situations where it is not very illustrative. For example, if the designer wishes to be able to analyze how much a specific component change may cost in order to be feasible, the calculated costs of energy do not give a direct answer. Therefore, we will develop a slightly different formulation of the same expression.

The income over the life of a wind turbine equals the sum of the present values of exported electricity minus the annual overhead expenses, minus the initial investment cost plus the present value of the scrap value of the turbine,

$$J = \sum_{t=0}^{T-1} \left[\frac{\overline{\pi}_t E_{\mathrm{ao}} - C_{\mathrm{omr}}}{(1+p)^t} \right] - C_{\mathrm{i}} + \frac{S}{(1+p)^{T-1}}, \tag{2.19}$$

where J is the income, T is the life of the turbine, $\overline{\pi}_t$ is the average price of electricity for year t, E_{ao} is the annual energy output, C_{omr} are the annual operations, maintenance, and repair costs (annual overhead expenses), C_{i} are the investment costs (including materials, installation, land, civil works etc.) p is the real (inflation-corrected) interest rate, and S is the scrap value of the installation. In the expression, the effect of inflation and interest rate have

been combined to form the real interest rate. Using Lysen's symbols, this real interest rate may be calculated from the nominal interest rate r and the inflation rate i with the equation

$$1+p=\frac{1+r}{1+i}. \tag{2.20}$$

Additionally, it should be noted that the lower index of the sum is zero instead of (the more conventional) one. This would mean that the annual income and expenses are to be paid at the beginning of the year and not the end (the "time origin" of the analysis is at the end of the first year of operation). The lower limit of the sum can, however, be freely changed (modifying the upper limit of the sum and the present value term of S accordingly). For the time being, we will let it remain zero.

If there are two[2] alternative configurations, Configuration 1 and Configuration 2, to be compared, the income difference ΔJ can be expressed as

$$\Delta J=\sum_{t=0}^{T-1}\left[\frac{\overline{\pi}_t\Delta E_{\mathrm{ao}}-\Delta C_{\mathrm{omr}}}{(1+p)^t}\right]-\Delta C_{\mathrm{i}}+\frac{\Delta S}{(1+p)^{T-1}}, \tag{2.21}$$

where the income difference $\Delta J=J_2-J_1$, the electricity prices $\overline{\pi}_{t,1}=\overline{\pi}_{t,2}=\overline{\pi}_t$, the AEO difference $\Delta E_{\mathrm{ao}}=E_{ao,2}-E_{ao,1}$, the OMR cost difference $\Delta C_{omr}=C_{\mathrm{omr},2}-C_{\mathrm{omr},1}$, the investment cost difference $\Delta C_{\mathrm{i}}=C_{\mathrm{i},2}-C_{\mathrm{i},1}$, the interest rate $p_1=p_2=p$, and the scrap value $S_1=S_2=S$. Thus, this formulation assumes that the lives of both turbines, and the economic parameters (the interest rate and the price of electricity), are equal.

Generally, estimating the annual OMR costs is difficult since failures and therefore repair costs cannot be known beforehand. In the design phase, however, it might be safe to assume that the two compared configurations are more or less identical in terms of reliability and need for maintenance (especially, since the environmental conditions for both alternatives will be the same). In this case, the term ΔC_{omr} can be assumed to be zero. There are, however, cases where OMR costs do have a significant impact on the analysis. Examples of this kind of situations are comparing converters with different capacitor types in the DC link (film capacitors, electrolyte capacitors), comparing geared and gearless turbines, and comparing generators with slip rings (doubly fed generators) and ones without them (PM generators). Simulations presented in this thesis are not of use in determining the OMR costs, but simulations could be used to obtain the energy outputs of the compared configurations in some cases. In this thesis, OMR costs are not included in the analysis. The situation is somewhat similar for the scrap value; its precise value is impossible to know exactly (an estimate of approx. 10 % of the initial investment has been used by Lysen (1983), Rehman et al. (2003)), but in many cases, it, also, can be assumed approximately equal for both compared configurations, resulting in $\Delta S=0$. With these assumptions, the income difference equation can be written

$$\Delta J=\sum_{t=0}^{T-1}\left[\frac{\overline{\pi}_t\Delta E_{\mathrm{ao}}}{(1+p)^t}\right]-\Delta C_{\mathrm{i}}. \tag{2.22}$$

[2]If there are more than two configurations, the configurations can be compared in pairs using the method presented here.

Equation 2.22 represents the change in the present value of the income generated during the life of the turbine when selecting one configuration (Configuration 2) instead of the other (Configuration 1). The selection may be such that it improves the overall performance (ΔE_{ao} is positive). In this case, the improved system will probably cost more (ΔC_{i} positive), because otherwise selection would obviously be Configuration 2. If, now, the income change ΔJ is positive, selecting Configuration 2 instead of Configuration 1 is in principle economically justified. Similarly, the change from Conf. 1 to Conf. 2 may aim to decrease the investment cost (ΔC_{i} negative) while also degrading the performance (ΔE_{ao} negative). In this case, the income change ΔJ will again be positive, if the change is economically feasible.

Aside from analyzing the feasibility of a configuration change, the equation can also be used to find limits for the price of Configuration 2 in order for it to remain feasible. Supposing, for example, that the designer considers upgrading a component of the drive train in Configuration 1 with one with lower losses, thus forming Configuration 2. The designer can then calculate the value of ΔJ in Equation 2.22 with $\Delta C_{\mathrm{i}} = 0$. The resulting value represents the maximum price increase. A similar method can also be used for a case where Conf. 2 has higher losses than Conf. 1. In this case, the question is, how much lower the investment cost of Conf. 2 must be in order to be more feasible than Conf. 1. Both these types of analysis will be discussed in the example cases in the next chapter.

The lower index of the sum is determined by the time from the investment to obtaining the first revenue from generated electricity. A value of one would correspond to the turbine being commissioned at time 0 and the first remuneration being received at the end of the first year. All income generated during a year is thus discounted to time 0 as if it occurred at the end of the year. The actual moment when the remuneration for the generated electrical energy is paid depends on the system used. To simplify the matter, we will use the end of the year as the remuneration moment. If the method is used for analyzing a real case, the year can be divided into smaller remuneration periods if appropriate. The time between the investment moment and receiving the first remuneration payments varies in practice case by case. Therefore, we will replace the lower index of the sum with the generic value t_0 and call it the initial time index. This gives

$$\begin{aligned}\Delta J &= \sum_{t=t_0}^{t_0+T-1} \left[\frac{\overline{\pi}_t \Delta E_{\mathrm{ao}}}{(1+p)^t} \right] - \Delta C_{\mathrm{i}} \\ &= \frac{1}{(1+p)^{t_0}} \sum_{t=0}^{T-1} \left[\frac{\overline{\pi}_t \Delta E_{\mathrm{ao}}}{(1+p)^t} \right] - \Delta C_{\mathrm{i}} \end{aligned} \tag{2.23}$$

This expression assumes that the price of electricity is constant over the whole life of the turbine. In liberalized electricity markets, the price is in principle determined by production and consumption, and cannot thus be known beforehand (although numerous attempts have been made to predict it at least on short time scales; for a recent review, see (Aggarwal et al., 2009)). To reduce uncertainty in the investment analysis and by that means encourage investment in wind energy, different support mechanisms have been devised and utilized in various countries. The details of the schemes vary, but they could generally be grouped into two major categories illustrated in Figure 2.7. In premium-based systems (Figure 2.7a), the

wind energy producer gets the market price of electricity plus a premium for the produced energy. In this scheme, the price of the electricity is still very much unknown. Alternatively (Figure 2.7b), there exists a guaranteed price (wind power feed-in tariff) which will be paid to the producer in case the market price is lower than the guaranteed price (or sometimes the guaranteed price is paid always, even if the market price is higher). In this case, if there is uncertainty in the electricity price, it is unidirectional, and assuming the price constant produces the minimum generated revenue.

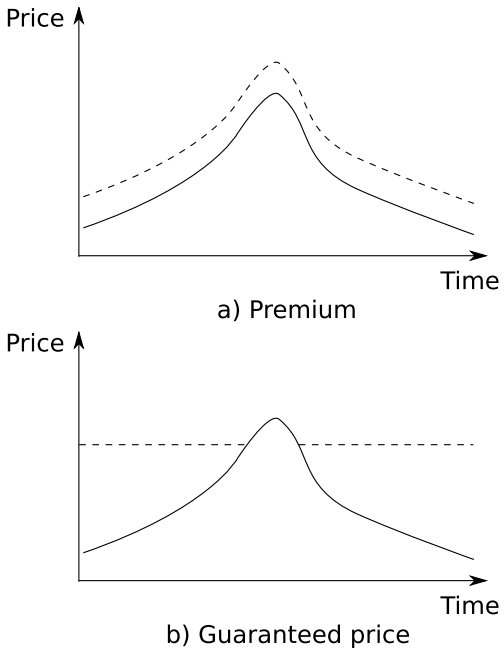

Fig. 2.7. Principles of two wind power economic support schemes: premium (a) and guaranteed price (b). In the premium-based system, the wind power producer is paid the market price plus the premium, whereas in the guaranteed price scheme, the producer receives the market price if it is higher than the guaranteed price and the guaranteed price otherwise.

Couture and Gagnon (2010) present an up-to-date and comprehensive overview of the different green energy support schemes. They conclude that generally feed-in tariff-based systems (guaranteed price) have been more successful in promoting renewable generation of electricity. The analysis method presented here must be adapted to the remuneration scheme applied. For all the analyses presented in this work, the same remuneration scheme was used. It is based on the proposal for the new Finnish feed-in tariff (dated Apr 2, 2009). This scheme was selected for its simplicity. It provides a guaranteed minimum price of electricity of 83.5 €/MWh during the first 12 years of wind turbine operation. If the (averaged) market electricity price for a period exceeds this value, the market price will be used (as in Figure 2.7b). However, it can be assumed that this occurs rarely, and the tariff price will be used for the whole tariff duration. In some tariff-based systems already implemented in other countries (for example, Germany), the performance of the plant has an effect on the tariff duration so that the more the installation produces energy, the shorter the tariff duration will be. (For

discussion on European policies for the promotion of renewable energy production, see for example Reiche and Bechberger (2004), Ringel (2005), Fouquet and Johansson (2008).) In the following, we will assume that the principle of the remuneration scheme applied is the same as in the Finnish tariff proposal. The tariff price is denoted $\overline{\pi}_1$ and the tariff duration is t_1 years. After the tariff duration, market price ($\overline{\pi}_2$, used as a constant in the analysis) is paid during the rest of the life of the turbine. Equation 2.23 can now be divided into two parts,

$$\Delta J = \frac{1}{(1+p)^{t_0}} \left[\sum_{t=0}^{t_1-1} \frac{\overline{\pi}_1 \Delta E_{\mathrm{ao}}}{(1+p)^t} + \sum_{t=t_1}^{T-1} \frac{\overline{\pi}_2 \Delta E_{\mathrm{ao}}}{(1+p)^t} \right] - \Delta C_{\mathrm{i}}. \tag{2.24}$$

The sums in this expression can be eliminated utilizing the well-known equation for the sum of the first n elements of a geometric series,

$$\sum_{i=0}^{n-1} ax^i = a\frac{1-x^n}{1-x}, \quad x \neq 0. \tag{2.25}$$

For this equation to be applicable to the second sum, it must be modified so that the first index is zero. Equation 2.24 takes now the form

$$\Delta J = \frac{1}{(1+p)^{t_0}} \left[\sum_{t=0}^{t_1-1} \frac{\overline{\pi}_1 \Delta E_{\mathrm{ao}}}{(1+p)^t} + \frac{1}{(1+p)^{t_1}} \sum_{t=0}^{T-t_1-1} \frac{\overline{\pi}_2 \Delta E_{\mathrm{ao}}}{(1+p)^t} \right] - \Delta C_{\mathrm{i}}. \tag{2.26}$$

The resulting form for the income difference equation is

$$\Delta J = \frac{\overline{\pi}_1 \Delta E}{(1+p)^{t_0}} \frac{(1+p)^{t_1}-1}{p(1+p)^{t_1-1}} + \frac{\overline{\pi}_2 \Delta E}{(1+p)^{t_0+t_1}} \frac{(1+p)^{T-t_1}-1}{p(1+p)^{T-t_1-1}} - \Delta C_{\mathrm{i}}. \tag{2.27}$$

This form is easier to work with than Equation 2.24 when doing calculations on paper with a simple calculator, but otherwise Equations 2.24 and 2.27 are equal.

Several parameters in Equation 2.27 have uncertainty. As already discussed in connection with the Weibull statistics, a commonly used method to assess the effect of uncertainty in the parameters to the value of an equation is the sensitivity analysis Tande and Hunter (1994), Kaldellis and Gavras (2000). In practice, this means calculating the partial derivatives of the equation with respect to all of the parameters (keeping others constant). This was done for

Equation 2.27. The partial derivatives are

$$\frac{\partial \Delta J}{\partial \Delta C_{\mathrm{i}}} = -1 \tag{2.28}$$

$$\frac{\partial \Delta J}{\partial \Delta E} = \frac{\overline{\pi}_1}{(1+p)^{t_0}} \frac{(1+p)^{t_1}-1}{p(1+p)^{t_1-1}} + \frac{\overline{\pi}_2}{(1+p)^{t_0+t_1}} \frac{(1+p)^{T-t_1}-1}{p(1+p)^{T-t_1-1}} \tag{2.29}$$

$$\frac{\partial \Delta J}{\partial \overline{\pi}_1} = \frac{\Delta E}{(1+p)^{t_0}} \frac{(1+p)^{t_1}-1}{p(1+p)^{t_1-1}} \tag{2.30}$$

$$\frac{\partial \Delta J}{\partial \overline{\pi}_2} = \frac{\Delta E}{(1+p)^{t_0+t_1}} \frac{(1+p)^{T-t_1}-1}{p(1+p)^{T-t_1-1}} \tag{2.31}$$

$$\begin{aligned} \frac{\partial \Delta J}{\partial p} = & -\frac{\Delta E}{p^2(1+p)^{T+t_0+t_1}} [\overline{\pi}_1(1+pt_0)(1+p)^{T+t_1} - \\ & (1+p(t_0+t_1))(\overline{\pi}_1-\overline{\pi}_2)(1+p)^T - \\ & \overline{\pi}_2(p(T+t_0)+1)(1+p)^{t_1}] \end{aligned} \tag{2.32}$$

$$\frac{\partial \Delta J}{\partial T} = \frac{\Delta E \overline{\pi}_2}{p(1+p)^{T+t_0-1}} \ln(1+p) \tag{2.33}$$

$$\begin{aligned} \frac{\partial \Delta J}{\partial t_0} = & -\frac{\Delta E \ln(1+p)}{p(1+p)^{T+t_0+t_1-1}} [((1+p)^{T+t_1} - (1+p)^T)\overline{\pi}_1 + \\ & ((1+p)^T - (1+p)^{t_1})\overline{\pi}_2] \end{aligned} \tag{2.34}$$

$$\frac{\partial \Delta J}{\partial t_1} = \frac{\Delta E \ln(1+p)}{p(1+p)^{t_0+t_1-1}} (\overline{\pi}_1 - \overline{\pi}_2) \tag{2.35}$$

Equation (2.27) is nonlinear with respect to p, T, t_0, and t_1. Thus, the corresponding partial derivatives (Equations 2.32 through 2.35) depend on the point where the derivative is calculated. The expressions themselves are not particularly illustrative. Numerical values for the partial derivatives are presented in the next chapter in connection with the example cases, where the analysis results are discussed.

2.4.4 Supplementing the Analysis with the Payback Time

The present value of the generated income over the life of a wind turbine is generally a good metric to compare two different configurations. However, more insight into the selection problem can be provided by supplementing the described analysis method with the calculation of the payback time difference of the compared configurations. In some cases, the compared configurations can differ only slightly in terms of the present value of the income and yet have significantly different payback times. In this case, the configuration with the shortest payback time (i.e., the lowest risk) is the natural choice. Furthermore, wind power technology has been developed extensively during the past decades, and, as a result, the cost of wind energy has decreased steadily. Therefore, it might be a justifiable choice to invest in

technology that will pay the investment back as quickly as possible, even if the total expected income is lower than in the alternative configurations.

In the most basic form, the payback time of a wind turbine (not taking into account the scrap value) can be expressed as

$$T_{\mathrm{pb}} = \frac{C_{\mathrm{i}}}{\overline{\pi} E_{\mathrm{ao}} - C_{\mathrm{omr}}}, \tag{2.36}$$

which is the investment cost divided by the annual income (generated revenue minus the OMR costs), assuming constant price of electricity indefinitely into the future. This formulation fails to take into account the time-value of money or the properties of the used tariff. Since the time-value of money is not taken into account, this equation gives overly optimistic (small) values for the payback time. However, the equation can be used to note the fact that if we calculate the payback time difference of two configurations, $\Delta T_{\mathrm{pb}} = T_{\mathrm{pb},2} - T_{\mathrm{pb},1}$, the annual operations and maintenance costs cannot be eliminated.

Deriving an analytic expression for the payback time taking into account the time value of money is not as straightforward. However, when using a computer, this can be calculated using a loop construction with the following principle,

1. Set $J = C_{\mathrm{i}}$ and $t = t_0$
2. Calculate $J_t = \dfrac{\overline{\pi}_t E_{\mathrm{ao}} - C_{\mathrm{omr}}}{(1+p)^t}$
3. If $J - J_t \geq 0$, then

   set $J = J - J_t$

   set $t = t + 1$

   go to step 2

   else

   set $T_{\mathrm{pb}} = t - 1 + \dfrac{J_t - J}{J_t}$

   end program

The annual energy outputs (E_{ao}), the annual mean electricity prices ($\overline{\pi}_t$), and the annual OMR costs (C_{omr}) are assumed to be available in the program. The algorithm simply subtracts the generated revenue for year t from the initial investment cost until the result would go below zero adding whole years to the payback time T_{pb} (actually, T_{pb} is not modified until the end of the program, because t already keeps track on the number of years). Then, when the result would go below zero, the fraction of the final year required to get the accumulated income (J) zero is calculated using a simple linear approximation. The scrap value is not taken into account, but if it were, its discounted value would be subtracted from the initial investment cost at the beginning of the program (step 1). Upon program termination, T_{pb} will hold the estimated payback time that takes into account the time value of money.

This variant of payback calculation was used in the analyses presented in this thesis. Unless otherwise stated, the annual OMR costs were assumed zero and the scrap value was not taken into account.

2.4.5 Implemented Tools

An Excel sheet was developed for the comparison of two alternative configurations. The sheet consists of two parts. The purpose of the first one is to calculate the annual energy output of a configuration, whereas the second part calculates the economic analysis. The output of the AEO calculator (for two different configurations) is input to the economic analysis. Additionally, the tool calculates the partial derivatives of the AEO expression (Equations 2.15 and 2.16).

In the AEO calculation sheet, for each configuration, the user specifies properties in three categories: the wind, the turbine, and the electric drive train. The parameters are described in Table 2.2. The turbine power coefficient C_p is calculated based on the nominal power, diameter, nominal wind speed, and air density. The power coefficient is assumed constant between the cut-in speed and the nominal speed. Above the nominal speed and below the cut-out speed, the turbine power is assumed constant. These assumptions idealize the behavior of the turbine, which in reality, as demonstrated for instance by Kwon (2010), has statistical variation. When comparing different electric drive train configurations used with the same turbine, the effect of these deviations from the ideal do not have as strong an effect on the outcome as when comparing different turbines. If desired, they could, however, be accounted for in the analysis.

The tool accepts Weibull distribution parameters to describe the wind conditions of the site. Furthermore, the user gives the desired number of bins and the lower and upper limits of the wind speed range that is divided into those bins. These must be selected by the user so that no hours remain outside the bins; in practice, this means that the low limit is set to zero and the high limit ”high enough”, somewhere around 30 m/s, for example. The tool calculates the durations of the bins based on the given Weibull parameters. The bins can also be created or modified manually to facilitate input of time-series data or the creation of non-equal bin widths.

The total efficiency of the electric drive train (from mechanical input to electric output) is given as a table, where the efficiency is given as a function of wind speed. Thus, also the efficiency is given in the form of bins. These efficiency bins need not be the same as the wind speed frequency bins. Furthermore, the user can give an electric input power limit. This is meant to be used in situations where the electric drive train is undersized with respect to the turbine, and the turbine output power must thus be limited. This kind of a situation is discussed in Case 2 in the next chapter. The efficiencies are obtained using a time domain simulation tool, which calculates the output power of the system in various operating points. The tool is described in more detail in the next chapter.

In the economic analysis tool, the user specifies the parameters given in Table 2.3. Based

Table 2.2. Parameters that the user gives to the AEO calculation tool.

Category	Parameter	Unit	Typical data source / Notes
Turbine	Nominal power	MW	Turbine manufacturer
	Diameter	m	”
	Nominal speed	r/min	”
	Nominal wind speed	m/s	”
	Cut-in wind speed	m/s	”
	Cut-out wind speed	m/s	”
Wind	Density of air	$\mathrm{kg/m^3}$	Meteorological data; $\rho = 1.225\ \mathrm{kg/m^3}$ commonly used
	Weibull scale parameter	m/s	Wind atlases; measurements
	Weibull shape parameter		”
	Number of bins		Set so that all time is allocated to
	Wind speed range	[m/s m/s]	bins and the bin width is small enough
Electric drive train	Efficiency table		As a function of wind speed; obtaining from simulations discussed in the next chapter
	Maximum power	MW	For limiting the turbine output

Table 2.3. Parameters that the user gives to the economic analysis tool.

Parameter	Unit	Notes
Interest rate	%	Common to both configurations
AEO	MWh	For both conf’s, from the AEO calc. tool.
Turbine life	years	Estimated, often taken as 20 years
Initial time index		Time to commissioning (years) + 1
Tariff price	€	
Tariff duration	years	
Post-tariff price	€	

on these, the income difference (Equation 2.23) between the configurations is calculated. The same interest rate is used for both configurations; other parameters can be set for each configuration separately. The tariff system is currently limited to a fixed-price tariff with a fixed duration. It would be relatively straightforward to make the tariff duration dependent on the performance of the plant (ending the tariff period after the first E MWh have been produced, for example); if the tool were to be used for a specific country, this would need to be done. The tool also calculates the payback time applying the method described in the previous section. In the present version, OMR costs are taken as zero, which causes slightly underestimated payback times. Furthermore, the values of the partial derivatives of the income change expression (Equations 2.28 through 2.35) are calculated.

2.5 Summary

This chapter discussed the fundamental physics of wind power production. An essential feature is that the power of wind is proportional to the cube of the velocity of the wind. This brings forth the fact that the output power of a wind turbine decreases rather rapidly from the nominal, when the wind speed decreases from the nominal. Additionally, above the nominal wind speed, the power of a wind turbine is limited to the nominal value. Above the cut-out speed or below the cut-in speed, the wind turbine is stopped. The description of statistical wind properties was discussed. An estimate for the annual energy output (AEO) of a wind turbine can be calculated, if the properties of the turbine (and the electric drive train) and the wind statistics are known. The calculation can be done by integrating over the distribution, or using a discrete bin-based approach. It was shown that the methods give practically identical results provided that the bin width is sufficiently small, approximately 1 m/s or less. The sensitivity of the AEO estimate to changes in the Weibull parameters was analyzed. A very brief overview of the regulations concerning wind turbine design was given. The design (and possible optimization of it) needs to be done so that all relevant regulations are met. Simulations are often used to verify compliance with regulations.

In the latter part of the chapter, an economic analysis method was developed for comparing two alternative wind turbine configurations, with the focus on the properties of the electric drive train. The idea of the method is to calculate the difference of the present value of the generated revenue over the life of the compared configurations. This comparison can answer at least two types of questions, namely 1) *Should Configuration 1 or Configuration 2 be selected on economic grounds?*, and 2) *How much can a performance-improving modification of a configuration cost in order to be feasible?*, or, conversely, *how much do we have to save with a performance-degrading modification of a configuration in order for it to be feasible?*, both being subject to a regulations-induced framework. In addition to calculating the income change, it was suggested that the calculation of the payback time could be used to supplement the analysis to assess the risk associated with the change. An Excel sheet was created to automate the analysis process.

Traditionally, economic analyses have been limited to rough feasible/not feasible analyses and determining the turbine power. After the feasibility of an installation is determined at this level, the configuration of the electric drive train can be analyzed. The presented method quantifies the economic performance of a change in the configuration, and gives the designer the ability to express the economic feasibility of the change as a sum of money (and a payback time) instead of a mere efficiency change. The presented method requires information on the losses in the electric drive train. This information can be supplied by a time domain simulator. Such a tool is discussed in detail in the next chapter.

Chapter 3

Simulations in the Wind Turbine Technical and Economic Analysis

This chapter builds upon the material presented in the previous chapter, which introduced a technical and economic analysis method for the assessment of the performance of a wind turbine electric power train and comparison of alternative configurations. In this chapter, first, the principles of loss modelling in a general-purpose transient simulation environment are studied. The applicability of time domain simulations to be used in connection with the economic analysis method presented in the previous chapter is tested with three (fictitious) example cases: component selection, electric drive train nominal power selection (with fixed turbine size), and high-level control principle selection in a modular low-voltage wind turbine drive. Finally, suggestions for further use cases are given.

3.1 Introduction

The previous chapter discussed the fundamentals of turning the kinetic energy of wind into electric energy and proposed a technical and economic analysis method to compare alternative configurations. It was stated that the annual energy output of a wind turbine can be calculated, if the wind speed distribution, the power curve of the turbine, and the efficiency (as a function of wind speed or power) of the electric drive train are known. The first two – wind speed distribution and properties of the turbine – were discussed in the previous chapter. However, the efficiency of the electric drive train (which appears in the title of this book) was not yet covered.

This chapter consists of two rather distinct parts. In the first part, the components of a wind turbine drive train are described, and modeling of their losses are discussed. In the second part, three different use cases of the technical and economic analysis utilizing the results of

the simulations are presented. We will begin this chapter by describing the calculation of electrical losses in general.

3.2 Calculation of Powers and Losses

Efficiency is generally defined as the ratio of output power and input power,

$$\eta = \frac{P_{\text{out}}}{P_{\text{in}}}. \tag{3.1}$$

For a wind power plant, the efficiency of the electric drive train is

$$\eta_{\text{e}} = \frac{P_{\text{pcc}}}{P_{\text{mech}}}, \tag{3.2}$$

where P_{pcc} is the power at the point of common coupling (PCC, the point where the generating plant is connected to the utility) and P_{mech} is the generator input mechanical power. Alternatively, using the loss term, this can be expressed as

$$\eta_{\text{e}} = \frac{P_{\text{mech}} - P_{\text{loss,e}}}{P_{\text{mech}}}, \tag{3.3}$$

where $P_{\text{loss,e}}$ represents the total losses of the electric drive train. Thus, for the determination of the efficiency at various operating points, a method to calculate the electric power or the losses at different points of the drive train is required.

Instantaneous electric power is, as is well known, defined as the product of a voltage accross a circuit element and the current flowing through that element,

$$p(t) = u(t)i(t), \tag{3.4}$$

where the power p, the voltage u, and the current i are generally functions of time t. If the voltage and current are sine waves with a constant frequency, the power can be calculated using phasors with the equation

$$p = \underline{u}\,\underline{i}^{*}, \tag{3.5}$$

where the asterisk (*) denotes the complex conjugate. In the commonly used three-phase system with a 120-degree phase shift between the phase voltages, the power is

$$p(t) = u_{10}(t)i_1(t) + u_{20}(t)i_2(t) + u_{30}(t)i_3(t), \tag{3.6}$$

where u_{x0} denotes the phase-to-neutral voltage of phase x. In the space vector form (peak value scaling) the instantaneous power can be expressed in various forms,

$$p(t) = \frac{3}{2}\text{Re}\{\boldsymbol{u}\,\boldsymbol{i}^{*}\} = \frac{3}{2}\boldsymbol{u}\cdot\boldsymbol{i} = \frac{3}{2}|\boldsymbol{u}||\boldsymbol{i}|\cos\varphi. \tag{3.7}$$

In practical electric drives, especially those based on power electronic converters, the voltage and current waveforms are never perfectly sinusoidal; aside from the fundamental frequency they contain to various degree harmonics, interharmonics, subharmonics, and a zero-frequency (DC) component. Furthermore, the phase sequence can be positive (L1 leading L2 leading L3), negative (L1 leading L3 leading L2), or zero (L1, L2, L3 in the same phase). Space vectors can represent all positive and negative sequence components. However, the zero sequence components of a voltage or current do not show in the corresponding space vector.

Measurements always attainable from a time-domain simulation are the phase currents and phase-to-phase voltages. Phase-to-neutral voltages are not directly available, if there is no neutral wire. A virtual star point using three identical resistors can be created, but, again, for the zero sequence voltages, the phase to virtual star point voltages would be zero. If the common-mode current does not exist, the instantaneous three-phase power can be obtained using the Aron method, which requires two phase-to-phase voltage measurements, two current measurements, and assumes that the sum of the currents equals zero Tumański (2006). Depending on the choices made in the derivation of the expression, different forms will be obtained. One option is, with time indices omitted for all quantities,

$$p = u_{31} i_3 - u_{12} i_2, \tag{3.8}$$

where p is the instantaneous power, u_{31} is the voltage measured between phases 3 (positive) and 1 (negative), u_{12} is the voltage between phases 1 and 2, and i_2 and i_3 are the phase currents of phases 2 and 3, respectively.

If the three-phase system under study does not have a neutral wire, then there is no galvanic path for the zero sequence current to flow[1]. If there is a neutral wire connected to the component under study, Equation 3.6 gives also the zero sequence power. Between these two cases, there is a third alternative, in which there is a neutral wire or ground connected to some components of the system, but not all. This kind of situation is depicted in Figure 3.1, where the generator star point and the transformer (generator side) star point are grounded. In that system, the zero sequence currents may flow through the device even if there apparently is no neutral conductor.

If, instead of power, we calculate the power loss over a component, even the contribution of the zero sequence can be detected. The component has two three-phase terminals, A and B. The phase-to-phase voltages and phase currents are measured at both terminals. Additionally, the voltages between the terminals A and B (voltages over the component) are measured. With these measurements, the loss can be expressed (Appendix A) as

$$\begin{aligned} p_{\text{loss}} =& (u_{\text{AB3}} - u_{\text{A31}}) i_{\text{A1}} + (u_{\text{AB3}} - u_{\text{AB1}} - u_{\text{A31}}) i_{\text{B1}} \\ &+ (u_{\text{AB3}} + u_{\text{A23}}) i_{\text{A2}} + (u_{\text{AB3}} - u_{\text{AB2}} + u_{\text{A23}}) i_{\text{B2}} \\ &+ u_{\text{AB3}} i_{\text{A3}}, \end{aligned} \tag{3.9}$$

where i_{An}, n $= 1,2,3$, are the phase currents at the A terminal, i_{Bn}, n $= 1,2$, are the phase currents at the B terminal, u_{A31} is the voltage between phases 3 and 1 and u_{A23} the voltage

[1] In a real system, the current may flow as a capacitive displacement current through various stray capacitances. No such mechanisms were modeled in the simulation models created for this study, however.

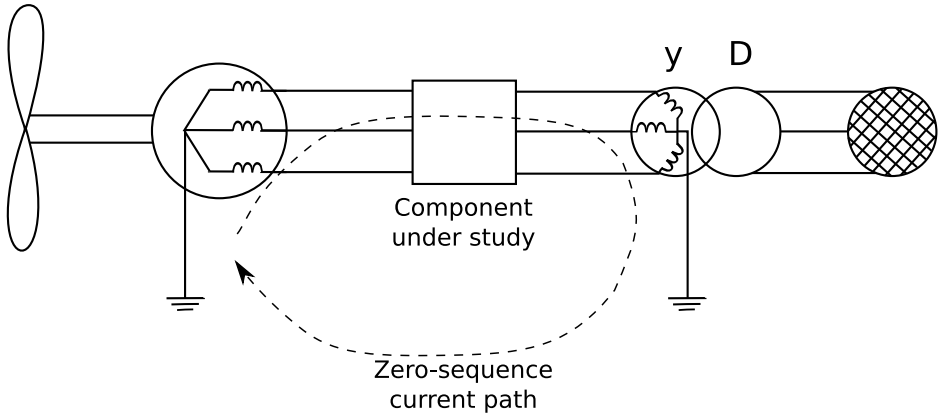

Fig. 3.1. Measuring losses in the component under study. There can be losses caused by zero-sequence currents even though the component itself does not have a neutral wire. The path for the current is formed because the star points of the generator and the transformer are grounded.

between the phases 2 and 3 at the A terminal, and u_{ABn}, n $= 1,2,3$, are the voltages over the component (A to B). The only assumption in the calculation (aside from assuming no neutral wire) is that the sum of the currents entering and exiting the component is zero (i.e., the component does not have a third terminal).

To conclude, three different methods for power and loss measurement were used,

1. Equation 3.6. Power calculation. Neutral wire (reference potential) must be available. Includes the contribution of all positive and negative sequence components as well as the zero sequence.
2. Equation 3.8. Power calculation. No neutral wire. The Aron method. Includes the contribution of all positive and negative sequence components but not the zero sequence component.
3. Equation 3.9. Loss calculation. No neutral wire. Includes the contribution of all positive and negative sequence components as well as the zero sequence.

3.3 Modeling the Losses in the Simulation

The design of a wind turbine is a very multi-disciplined task. Electrical aspects of the process include the design of the generator and other drive train components, as well as the control algorithms, the network connection, and fault tolerance. Simulations are a very useful tool analyzing many of the subproblems associated. Accurate simulation of all loss mechanisms in a subsystem would require a detailed and comprehensive model of the subsystem. Generally, however, when implementing a loss model for a simulation, the goal is to obtain a model that can take into account those mechanisms which are relevant for the analyzed case. Therefore,

the requirements of the simulator and the simulation model will differ from case to case. Modeling of high-frequency phenomena might, for example, require tuning equivalent circuit parameters based on measurements. The required bandwidth could be estimated based on a power spectrum analysis, for example.

Many papers have been published about using simulation software in the study of the behavior of the wind energy conversion system in transient situations, including network disturbances. Simulations that aim at studying the dynamics of the power system containing wind generation often use a time step significantly longer than the period of the frequencies occurring in voltage-source inverter drives and, consequently, ignore the details of how the electric drive operates. For example, Slootweg et al. (2003) have presented a general model utilizable to represent both DFIG-based and full power converter (with PM machine) based variable speed turbines. In their simulations, a time step of 10 ms is used, and the generator is modeled as a torque source. Akhmatov et al. (2000) present a thorough analysis of the interaction between the power network and a wind turbine equipped with a constant speed induction generator. Their study concentrates on the modeling of the turbine itself, including the mechanical resonances of the turbine rotor. In another article largely by the same authors (Akhmatov et al., 2003), the modeling of a wind farm of 80 such wind turbines (2 MW each) is discussed. In both papers, the electric drive train consists of the generator only, and the generator is modeled basically as a speed-torque curve. The effects of different generator parameter (resistances, inductances) selections on the stable operating area of the generator are analyzed, but the efficiency of the electric drive train is not considered.

Furthermore, a lot of scientific contribution has been made recently in the field of fault ride-through studies. Seman et al. (2006) compared three different approaches to voltage dip ride through capability of a DFIG-based turbine. They found out that simplifying the turbine model to a constant speed, constant torque representation did not have a significant effect on the results. Furthermore, they note that a FEM (finite element method) model of the generator can be used in conjunction with the transient simulator to model high-frequency phenomena such as skin effect. This did not have a significant effect on the transient study results in this case. In the efficiency analysis, skin and proximity effect as well as saturation might have to be taken into account in some cases. This cannot be done using the standard two-axis model of an electric machine. Modified two-axis models with parallel current paths in the stator winding have been developed to take into account skin effect (see e.g. (Thiringer, 1996)), and these could be used as an alternative to FEM modeling. Generally, it can be concluded that simulators and models utilized in FRT studies are more suitable to the efficiency analysis than those applied in power system dynamics studies.

There is a vast array of commercial simulation tools available that can be utilized to simulate the electric behavior of a wind turbine. Some, such as PSS/E and PSCAD, are more suitable for simulating the power network and its interactions with the generating plant, whereas others, such as Saber or PSpice, are focused on simulating electronics (Akhmatov et al., 2000, Lund et al., 2005, Iov et al., 2002). MATLAB/Simulink, on the other hand, is a general purpose simulation platform for simulating dynamic systems. It can be used stand-alone, or in connection with other software. Uski et al. (2004) have demonstrated the use of Simulink in connection with PSCAD and ADAMS (a mechanics simulator). Iov et al. (2004) presented a

wind power simulation platform with MATLAB/Simulink as the basic modelling tool that can be connected to other simulation software (Saber, HAWC, DIgSILENT). In 2008, a project was started at Lappeenranta University of Technology in co-operation with The Switch Ltd. to develop a MATLAB/Simulink-based tool for the simulation of wind power electrical systems. The tool, called SwitchTool, includes models for transformers, filters, bridges, machines and the like as well as the required generator and network control blocks (Luukko et al., 2009b). The models utilize standard Simulink blocks and blocks from the SimPowerSystems extension. SwitchTool is capable of simulating both fixed-speed and variable-speed systems, and aims to be user friendly and extensible. The tool can be used for instance to develop control algorithms and analyze the behavior of the generating plant in the case of a network disturbance (protection, regulations compliance).

As a part of SwitchTool, a dedicated tool for efficiency analysis was developed. The tool simulates a SwitchTool model in specified operating points and calculates the losses and the exported power. The calculations are defined by the user. Likewise, the operating points (in the form of wind speeds) are specified by the user. Figure 3.2 illustrates the parts of the analysis system. The procedure for comparing two alternative configurations could be the following:

1. Create models for the compared configurations. SwitchTool blocks can be used (they utilize both plain Simulink blocks and blocks from the SimPowerSystems extension). Also, other blocks could be used. Ideally, the models (or one of them) already exist and are used for other purposes.
2. Select powers and losses to be recorded. Add required power/loss measurement blocks (found in the SwitchTool library). Create expressions for the required calculations (calculation of the total efficiency); input to SwitchToolEff as an XML file.
3. Select operating points; input to SwitchToolEff as an XML file.
4. Allow SwitchToolEff to run the simulations for the selected operating points and calculate the efficiencies. Repeat for all compared configurations.
5. Import efficiencies to the economic analysis Excel sheet (discussed in the previous chapter). Select the wind data. Calculate analysis.

A power/loss calculation block was implemented in SwitchTool. This block can be used to calculate and export the instantaneous power at a node (using Equation 3.8) or the loss over a component (Equation 3.9) with a PUI_loss block connected to both terminals of the component. The average values of losses are calculated by SwitchToolEff after the simulation is finished. Since the total efficiency is calculated from the generator input mechanical power to the electrical power exported to the network, also the mechanical power needs to be calculated. Since the generator load torque and the rotation speed are known, the mechanical power can be calculated using the equation

$$P = \omega T, \tag{3.10}$$

where P is the power, ω is the angular frequency of the rotation ($\omega = 2\pi n/60$, where n is the rotation speed in RPM), and T is the torque. An example of models used with SwitchToolEff can be found later in this chapter, for example in Figure 3.7.

The value of simulations in the technical and economic analysis depends on the loss mech-

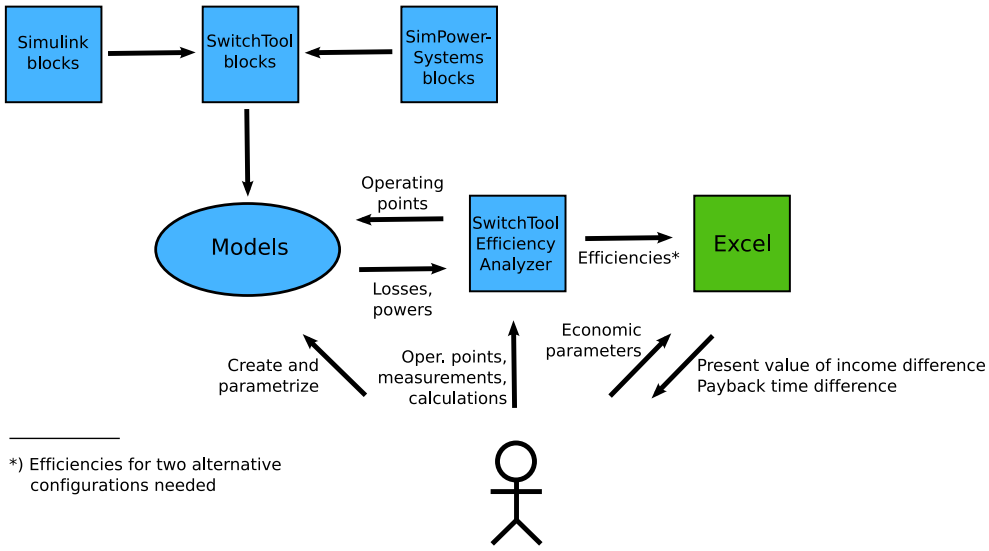

Fig. 3.2. Simulation and analysis software as a block diagram.

anisms that show in the simulations. The following sections detail the loss mechanisms in a wind power drive based on a permanent magnet generator and a full-power converter, which is the type of the wind power drive in all of the simulation examples presented in this chapter. An example of the main components of the electric power train of a such system is presented in Figure 3.3. In the figure, the wind turbine feeds mechanical power to the PM generator, which is connected to the frequency converter through a generator filter. The converter is connected to the power network through the transformer, and there is a network filter between the transformer and the converter. The applicability of the utilized simulator to the analysis of each loss mechanism is discussed in connection with the discussion of the loss mechanism.

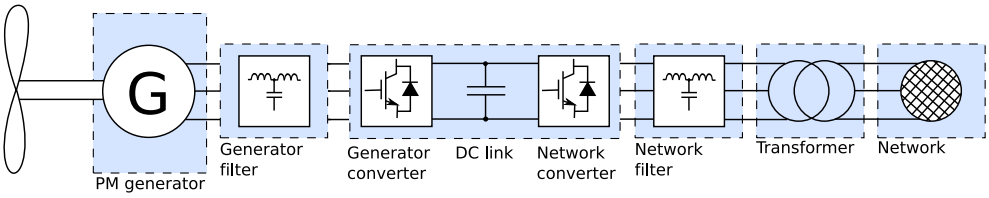

Fig. 3.3. Main components of a wind power drive train based on a PM generator and a full power converter. The generator and network filters are shown here as LCL filters, but they could be of any type, or there might be no generator filter at all. Switchgear and protective devices not shown.

3.3.1 Generator

Losses in an electrical machine generally consist of copper losses, iron losses, mechanical losses, and additional losses (Pyrhönen et al., 2008). Copper losses (or, Joule losses) are resistive losses caused by current flowing in the windings of the machine. For a three-phase machine,

$$P_{\mathrm{Cu}} = 3I^2R, \tag{3.11}$$

where R is the resistance of one winding. In principle, copper losses are straightforward to model by including a stator resistance in the generator model. However, the resistance is generally frequency-dependent; the resistance increases with increasing frequency as a result of skin effect and proximity effect. Since the generator is supplied by a frequency converter, the generator voltage contains harmonics of the fundamental frequency component. Using a constant stator resistance in the generator model, copper losses caused by both the fundamental and the harmonics will be captured. However, the frequency-dependent phenomena will be ignored. The rotation speed of a gearless wind power turbine is relatively small (approx. 10–30 RPM). Therefore, the supply fundamental frequency can also be low (although it may also be higher, over 50 Hz). It can be assumed, however, that the constant resistor model is sufficient in many cases. Copper losses are the dominant loss mechanism in such slowly rotating PM generators (see, e.g., simulation results by Polinder et al. (2006) and Tan et al. (2005)).

The stator resistance is also a function of temperature and thus dependent on the operating point of the generator and the ambient temperature. The temperature of the winding can be estimated, if the power dissipation is known and there is a thermal model of the generator. Since the power dissipation (the losses) is a function of temperature, the process is iterative. No thermal modelling was included in the simulator, and thus the effect of temperature was ignored. The effect of temperature could, however, be taken into account either by manually adjusting the resistance (e.g. for different ambient temperatures) or including a thermal model in the model with the power loss as an input and stator resistance as an output.

Iron losses (core losses) are usually the second most important loss mechanism in a PM generator. Iron losses consist of two parts: hysteresis losses ($\propto f$) and eddy current losses ($\propto f^2$) (Hanselman, 2003). To represent the core losses of a PM machine, a core loss resistor R_{c} is added to the machine model and equations. Wijenayake and Schmidt (1997), for example, present a modified $\mathrm{d^e} - \mathrm{q^e}$ equivalent model for a PM machine starting from a per-phase equivalent circuit with the core loss resistor in parallel with the internal voltage source. Model parameters (magnetizing inductances, stator resistance, voltage and current sources) are modified to include the effect of the core losses. For example, the Simulink model of a PM generator included in the Wind Turbine Blockset developed by Aalborg University and RISØ National Laboratory includes an optional iron loss resistor (Iov et al., 2004). The resistor value is a function of the mechanical rotation speed of the generator thus taking into account the core loss variation as a function of electrical frequency. However, the effect of harmonics is more difficult to take into account in this model. For more accurate representation of the iron losses, a FEM model can be used (Mi et al., 2003), and the model can be combined with a time domain simulator (Seman, 2006). Iron losses and saturation may have to be taken into account when the compared systems differ in terms of for example harmonic content in the

generator terminal voltage. Notwithstanding the difficulties in iron loss modeling, it can still be said that it is more straightforward to do using the simulation-based loss calculation than the analytical one. However, in the case examples presented in this chapter, it was assumed that the iron losses in the compared configurations were negligible in comparison with copper losses, and they were not included in the models.

Mechanical losses and additional losses comprise losses for instance from friction ($\propto \omega_{\mathrm{mech}}$), generator cooling and electromagnetic losses other than resistive and iron losses (Pyrhönen et al., 2008). Due to their diversity, they are difficult to estimate and model. However, their effect is often insignificant compared with copper and iron losses. For example, the IEC 60034-2:1996 standard (IEC, 1996) defined additional losses to be equal to 0.5 % of the estimated input power at rated load.

The models used in the simulation included only copper loss resistance, and thus no other loss mechanisms were taken into account. Therefore, in the simulations, it was assumed that the iron losses (as well as friction losses and additional losses) are insignificant compared with the copper losses, and that the compared generators do not differ significantly in terms of iron loss characteristics. These might be justifiable assumptions, especially if the generators are slowly rotating and the voltage waveforms (in terms of harmonic content) in their terminals are relatively similar. If the simulator is used for comparing generators with different iron loss characteristics, then the generator model has to be modified to include an iron loss resistance in the machine equations. For accurate modeling, again, measurements of actual components in different operating points would be needed.

3.3.2 Filters

Loss mechanisms in filter inductors are rather similar to those in the generator; losses occur in the conductors (copper loss) and the core (hysteresis loss, eddy current loss). The inductors can be modeled using some of the standard Foster or Cauer equivalent circuits. Figure 3.4 presents a series-Foster equivalent circuit of an inductor. The circuit consists of the DC resistance and N elements in series, each of the elements consisting of an ideal inductor and an ideal resistor in parallel. The idea of the model can be qualitatively understood by considering the circuit at different frequencies. With a DC input, current flows through the DC resistance and through the series-connected ideal inductors (which represent a zero impedance at DC). The loss in this resistance corresponds to zero-frequency (no skin effect) copper loss. As the input frequency is increased, more and more current is diverted to the resistances in parallel with the inductances thus increasing the losses. The number of segments in the model must be selected by the user. The model parameters are most accurately defined by measurements. When based on a loss measurement, this kind of a model models the losses of the inductor as a function of frequency, and the loss modeled contains contribution of all frequency-dependent loss mechanisms (copper loss increase caused by skin effect and iron losses).

This equivalent circuit was used in all the simulations presented in this chapter. As no real filter components or data were available, a very simple version of the circuit was used. The circuit consisted of the DC resistance with one RL element in series. The value of the in-

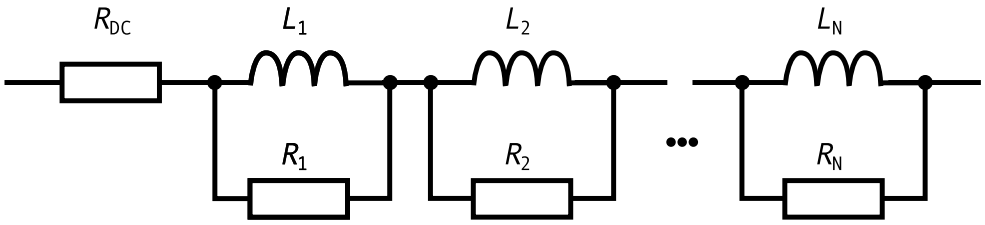

Fig. 3.4. Foster series equivalent circuit with N elements for an inductor.

ductance was taken as the nominal inductance of the inductor, and the parallel resistance was selected such that it is approximately equal to the reactance ($X_L = \omega L$) of the inductor at a frequency of tens of kilohertz to a hundred kilohertz.

In addition to the inductors, also the filter capacitors are lossy components. A commonly used simple model of a capacitor is the series connection of an ideal capacitor (equal to the nominal capacitance), an ideal resistor (the equivalent series resistance, ESR), and an ideal inductor (the equivalent series inductance, ESL), shown in Figure 3.5. In this work, the capacitors were modeled simply as an ideal capacitance with the ESR in series (ESL equal to 0).

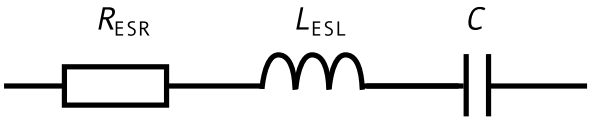

Fig. 3.5. RLC equivalent circuit of a capacitor.

The voltage waveforms in the terminals of a voltage source converter contain, in addition to the fundamental frequency, various higher-frequency components extending up to the megahertz range (Skibinski et al., 1999). The simulation-based approach, although not entirely trivial, is thus nonetheless more straightforward than forming an analytical expressions for the losses in a filter.

3.3.3 Power Electronic Converter

The converter consists of a generator-side converter and a network-side converter, which are connected back-to-back by the DC link. The DC link can be a voltage source (capacitor) or a current source (inductor). Here, it is assumed that the DC link is of the voltage source type, but nothing prevents the simulation of current source inverters. The converter is assumed to be a four-quadrant one with both the generator and network converters implemented using IGBT (insulated gate bipolar transistor) switches.

Table 3.1. Switching energies as a function of load current direction (I_L positive towards the load) and gate command change (1: upper leg conducting; 0: lower leg conducting).

	$0 \rightarrow 1$	$1 \rightarrow 0$
$I_L > 0$	E_{on}	E_{off}
$I_L < 0$	E_{off}	E_{on}

IGBT Bridges. An IGBT-based power electronic switch contains an IGBT transistor and an antiparallel diode. The losses of the switch can be divided into two parts: conduction losses and switching losses. Conduction losses can be modelled with an on-state resistance and voltage drop over the device. Modeling the switching losses is more difficult with the simulation environment and models used in the present work. The IGBT models may enable a simulation using non-ideal switching waveforms. However, switching the transistor or the diode on or off is a very fast phenomenon (in the order of hundreds of ns or less) compared with the simulation time step used (ca. 1 µs). Therefore, the switching losses cannot directly be contained in the simulation results, but the switching times must be set to zero and the switching losses have to be obtained by other means.

The switching losses can be obtained by simulating the modeled system over a short period with a small time step (separately from the main simulation, solely to obtain the switching losses). Because of the limitations of the particular simulation environment, this could not be done. Switching losses can also be estimated based on the information found in the data sheet of the device, which typically contains a graph of switching energies as a function of device (collector) current for one or more device voltages. Switchings can be grouped into two cases:

1. The IGBT turns on and the antiparallel diode turns off. Switching energy E_{on}.
2. The IGBT turns off and the antiparallel diode turns on. Switching energy E_{off}.

The diode turn-on energy is typically insignificant compared with the other energies, and can therefore be assumed zero (Kouro et al., 2008). Therefore, switching energies can be expressed as (Kouro et al., 2008)

$$E_{on} = E_{IGBT,on} + E_{diode,off} \tag{3.12}$$

$$E_{off} = E_{IGBT,off} \tag{3.13}$$

When a gate command changes, the associated loss (E_{on} or E_{off}) depends on the direction of the change ($0 \rightarrow 1$, $1 \rightarrow 0$, 1 denoting "upper leg switch on, lower leg switch off" and 0 correspondingly "upper leg switch off, lower leg switch on") and the direction of the load current in the phase. If the current flowing towards the load is denoted positive, the switching energies have values presented in Table 3.1 (based on the work by Kouro et al. (2008)).

In the simulator, a Simulink block was implemented to record switching energies based on the logic presented in Table 3.1 and the switching energy values taken from the data sheet (as a function of collector current). The energies are converted to switching loss power by

the efficiency analysis tool. Switching waveform measurements can be used to obtain a more accurate estimate of the switching energies.

DC Link Circuit. The DC link capacitor can be modeled using the same models as in the case of filter capacitors. In the simulations, a simple ideal capacitance with an equivalent series resistance (ESR) was used. Similarly, if there is a DC filter inductor in the circuit, it can be modeled using some of the standard inductor models (Foster/Cauer). In the simulations, no DC link inductor was used.

3.3.4 Transformer

Transformer loss mechanisms are generally similar to those found in inductors and generators (for transformer modeling, see e.g. (de León and Semlyen, 1994)), that is, copper losses and core losses. In the simulations, the symmetrical transformer model provided by SimPowerSystems was used. Copper losses were modeled by the winding resistances, and the other loss mechanisms were ignored.

3.4 Example Cases

This section presents three example cases of the usages of the proposed method. All cases are fictitious (not based on any existing or planned installation); their intended meaning is to illustrate some of the possible uses of the method. The first case involves two alternative component selections, the second case two alternative electric drive trains, and the third case two alternative high-level control principles of a modular converter.

Component prices used in the calculations aim to be in a realistic order of magnitude, but it should be stressed that the results of the cases themselves are not the point of the section. Rather, the point is to test and illustrate the usage of the method in different kinds of situations. All simulations presented were run with a discretization sample time 1 μs and variable step Dormand-Prince ODE45 solver. In addition to the three cases, other possible use cases are suggested.

3.4.1 Case 1: Component Selection

This case tests the usage of the simulation-based approach in analyzing alternative component selections. The case shows how the effect of different component selections shows in the economic analysis, that is, what is the monetary value of the component change. This value can be used by the designer to gauge the feasibility of the alternatives.

The drive under study is, as in all the other cases, based on a permanent magnet synchronous generator (PMSG) and a full power converter (block diagram presented in Figure 3.6). The alternative components studied are two different IGBT modules. The modules differ in terms of nominal current, losses, and, presumably, price. The basic question that the designer wants answered is ”how much more can the component with lower losses cost in order to be more feasible?” The analysis is calculated for three different wind conditions, described later.

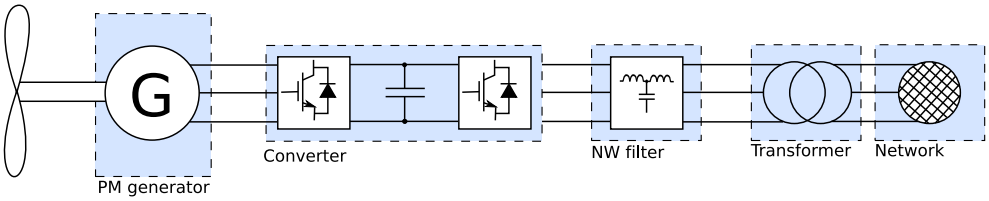

Fig. 3.6. Block diagram of the simulated system.

A simulation model was created for Simulink utilizing the SwitchTool models described by Luukko et al. (2009b). A screenshot of the model with explanatory labels is presented in Figure 3.7. Blocks indicated by blue arrows are specific to the loss calculation. The calculated quantities are the mechanical power, the generator electric output power, converter losses (switching losses and others), network filter losses, transformer losses, and power at the point of network connection. In addition to adding the loss calculation blocks, no other modifications of the basic simulation model were required for the efficiency analysis. Similar models were created also for the other cases. The model parameters are discussed in the following section.

Drive Train Parameters

The turbine specifications are based on the 1.5 MW direct drive configuration (generator stator outside diameter 5.3 m) analyzed by Bywaters et al. (2004). Some of the parameters and characteristics of the drive components and other simulation blocks are presented in Table 3.2. As can be seen, the only differing parts are the network and generator converters. Switching losses were modeled as described in the previous chapter. Switching loss values for different device currents (at junction temperature $T = 125\,^{\circ}\mathrm{C}$) were tabulated from the datasheets (Dynex Semiconductor, a,b).

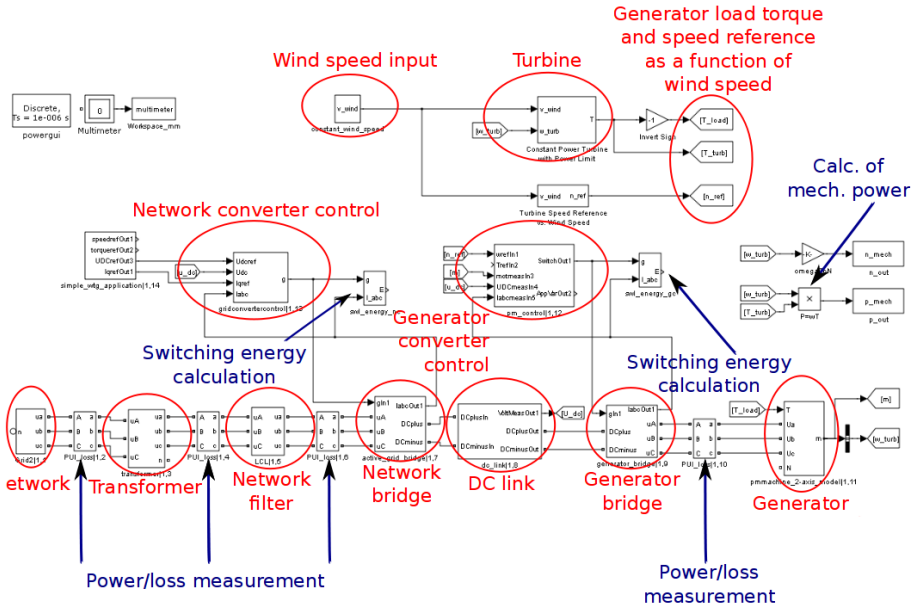

Fig. 3.7. Screenshot of the Simulink model used. Blue arrows denote blocks specific to the loss calculation.

Table 3.2. Parameter values and other properties of the compared configurations, Case 1. In connection with the switching losses, the nominal current I_{nom} is the nominal current of the module (1600 A/1800 A). Transformer parameters are non-reduced.

		Configuration 1 ("Basic")	Configuration 2 ("Oversized")
Turbine	nominal power, MW	1.55	
	nominal wind speed, m/s	12	
	cut-in wind speed, m/s	3	
	cut-out wind speed, m/s	25	
	nom. rotation speed, RPM	19.6	
	diameter, m	70.5	
Generator	nominal apparent power, MVA	1.7	
	nominal power, MW	1.55	
	nom. voltage (line-to-line), V	690	
	nominal frequency, Hz	12.77	
	pole pairs	39	
	stator resistance, mΩ	15	

Continued on the next page

Table 3.2 – Continued

		Configuration 1 ("Basic")	Configuration 2 ("Oversized")
Converter	DC link capacitance, mF	57.6	57.6
	DC link capacitor ESR, mΩ	1.0	1.0
	switches	IGBT + diode	IGBT + diode
	switch module nom. current, A	1600	1800
	switching freq., network/gen., kHz	3.6/3.0	3.6/3.0
	IGBT forward voltage, V	2.6	2.6
	diode forward voltage, V	2.1	2.6
	on-state resistance, mΩ	0.27	0.09
	IGBT switch-on loss at I_{nom}, mJ	150	175
	IGBT switch-off loss at I_{nom}, mJ	350	390
	diode switch-on loss at I_{nom}, mJ	0	0
	diode switch-off loss at I_{nom}, mJ	160	195
Network filter	type	LCL	
	network-side (NS) inductance, µH	62.8	
	converter-side (CS) inductance, µH	105.2	
	capacitance, mF	0.53	
	total DC resistance, mΩ	4	
	NS inductor parallel resistance, Ω	40	
	GS inductor parallel resistance, Ω	66	
Transformer	nominal power, kVA	2000	
	nominal frequency, Hz	50	
	nominal voltage (HV/LV), V	20 000/690	
	vector group	Dyn11	
	HV resistance, Ω	0.02	
	HV inductance, mH	0.132	
	LV resistance, mΩ	2.0	
	LV inductance, µH	7.0	
	magnetization resistance, Ω	220 000	
	magnetization inductance, H	100	
Network	nominal line-to-line voltage, kV	20	
	nominal frequency, Hz	50	
	3-phase short circuit power, MW	100	
	reactance/resistance ratio	6	

Table 3.3. Weibull parameters of the wind speed distributions used in the simulation. Data for Bogskär from (Tammelin, 1991), others from (Finnish Wind Atlas 2009).

Location	c	k	Height, m	Notes
Bogskär	9.1	2.41	50	Open sea.
Enontekiö	9.2	2.2	100	Inland. Hilly terrain with no trees.
Lappeenranta	7.4	2.6	100	Inland, < 1 km from lake Saimaa.

Table 3.4. Bins and their durations used in the simulation.

Start	End	Midpoint	Duration			Notes
			Bogskär	Enontekiö	Lappeenranta	
0	3	1.5	584	714	799	Stopped
3	5	4	1259	1302	1855	
5	7	6	1768	1681	2420	
7	9	8	1841	1685	2027	
9	11	10	1503	1387	1129	
11	12	11.5	556	534	270	
12	25	18.5	1249	1455	261	Lim. to nom. power
25	30	27.5	0	1	0	Stopped

Wind Speed Distribution

The analysis was calculated with three wind speed distribution representing different types of locations in Finland. The Weibull coefficients for the locations are given in Table 3.3. The first location is based on the data given by Tammelin (1991) for the Bogskär weather station situated in the open sea approximately 60 km SSE from the city of Mariehamn in the Åland Islands off the south-western coast of mainland Finland. The parameters are taken at the mast heigth of 50 meters. The second location is Enontekiö in the extreme north-west of Finland. The landscape is generally hilly and open, trees being stunted or missing altogether. The mast height is taken as 100 m. The data were taken from the new Finnish wind atlas published online in November 2009 (Finnish Wind Atlas 2009). The third location is Lappeenranta in the south-east of Finland roughly 100 km from the southern coast. The wind conditions in the location are affected by the proximity of the largest lake in Finland, lake Saimaa. The coefficients were taken from the Finnish Wind Atlas 2009. Graphs of the wind speed distributions are presented in Appendix B.

The distributions were divided into bins of non-equal widths by an Excel program as depicted in Table 3.4. Bin midpoints were used as the wind speed value for the corresponding bin in the simulation. Thus, the simulation was run for wind speeds 4, 6, 8, 10, 11.5 and 18.5 m/s. Since the power is limited to nominal, 18.5 m/s corresponds to the nominal wind speed, 12 m/s.

Table 3.5. Total efficiencies of the drives in the simulated operating points.

	Efficiency	
v_w [m/s]	Conf. 1	Conf. 2
4	0.783	0.805
6	0.926	0.927
8	0.943	0.943
10	0.926	0.927
11.5	0.908	0.909
12-25	0.901	0.901

Table 3.6. AEO for the compared configurations in different wind conditions with the corresponding AEO differences.

Location	$E_{AO,1}$, MWh	$E_{AO,2}$, MWh	ΔE_{AO}, MWh
Bogskär	4885	4891	6
Enontekiö	4970	4976	6
Lappeenranta	3021	3026	5

Simulation Results

The total efficiencies of the drives in the simulated operating points are given in Table 3.5. The annual energy outputs (E_{AO}) of the compared configurations and their differences (ΔE_{AO}) were calculated using the wind speed distributions discussed above. The AEO calculation was performed using the bin method (using the bin midpoint wind speed as the wind speed value and assuming the efficiency constant over the whole bin) with bin width 0.5 m/s. The results are given in Table 3.6.

Economic Analysis

The alternative configurations were compared applying methods presented in section 2.4. The question was: "How much more can Configuration 2 cost than Configuration 1 in order to be more feasible?" To answer this question, the difference of the generated revenue was calculated using Equation 2.24 with $\Delta C_i = 0$ and ΔE taken from Table 3.6. Payback time differences were not calculated in this case. In the calculation, the values presented in Table 3.7 were used. The results are presented in Table 3.8.

With these values, it was obtained that the maximum investment cost increase is approximately 3 000–4 000 €, which corresponds to 0.2–0.4 % of the investment cost. The investment costs were taken directly from the report by Bywaters et al. (2004). The estimate is from the year 2004, the dollar-to-euro conversion has been made with simply replacing the unit (i.e., exchange rate 1.000), the prices do not include the price of the transformer or the network filter, and the estimate is the manufacturing cost, not the sales price. All these factors contribute to uncertainty in the investment cost. However, it should be noted that in this kind

Table 3.7. Parameters used in the economic analysis.

Parameter	Value	Notes
Interest rate (p)	8 %	
Time to commissioning (t_0)	2 years	
Turbine life (T)	20 years	
Investment cost (c_i)	1 092 800 €	Bywaters et al. (2004) estimate with 1 $=1 €
Tariff price of electricity ($\overline{\pi}_1$)	83.50 €/MWh	Proposal for the Finnish tariff
Tariff duration (t_1)	12 years	Proposal for the Finnish tariff
Market price of electricity ($\overline{\pi}_2$)	30.00 €/MWh	

Table 3.8. Results of the analysis: difference of the generated revenue when selecting Configuration 2 instead of Configuration 1.

Wind Profile	ΔJ, €(%)
Bogskär	4 022 (0.37)
Enontekiö	4 159 (0.38)
Lappeenranta	3 168 (0.29)

of an analysis the investment cost itself is not needed; it was included here only for normalizing the maximum investment cost increase. The investment costs are discussed in more detail in connection with the next case.

The sensivity of the results to changes in parameter values can be estimated with a sensitivity analysis. To illustrate, the values of the partial derivatives of the income change expression (Equations 2.28–2.35) for the Bogskär case (Table 3.7, $\Delta E_{\mathrm{AO}} = 6$ MWh) are presented in Table 3.9. The values in the table give an estimate of the change in the income difference ΔJ (Equation (2.27)) when a parameter is changed (change in € per amount in parentheses).

It can be seen that the result is very sensitive to changes in the annual energy output difference. The sensitivity of the AEO to changes in the wind conditions were analyzed previously, see

Table 3.9. Sensitivity analysis of the income difference ΔJ (Equation (2.27)). Localized to the point defined by the parameter values in Table 3.7 and $\Delta E_{\mathrm{AO}} = 6$ MWh.

Changed Parameter	Change in ΔJ, €
Interest rate (p)	-612 (%-unit)$^{-1}$
AEO difference (ΔE_{AO})	808 (MWh)$^{-1}$
Turbine life (T)	63 (year)$^{-1}$
Time to commissioning (t_0)	-236 (year)$^{-1}$
Inv. cost difference (Δc_i)	-1 (€)$^{-1}$
Tariff price ($\overline{\pi}_1$)	51 (€)$^{-1}$
Tariff duration (t_1)	166 (year)$^{-1}$
Market price of electricity ($\overline{\pi}_2$)	21 (€)$^{-1}$

Table 3.10. Sensitivity of the AEO difference to changes in Weibull parameter values.

Wind Profile	$\frac{\partial \Delta E_{\mathrm{ao}}}{\partial c}$, MWh/(ms^{-1})	$\frac{\partial \Delta E_{\mathrm{ao}}}{\partial k}$, MWh
Bogskär	0.8	-0.3
Enontekiö	0.7	-0.2
Lappeenranta	0.4	-0.4

Table 3.11. Absolute maximum errors in the Weibull parameters.

Wind Profile	c, m/s	k	AEO
Bogskär	9.1 ± 0.9	2.41 ± 0.24	6 ± 0.8
Enontekiö	9.2 ± 0.9	2.2 ± 0.22	6 ± 0.7
Lappeenranta	7.4 ± 0.7	2.6 ± 0.26	5 ± 0.4

Equations 2.15 and 2.16. Now that we are analyzing the sensitivity of the AEO difference instead of the plain AEO, these equations can be rewritten as

$$\frac{\partial \Delta E_{\mathrm{ao}}}{\partial c} = T \frac{k}{c} \sum_{i=0}^{\mathrm{N}-1} \left[\left(\frac{v_{i,\mathrm{l}}}{c} \right)^k \exp\left(- \left(\frac{v_{i,\mathrm{l}}}{c} \right)^k \right) - \left(\frac{v_{i,\mathrm{h}}}{c} \right)^k \exp\left(- \left(\frac{v_{i,\mathrm{h}}}{c} \right)^k \right) \right] \Delta P_{\mathrm{e},i}, \tag{3.14}$$

$$\frac{\partial \Delta E_{\mathrm{ao}}}{\partial k} = T \frac{k}{c} \sum_{i=0}^{\mathrm{N}-1} \left[\left(\frac{v_{i,\mathrm{h}}}{c} \right)^k \exp\left(- \left(\frac{v_{i,\mathrm{h}}}{c} \right)^k \right) \ln\left(\frac{v_{i,\mathrm{h}}}{c} \right) - \left(\frac{v_{i,\mathrm{l}}}{c} \right)^k \exp\left(- \left(\frac{v_{i,\mathrm{l}}}{c} \right)^k \right) \ln\left(\frac{v_{i,\mathrm{h}}}{c} \right) \right] \Delta P_{\mathrm{e},i}, \tag{3.15}$$

where $\Delta P_{\mathrm{e},i}$ is the electrical power difference between the configurations in bin i. The values of the partial derivatives were calculated for each of the wind profiles. Table 3.10 presents the results.

Let us assume that both of the Weibull parameters have an error of 10 %. Furthermore, let us for now assume that the electric power (mechanical power times the total efficiency) exported to the network is correct for all bins. This gives the absolute Weibull parameter values given in Table 3.11. Table 3.11 also lists the AEO errors with these assumptions.

If the two compared cases share similar wind conditions (as in this case), then the AEO difference can be written as

$$\Delta E_{\mathrm{ao}} = \sum_{i=0}^{\mathrm{N}-1} \Delta\eta(v_i) P(v_i) T_i, \tag{3.16}$$

where $\Delta\eta(v_i)$ are the efficiency differences for different wind speeds (obtained from simulations). Assuming that the mechanical power P is known exactly and keeping the Weibull parameters and thus the bin durations T_i constant, it can be seen (applying the triangle inequation, $|x+y| \leq |x| + |y|$) that the error in ΔE_{ao} is less than or equal to the sum of the errors in each bin,

$$|\Delta(\Delta E_{\mathrm{ao}})| \leq \sum_{i=0}^{\mathrm{N}-1} |\Delta(\Delta\eta(v_i)) P(v_i) T_i|. \tag{3.17}$$

Table 3.12. Annual energy output differences for the three locations, with tolerances.

Wind Profile	AEO	Max. error, %
Bogskär	6 ± 1.8	30
Enontekiö	6 ± 1.8	30
Lappeenranta	5 ± 1.3	26

Thus, for example, if each of the efficiency differences can be assumed to be known with an accuracy of 20 %, then the maximum error in the AEO difference caused by this is 20 % as well. Continuing the previous example, the lower and upper limits of the AEO difference presented in Table 3.11 can be expanded to values given in Table 3.12. The assumptions were that the maximum error in the Weibull parameters is 10 % and the maximum error in the efficiency differences was 20 %. Furthermore, the two errors were calculated independent of each other (assuming the other variable known).

It can be concluded that the AEO differences can be assumed to be known (in this case) with an accuracy of approximately ± 2 MWh or better. This would create a maximum error of approximately 1 000–2 000 € in the difference of the present values of the generated income of the compared configurations, which corresponds to roughly 20–50 %.

Looking at Table 3.9, we can see that also the interest rate p has a relatively large influence on the present value of the income difference, ΔJ. Increasing interest rate will decrease ΔJ. Therefore, selecting a high interest rate will favor Configuration 1. Changes of approximately 2–4 %-unit would be required to create a similar effect on ΔJ as the uncertainty of the AEO difference calculated above.

With this kind of a tariff, the tariff price and duration are known at the investment moment. The market price of electricity after the tariff period does not have a significant effect on the analysis result. The investment cost difference can be expected to be reasonably well known to the turbine manufacturer. The time to commissioning is also known with an accuracy of one to two years, and the turbine life does not have a significant impact on the result.

It can thus be concluded that the two significant contributors to the uncertainty in the analysis result are (in this case) the uncertainty in the AEO difference and the future interest (and inflation) rate. Uncertainty in the AEO difference is caused both by uncertainty in the future wind conditions and the uncertainty in the efficiency differences. The former can never be totally eliminated, since there is annual variation in the wind conditions. Accurate measurement data are needed to minimize that effect. The latter can, in principle, be eliminated very well with good simulation models. The models used in this example case are far from perfect, and that they must be, since there are no real configurations which they would attempt to model. With actual components and configurations, more accurate models could be constructed.

Finally, it could noted that although the income differences obtained in this example are small, less than 5 000 €, the cumulative effect might be significant. In 2008, the new installed wind power capacity was 27 GW (Global Wind Energy Council). This corresponds to approximately 18 000 wind turbines like the one discussed in the example. So, although

the maximum cost increase in this example was less than 5 000 €, the great number of new installations scales this to 90 million € globally.

Conclusion

This case demonstrated the utilization of the simulation-based approach to the output energy calculation in the technical and economic analysis of a wind turbine electric drive train. Two alternative IGBT module selections were analyzed in three different wind conditions. An estimate was obtained for the monetary value of selecting an oversized module instead of the nominally sized one. This value depends on the wind conditions, and can be used by the designer to gauge the feasibility of component selections. Loss calculation blocks were added to simulation models utilized in the study of control algorithms and fault ride-through; no other modifications were made.

A benefit of the simulation-based approach over analytic calculation of losses is the fact that voltage waveforms in the simulation resemble, depending on the quality of the models, waveforms occuring in real systems. Therefore, loss contribution from all frequencies could be included in the calculation. However, models applied in the case did not include mechanisms to take into account some frequency-dependent phenomena, such as skin effect in the generator windings. This kind of phenomena would nonetheless be more straightforward to include in the calculation using the simulation-based approach than analytic calculation of losses. Simulation model development is required if more accurate loss figures are needed.

Another significant benefit of the simulation-based approach is the fact that the effect of the control principle of the generator can be taken into account. In this example, the control method applied was the standard $i_\mathrm{d} = 0$ control. If there were alternative implementations of the generator control, the different control blocks could be the components under study.

It can be concluded that the simulation-based approach is very useful in this kind of a study. The electric drive train must be considered as a whole, where changes in one component may result in changes in losses of other components. It is more straightforward to take this kind of interactions into account by using the simulation-based approach than it is using analytic calculation of losses. A simulation of this kind can be used to refine component selections after the basic topology and size of the wind energy conversion system have been decided upon.

3.4.2 Case 2: Electric Drive Train Sizing

In the second case, the simulation-based approach is tested in a site matching-type problem. Site matching of wind energy conversion systems has been traditionally done ignoring the effect of the electric drive train, as was discussed in the previous chapter. This case example aims to test if the inclusion of the electric drive train could have an effect on the analysis.

The example problem is partial site matching in the sense that the size and other properties of the turbine are fixed. The nominal power of the turbine is 2 MW. However, the company (wind power manufacturer or integrator) has at its disposal full power converters with ratings of 1.5 MW and 3 MW, and the generator power can be selected to match the power of the turbine or the converter. Thus, two different configurations can be offered to the customer:

- **Configuration 1** (undersized): 2-MW turbine, 1.5-MW generator, 1.5-MW full power converter
- **Configuration 2** (oversized): 2-MW turbine, 2-MW generator, 3-MW full power converter

With configuration 1, the power output of the 2-MW turbine must be limited to 1.5 MW by blade pitch control, whereas with configuration 2, the full nominal output power of the turbine can be fed to the converter. Figure 3.8 illustrates the output power of a 2-MW turbine as a function of wind speed without power limitation (solid line) and with power limited to 1.5 MW (dashed line).

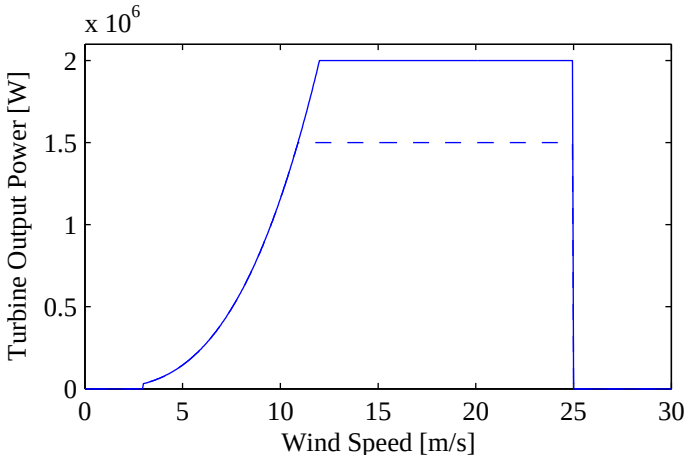

Fig. 3.8. Theoretical power output of a 2-MW turbine (solid line), limited to 1.5 MW (dashed line).

The effect of the power limitation on the mean annual power (and annual energy output) of the turbine cannot be determined from Figure 3.8 alone, because the wind speed distribution determines the duration of hours when the power output is limited. The effect of the limitation can be graphically gauged by weighing the turbine power output curve with the wind speed frequency distribution function and plotting the resulting curve. The weighed curve corresponds to the integrand $(P_{\mathrm{w}}(v)p(v))$ in Equation 2.6. Figure 3.9 presents an example of such a curve. The wind speed Weibull distribution parameters are $k = 2.41$ and $c = 9.10$ m/s (the ones used for Bogskär in the previous Case).

The area below each curve corresponds to the annual average power output of the configuration. This multiplied by one year (8760 hours) yields the average annual energy output. The

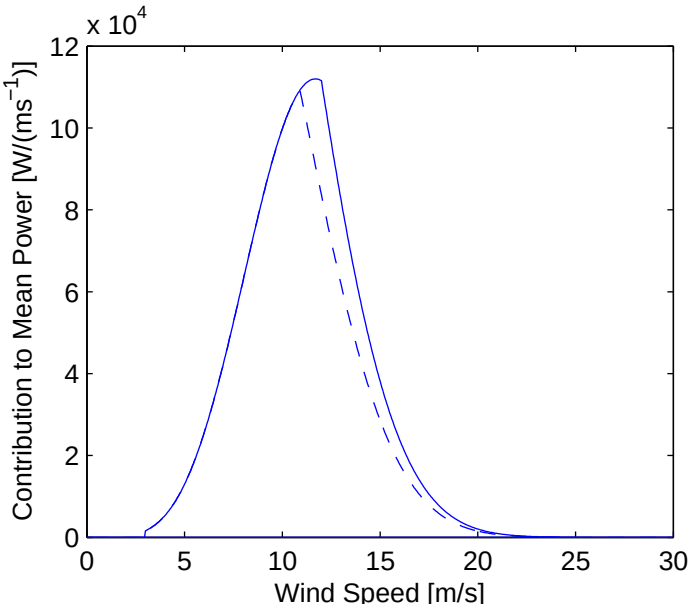

Fig. 3.9. Contribution of different wind speeds to the mean annual output ($P_w(v)p(v)$ in Equation 2.6) with the turbine power not limited (solid line) and limited to 1.5 MW (dashed line). Calculated with Weibull parameters $k = 2.41$ and $c = 9.10$.

area above the dashed line and below the solid line corresponds thus to the lost production due to power limitation. Using numerical integration (trapezoidal rule), the AEO difference in this case can be calculated to be 767 MWh, which corresponds to a 11-% decrease compared with the non-limited case.

This analysis does not take into account the efficiency of the electric drive train, but might be a good starting point. Some of the income change equations (e.g. Equation 2.27) can be used to calculate the relative feasibility of the two configurations. However, in reality, the configurations might not be identical in the area below the power limitation. To take this into account, we will again utilize simulations.

Drive Train

Both configurations have a low-voltage (LV) permanent magnet (PM) generator supplied by a full-power four-quadrant frequency converter. The LV converter is connected to the 20-kV network using a transformer. A network filter is connected between the converter and the transformer. In the models, the filter is an LCL filter. Alternatively, a CL filter could be used, effectively using the transformer as an additional filter inductance. Some parameter values and other properties of the subsystem simulation models for the two alternative configurations are presented in Table 3.13. It can be noted that only those parts that are not part of the electric power train (the turbine and the network) are completely identical in both cases.

The two drive train configurations were modeled in Simulink/SwitchTool. Simulations were run in different operating points, and the total efficiencies of the configurations were calculated. The results are presented in Table 3.14.

Drive Train Cost Estimates

Prices of wind turbines and their components and subsystems are generally trade secrets. This is not a problem, however, because the aim of this book is not to present absolute feasibility calculations of any particular turbine or turbine type but, rather, to present an analysis method that can be used by those who can better estimate the costs. However, cost estimates of some grade are required to be able to illustrate the usage of the method. Bywaters et al. (2004) compared various wind turbine configurations in terms of their costs. Their estimates for two direct-drive permanent magnet configurations are presented in Table 3.15. Bywaters et al. (2004) discuss two 1.5-MW DD configurations, the one in the table is the variant with a diameter of 5.3 m.

The ”normalized sales price” (dollars/kilowatt) can be used to estimate the price of corresponding systems or components of different power ratings. Alternatively, the nominal torque of the machine could be used as the basis of the normalization. The electrical torque can be

Table 3.13. Parameter values and other properties of the compared configurations. Transformer parameters are non-reduced.

		Configuration 1 (undersized)	Configuration 2 (oversized)
Turbine	nominal power, MW	2.0	
	nominal wind speed, m/s	12	
	cut-in wind speed, m/s	3	
	cut-out wind speed, m/s	25	
	nom. rotation speed, RPM	15.3	
	diameter, m	88	
Generator	nominal power, MW	1.5	2.0
	nom. voltage (line-to-line), V	690	690
	nominal frequency, Hz	12.77	12.77
	pole pairs	50	50
	stator resistance, mΩ	0.015	0.0113
Converter	switches	IGBT + diode	IGBT + diode
	IGBT forward voltage, V	2.6	2.6
	diode forward voltage, V	2.1	2.1
	on-state resistance, mΩ	0.27	0.09
	DC link capacitance, mF	57.6	115.2
	DC link capacitor ESR, mΩ	1.0	0.5
	IGBT switch-on loss at I_{nom}, mJ	150	200
	IGBT switch-off loss at I_{nom}, mJ	350	600
	diode switch-on loss at I_{nom}, mJ	0	0
	diode switch-off loss at I_{nom}, mJ	160	260
Network filter	type	LCL	LCL
	network-side (NS) inductance, µH	41.9	31.4
	converter-side (CS) inductance, µH	70.1	52.6
	capacitance, mF	0.795	1.06
	total DC resistance, mΩ	1.33	1
	NS inductor parallel resistance, Ω	26	20
	GS inductor parallel resistance, Ω	44	33
Transformer	nominal power, kVA	2000	2500
	nominal frequency, Hz	50	50
	nominal voltage (HV/LV), V	20 000/690	20 000/690
	vector group	Dyn11	Dyn11
	HV resistance, Ω	0.8	0.6
	HV inductance, mH	0.132	0.106
	LV resistance, mΩ	0.7	0.55
	LV inductance, µH	7.0	5.6
	magnetization resistance, Ω	220 000	220 000
	magnetization inductance, H	100	100
Network	nominal line-to-line voltage, kV	20	
	nominal frequency, Hz	50	
	3-phase short circuit power, MW	100	
	reactance/resistance ratio	6	

Table 3.14. Efficiencies of the compared configurations in different wind speed bins. The value is obtained by simulations with the bin midpoint as the wind speed.

Wind speed, m/s	Configuration 1 (undersized)	Configuration 2 (oversized)	Notes
0 – 3	0	0	Stopped
3 – 5	0.827	0.813	
5 – 7	0.931	0.932	
7 – 9	0.940	0.944	
9 – 11	0.923	0.937	
11 – 12	0.911	0.922	
12 – 25	0.911	0.915	
25 –	0	0	Stopped

Table 3.15. Cost estimates for subsystems in direct drive permanent magnet (DDPM) wind turbines (Bywaters et al., 2004, Section 9.1).

	1.5 MW	3 MW
Generator	\$185 000 (17.0 %)	\$420 000 (21.5 %)
Nacelle	\$90 000 (8.3 %)	\$131 000 (6.7 %)
Converter	\$121 000 (11.1 %)	\$180 000 (9.2 %)
Turbine, cabling, tower etc.	\$612 000 (56.4 %)	\$1 041 000 (53.2 %)
Freight, assembly	\$78 000 (7.2 %)	\$184 000 (9.4 %)
Total	\$1 086 000	\$1 956 000
Projected sales price	\$1 257 000	\$2 333 000
Price/kilowatt	\$838	\$778

Table 3.16. Normalized costs of the 1.5-MW and the 3-MW direct drive generators analyzed by Bywaters et al. (2004).

	1.5 MW	3 MW
Estimated cost	$185 000	$420 000
Nominal power	1.55 MW	3 MW
Nominal rotation speed	19.7 RPM	15.3 RPM
Nominal torque	751 kNm	1870 kNm
Cost/kW	$119	$140
Cost/kNm	$246	$224

expressed as

$$\boldsymbol{T}_\mathrm{e} = \frac{3}{2} p \boldsymbol{\psi}_\mathrm{s} \times \boldsymbol{i}_\mathrm{s}, \tag{3.18}$$

where $\boldsymbol{T}_\mathrm{e}$ is the electrical torque space vector, p is the number of pole pairs, $\boldsymbol{\psi}_\mathrm{m}$ is the stator flux linkage space vector, and $\boldsymbol{i}_\mathrm{s}$ is the stator current space vector (space vector lengths normalized to the peak value of the corresponding phase quantity sine wave). The electrical power, on the other hand, is

$$P_\mathrm{e} = \frac{3}{2} \boldsymbol{u}_\mathrm{s} \cdot \boldsymbol{i}_\mathrm{s}, \tag{3.19}$$

where P_e is the electrical power, $\boldsymbol{u}_\mathrm{s}$ is the stator voltage space vector, and $\boldsymbol{i}_\mathrm{s}$ is the stator current. As can be seen, both the power and the torque depend on the current and the voltage (in stationary state, $\boldsymbol{u}_\mathrm{s} = \mathrm{j}\omega\boldsymbol{\psi}_\mathrm{s}$). Additionally, the torque depends on the number of pole pairs in the machine. The nominal synchronous rotation speed (in revolutions per minute) of a generator is

$$n_\mathrm{nom} = \frac{60 f_\mathrm{nom}}{p}, \tag{3.20}$$

where f_nom is the nominal electrical frequency and p is the number of pole pairs. Thus, if n_nom is to be decreased while keeping f_nom constant, p must be increased. Consequently, slowly rotating machines require generally more pole pairs than faster-rotating machines of the same nominal power rating. A higher number of pole pairs may also complicate the assembly and add to the volume of the machine, thereby increasing costs. Therefore, the nominal torque is a more justified choice for the normalization than the nominal power. In practice, though, the compared generators often do not differ significantly in terms of their nominal rotation speed, and the nominal power can be used as well. Prices normalized with the nominal power and the nominal torque are given in Table 3.16. It can be seen that the cost-per-kW of the smaller generator is lower than that of the larger generator. However, if the nominal torque is used as the basis of the normalization, the situation is opposite.

The maximum torque of the undersized generator (nominal power 1.5 MW) is required at the wind speed where the power limitation becomes active, $v_\mathrm{w,lim}$. This wind speed is somewhat lower than the nominal wind speed $v_\mathrm{w,nom}$ of the non-limited turbine. The wind speed and rotation speed can be estimated with the following procedure. First, solving Equation 2.3 for the wind speed v_w, we obtain an expression for the required wind speed to produce power P,

$$v_\mathrm{w} = \left(\frac{2P}{\rho A C_\mathrm{p}} \right)^{\frac{1}{3}}. \tag{3.21}$$

Assuming the power coefficient C_p of the (non-limited) turbine constant in the interval $[v_{w,lim}, v_{w,nom}]$, this can be simplified to

$$v_w = \left(\frac{P}{P_{nom}}\right)^{\frac{1}{3}} v_{w,nom}. \tag{3.22}$$

For limiting power $P = P_{lim} = 1.5$ MW and nominal power $P_{nom} = 2$ MW, this yields $v_{w,lim} \approx 10.9$ m/s. To calculate the torque at this wind speed, the rotation speed of the turbine must be known. If the tip-speed-ratio λ (Equation 2.4) of the turbine is assumed constant over the interval $[v_{w,lim}, v_{w,nom}]$, the rotation speed n_{lim} can be calculated from

$$n_{lim} = \frac{v_{lim}}{v_{nom}} n_{nom}. \tag{3.23}$$

Setting $v_{nom} = 12$ m/s, $v_{lim} = 10.9$ m/s, and $n_{nom} = 15.3$ RPM gives $n_{lim} = 13.9$ RPM. Thus, the required generator torque is $T_{lim} = 1.03$ MNm. For the non-limited case, the maximum torque is the nominal torque ($P_{nom} = 2$ MW and $n_{nom} = 15.3$ RPM), which equals 1.25 MNm. Using the normalized generator cost \$246/kNm, the prices of the generators are \$253 000 (1.5 MW) and \$307 000 (2 MW). The 1.5-MW generator can be designed with 13.9 RPM as the nominal rotation speed (and with overspeed capability up to at least 15.3 RPM), or the generator can be designed with the nominal speed of 15.3 RPM but with sufficient torque handling capability at lower rotation speeds. The generator design affects the costs, but this is beyond the scope of this book. In the analysis, we will use the above-calculated costs for the generators.

The converter sizing is determined by the current handling capacity required, and this, in turn, is determined by the nominal apparent power of the generator. In this case, the two converter options were the 1.5-MW converter and the 3-MW converter. As cost estimates for these, the values in Table 3.15 were used.

The tower and foundation costs are affected by the weight of the nacelle. The main components of the nacelle are the turbine (which is the same in both configurations) and the generator. The power converter is assumed to be located on the ground. In this example case, the nacelle of the 2-MW turbine is presumably designed to support the weight of a 2-MW PM machine. In the undersized case (1.5-MW generator) the mechanical structure could be made lighter, but in this example it is assumed that the generator/converter supplier cannot influence the nacelle or tower design and, thus, these costs are assumed equal in both cases. Furthermore, the prices of the turbine, cabling, tower, and nacelle were assumed to be linearly dependent on the nominal power of the turbine, and the values for these costs were taken from the 1.5-MW configuration costs in Table 3.15 by multiplying them with 2/1.5 = 4/3.

At this point it should be noted that the estimates presented by Bywaters et al. (2004) do not include the cost of the transformer. In his article concerning the design of a 1.5-MW DD wind generator (Zephyros Z72), Versteegh (2004) estimates the cost of the transformer to be 2 % of the total cost of the turbine. Using the total cost of the undersized generator calculated so far, it can be estimated that the transformer cost is approximately \$30 000. Assuming the price of the transformer to be linearly dependent on the rated apparent power, the price of the oversized transformer can then be estimated to be $2.5/2 \cdot \$30\,000 \approx \$38\,000$. Furthermore,

Table 3.17. Cost estimates used in the Case.

	Configuration 1 (undersized)	Configuration 2 (oversized)
Generator	253 000 €	307 000 €
Converter	121 000 €	180 000 €
Turbine, tower, cabling; freight, assembly	1 040 000 €	1 040 000 €
Transformer & network filter	60 000 €	76 000 €
Total cost	1 474 000 €	1 603 000 €
Price with 20 % profit margin	1 769 000 €	1 924 000 €

Table 3.18. Weibull parameters for the analysis. All parameters taken from the European Wind Atlas (Troen and Petersen (1989)) at the height of 100 m.

Location	c	k	Roughness class	Notes
Ålborg, DK	9.8	2.24	1	Very flat terrain
Eindhoven, NL	7.9	2.42	2	Comparatively close to the sea
Hamburg, GER	7.8	2.43	2	Comparatively close to the sea
Saarbrücken, GER	7.0	2.27	2	Further inland
Munich, GER	5.8	1.45	2	Deep inland

the network filter costs are not included in the estimates presented by Bywaters et al. (2004). The costs can be estimated to be of the same order of magnitude as the transformer costs. In the analysis, we will assume that the network filter costs are identical to the corresponding transformer costs.

Table 3.17 summarizes the estimated costs of the compared configurations. In the table, dollars have been converted to euros with \$1 = 1 €. The values presented so far are the costs of the configurations; the sales prices will be higher. However, it is the sales price that the customer buying the turbine and producing the electricity needs to use in the analysis. In the analysis, sales prices 20 % higher than the costs were used.

Economic Analysis

The analysis was made for various wind distributions acquired from wind atlases. The locations and their corresponding Weibull parameters are listed in Table 3.18. Graphs of the distributions used are presented in Appendix B. Ålborg in northern Jutland represents a comparatively windy location. Eindhoven and Hamburg, both located less than 200 km from the North Sea, are rather similar in terms of wind conditions (noticeably less windy than Ålborg). Saarbrücken in Germany near the French border is about twice as far from the sea as Eindhoven and somewhat less windy. Munich in Bavaria is located yet farther from the sea, and is clearly less windy than the other locations.

Table 3.19. Parameters used in the economic analysis.

Parameter	Value	Notes
Interest rate (p)	8 %	
Time to commissioning (t_0)	2 years	
Turbine life (T)	20 years	
Investment cost (c_i)	1 769 000 €	Configuration 1
	1 924 000 €	Configuration 2
Tariff price of electricity ($\overline{\pi}_1$)	83.50 €/MWh	
Tariff duration (t_1)	12 years	
Market price of electricity ($\overline{\pi}_2$)	30.00 €/MWh	Assumed price after tariff period

Since the locations where the data have been acquired are in different countries, the locations will also differ in terms of the remuneration for the produced energy. Germany, for example, uses a tariff-based system for on-shore wind power, in which the basic tariff is 50.20 €/MWh except during the first five years of operation, when an initial tariff of 92.00 €/MWh is used. This initial tariff is extended based on the performance of the wind power installation in comparison with a reference installation. These values are valid for installations in operation before 1 Jan 2010, and they decrease with 1 % per a year's delay in commissioning (until 2015) (German Renewable Energy Act 2008, Article 1; §20,§29). Denmark, on the other hand, uses a premium-based system with a premium of 250 DKK/MWh (approximately 34 €/MWh 10 Nov 2009) added to the electricity price during the first 22 000 full load hours of an on-shore wind turbine, that is, until 22 000 h $\cdot P_\mathrm{nom}/\mathrm{MW}$ MWh of energy has been exported to the network (Danish Renewable Energy Promotion Act 2008, Ch. 1, §36). In both German and Danish legislation, the duration of the tariff is thus dependent on the performance of the turbine.

To simplify the analysis and to eliminate the effect of different energy policies, the same remuneration system is used with all wind speed distributions. The tariff selected is the same as in the previous case, 83.50 €/MWh (12 years from commissioning). The economic parameters are shown in Table 3.19.

Results and Discussion

For each wind profile, the difference between the annual energy output of the two considered configurations was calculated. Using this value and the estimated investment cost difference and economic parameters given in Table 3.19, the difference in the present value of the income over the life of the turbine (ΔJ) was calculated. Furthermore, the difference between the payback times of the two configurations was calculated as discussed in the previous case. The results are presented in Table 3.20.

In the first case (Ålborg), Configuration 2 (oversized converter) is clearly superior. The average wind speed is so high that a significant amount of energy (1 GWh) per year will be lost if an undersized converter and generator are selected. In the case of Eindhoven and Ham-

Table 3.20. Results of the economic analysis.

Wind profile	ΔAEO, MWh	ΔJ, €	ΔT_{pb}, months	Selected configuration
Ålborg	999	496 000	-4	Conf. 2
Eindhoven	373	88 000	0	Conf. 2 (or Conf. 1)
Hamburg	345	69 000	1	Either
Saarbrücken	211	-17 000	5	Conf. 1
Munich	286	N/A	N/A	Neither

burg, both configurations are approximately equal in terms of economic performance. In both cases, the present value of the generated electricity is slightly more when using Configuration 2 than with Configuration 1. For Eindhoven, the payback times are equal; for Hamburg, the payback time of Configuration is slightly less (1 month) than that of Configuration 2. There is no practical difference between the two configurations in terms of economic performance. For Saarbrücken, the present value of the generated electricity is practically equal for both configurations (17 000 € more for Configuration 1). However, the payback time of Configuration 1 is five months less than that of Configuration 2, and it could be said that in this case selecting Configuration 1 would be justified. For the final case, Munich, neither of the configurations is economically feasible; the generated income for Configuration 1 is negative, and for Configuration 2, barely above zero. The corresponding payback times are approximately equal to the life of the turbine.

As mentioned, site matching problems of this kind are usually calculated without taking into account the effect of the electric drive train. The additional value obtained by the simulator can be gauged by calculating the corresponding analyses without the use of the simulator. Table 3.21 shows the economic analysis results for Case 2 calculated without the simulator, assuming that the efficiency of the electric drive train is constant 0.9 (independent of the operating point). Values obtained using the simulator are shown in parentheses (first presented in Table 3.20). It can be seen that in none of the considered wind regimes, utilizing the simulator instead of merely using the (guessed) constant efficiency has an effect on the outcome of the analysis (i.e., the selection of the electric drive train configuration). Therefore, the use of a simulator with the kind of models presented here does not seem to bring much additional information to analyzing the problem. However, with more detailed generator models, generator control and overloading analysis would be possible and might yield additional information, which would be more complicated to obtain with analytic methods. Furthermore, a turbine aerodynamic model could be combined with the electrical model, enabling an analysis of the dynamic performance of the drive for instance in gusts.

3.4.3 Case 3: Drive Train Control Evaluation

In the previous two cases, the selections involved two alternative hardware configurations. The third case attempts to evaluate the simulation-based approach in the selection of the control methods and principles. Control development is very commonly carried out with the help of a simulator, so it might be useful to obtain figures of the economic performance

Table 3.21. Results of the economic analyses presented in the case with efficiency assumed constant 0.9*. The numbers in parentheses indicate results obtained using the simulator (Table 3.20).*

Wind profile	ΔAEO MWh	ΔJ, €	ΔT_{pb}, months	Selected configuration
Ålborg	952 (999)	466 000 (496 000)	-5 (-4)	Conf. 2
Eindhoven	342 (373)	68 000 (88 000)	0 (0)	Conf. 2 (or Conf. 1)
Hamburg	315 (345)	50 000 (69 000)	1 (1)	Either
Saarbrücken	189 (211)	-32 000 (-17 000)	5 (5)	Conf. 1
Munich	269 (286)	N/A	N/A	Neither

of the alternative control principles at the same time as obtaining figures of their technical performance. Furthermore, the effects created by selections in the control systems are often such that they are difficult to analyze analytically. The combined implication of these two notes is that this kind of an analysis can be expected to be one of the most suitable candidate usages of the simulation-based approach.

In this example, two high-level control principles of a modular low-voltage drive are compared. The nominal power of the wind turbine is a 4.5 MW, and the turbine drives a 4.5-MW permanent magnet generator. The generator is connected to the network utilizing three parallel-connected full-power IGBT-based converters each having a nominal power of 1.5 MW. Parallel connection of power electronic converters, generally, is useful when high power levels with low voltages are required. Other potential benefits over single-converter approach include higher reliability and lower harmonic levels (see, for example, (Ye, 2000)).

In this example, the converters are connected to the network using a common transformer. Each converter has a dedicated network filter. There are no generator filters; the generator-side IGBT bridges are connected to each other and to the generator terminals. In real devices, power imbalance and circulating currents could arise resulting from differences in parameters, but in the simulation model, all IGBTs and other components can be made perfectly similar. On the other hand, the effects of component imbalances could be taken into account in an equally straightforward way, and different parallelization schemes (e.g. separate stators for each converter, separate transformers or transformer secondaries for each converter) could be compared. A block diagram of the system is presented in Figure 3.10.

The network and the generator converter controllers give the same gate commands to all three network and generator converters, respectively. In the example, converter control algorithms were not compared. Instead, two higher-level control principles were compared:

- **Alternative 1** ("All on"): All three frequency converters active whenever the turbine is rotating,
- **Alternative 2** ("Staircase"): Different set of converters engaged at different power levels, such that converter 1 is always active ($P_{\mathrm{cut-in}} < P < P_{\mathrm{cut-out}}$), converter 2 is active when 1 MW $< P <$ $P_{\mathrm{cut-in}}$, and converter 3 is active when 2.5 MW $< P <$ $P_{\mathrm{cut-out}}$.

The capacity of the connected converters and the turbine output power as a function of wind

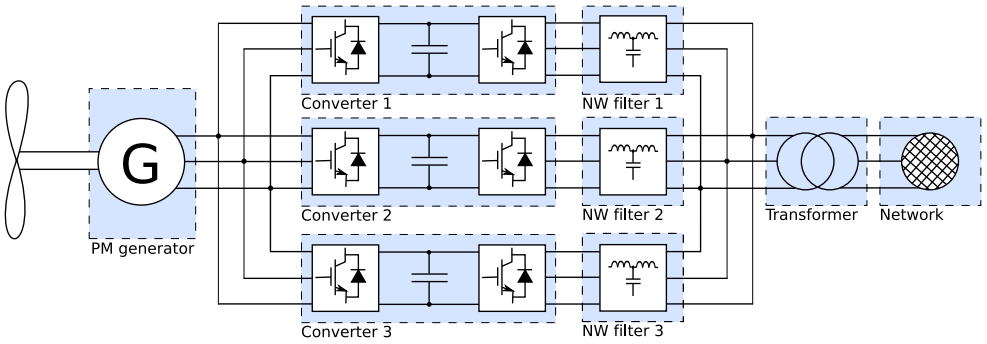

Fig. 3.10. Block diagram of the electric drive train of the system simulated in the case. One 4.5-MW PM generator is fed by three parallel-connected 1.5-MW full power converters.

speed is illustrated in Figure 3.11.

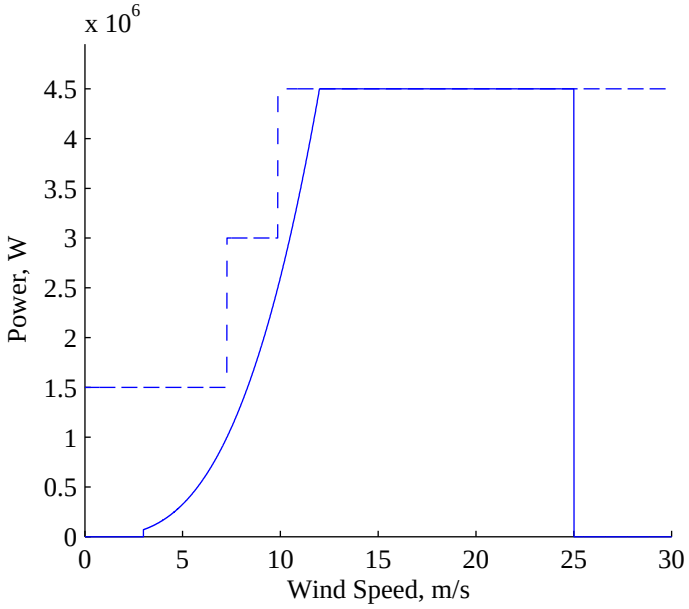

Fig. 3.11. Enabled converters in Alternative 2: turbine output power (solid line) and connected converter capacity (dashed line) as a function of wind speed.

In this case, the hardware configurations for both alternatives are the same, and thus the investment cost difference ΔC_i is zero. However, the monetary value of the changing of the high-level control principle can be calculated using the same method as in the previous cases. This can, then, be weighed against the estimated cost of for instance changing the existing controller software. Table 3.22 lists the efficiencies obtained using the simulator.

Table 3.22. Efficiencies of the alternative configurations (from simulations).

Wind speed, m/s	Alternative 1 (all on)	Alternative 2 (staircase)	Notes
0 – 3	0	0	Stopped
3 – 5	0.716	0.843	
5 – 7	0.883	0.932	
7 – 9	0.935	0.945	
9 – 11	0.940	0.937	
11 – 12	0.922	0.923	
12 – 25	0.918	0.917	Nominal
25 –	0	0	Stopped

Table 3.23. Increase in income (ΔJ) when the "staircase" converter utilization scheme is used instead of the "all on" scheme.

Wind profile	ΔAEO, MWh (%)	ΔJ, €
Ålborg	88 (0.5)	57 000
Eindhoven	114 (1.1)	74 000
Hamburg	116 (1.1)	75 000
Saarbrücken	124 (1.6)	81 000
Munich	98 (1.5)	64 000

As could have been expected, the "staircase" utilization yields higher efficiencies on low loads. With higher loads, the efficiencies are equal (within variation caused by the simulator). The monetary value of implementing the "staircase" converter utilization instead of the "all on" utilization was calculated for the same wind data as in Case 2. The investment costs were set equal for both configurations. Other economic parameters were taken from Table 3.19. Table 3.23 presents the results for different wind data (locations).

Utilization of the "staircase" principle could thus have a significant effect on the generated energy and revenue. The simulation method could be used to find the optimal wind speeds (powers) for the converter combination changes. In this example, the two combinations were simulated separately. However, adding parallel branches may increase the simulation time quite significantly. Therefore, a more feasible method could be to simulate only the efficiency of one converter as a function of power, and then analytically divide the generator power into the active converters and calculate the combined efficiency. This method could then be used to find good combination selection criteria. However, with this method, possible effects of component imbalances could not be taken into account. These imbalances result in circulating currents, which increase losses.

Conclusion

In this case, the simulation-based approach was tested with a rather simple example of selecting the converter utilization scheme in a full-power converter-based wind energy conversion system with three parallel-connected low-voltage converters. According to the simulations, one of the alternatives was clearly superior to the other. The simulation-based method is well suited for analyses of this kind, and it could be applied for instance to selection of generator control algorithms and analysis of the losses caused by parameter deviations between parallel-connected converters. Since power levels in wind energy conversion systems are constantly growing, a lot of research is focused on modularization, and several concepts have been proposed. Simulation-based technical and economic analysis can prove to be a very useful tool in comparing the alternative concepts.

3.4.4 Discussion

The three cases discussed above represented three different situations. The first one involved two alternative component selections, in this case alternative IGBT modules. Clearly, in this case, efficiency data for the considered components for different operating points is a prerequisite for the calculation of the technical and economic analysis. When designing a completely new product, this kind of an analysis could be performed. In practice, however, the number of different components and modules is usually kept to a minimum, and, thus, the same components utilized in other models (or, for example, components from the same manufacturer) are chosen for a new design. This limits the potential use of the method in this kind of situations.

In the second case, the method was applied to the selection of the nominal power of the electric drive train when the properties of the turbine were fixed (kind of a ”partial” site-matching problem). As seen in the Case, selection of the electric drive train may have a significant effect on the economic performance of the installation (Table 3.20). However, in many cases, the efficiency of the electric drive train has an insignificant effect on the outcome of the analysis. Generator overloading analysis and including a turbine model as well as a dynamic model of the wind conditions (including gusts) could provide additional information not obtainable using analytic calculation.

In the third Case, two high-level control principles were compared in the case of a turbine with three converters operating in parallel. The goal was to compare two systems, which had different criteria for selecting the combination of running converters. The simulator can be used to find a good (if not optimal) scheme. Since the hardware configuration is not changed, no direct investment cost difference is applicable to the analysis. However, for example, changing the required software may have a quantifiable cost.

Some cases that might be interesting to simulate are discussed in brief in the following paragraphs.

Multi-level converters. Simulation and technical and economic analysis of a multi-level (e.g. three-level) converter vs. a traditional two-level converter in a wind turbine. This has been previously discussed by e.g. Ikonen et al..

Modular converters. Discussed in Case 3. However, comparison of different topologies (see e.g. (Ye et al., 2000)) and comparison of multiple converters vs. multiple IGBT modules (see e.g. (Keller and Tadros, 1993)) could also be made.

Medium-voltage drives. As wind turbine sizes and power electronics ratings increase, medium-voltage (MV) turbines become feasible in more cases. Comparison of an MV and an LV (low-voltage) drive for a particular turbine and site could be made using the proposed method.

Control algorithms. Simulations can be used to estimate the performance of different control algorithms. The results can be weighed with the wind speed distribution. Investment cost difference might be applicable in some cases (for example, speed sensor vs. no speed sensor).

Selection of components. Discussed in Case 1. Can be applied for instance to network and generator filter selection (core material, parameters), cable sizing, design and sizing of the overvoltage protection (brake chopper, AC load), and others. Could also include, for example, selection of the switching frequency.

Chapter 4

Conclusion and Discussion

This work discussed the feasibility of utilizing a time domain simulation used for the technical analysis and development of a wind power drive train in the economic analysis and comparison of different component and parameter selections. The benefits of the approach compared with the analytical calculation of efficiencies were studied. The method was tested with three example cases, and suggestions for further cases were given.

Chapter 2 introduced the required fundamental physics of wind power production. It was pointed out that the power of wind is proportional to the cube of the velocity of the wind, which brings forth the fact that the output power of a wind turbine decreases rather rapidly from the nominal, when the wind speed decreases from the nominal. Chapter 2 also discussed the description of statistical wind properties. It was noted that an estimate for the annual energy output (AEO) of a wind turbine can be calculated, if the properties of the turbine (and the electric drive train) and the wind statistics are known. The calculation can be done integrating over the distribution, or using a discrete bin-based approach. It was shown for an example distribution that the methods give identical results provided that the bin width is sufficiently small, approximately 1 m/s or less. The sensitivity of the AEO estimate to changes in the Weibull parameters was analyzed. A very brief overview of the regulations concerning wind turbine design was given. The design (and possible optimization of it) need to be done so that all relevant regulations are met. Importantly, it was noted that simulations are often used to verify compliance with regulations.

In the latter part of Chapter 2, an economic analysis method was developed. The method is utilizable in the comparison of two alternative wind turbine configurations, with the focus on the properties of the electric drive train. With the method, the difference in the present value of the generated revenue over the life of the compared configurations is calculated. This comparison can answer at least two types of questions, namely 1) *Should Configuration 1 or Configuration 2 be selected on economic grounds?*, and 2) *How much can a performance-improving modification of a configuration cost in order to be feasible?*, or, conversely, *How much do we have to save with a performance-degrading modification of a configuration in*

order for it to be feasible?, both subject to the regulations-induced framework. In addition to calculating the income change, it was suggested that the calculation of the payback time could be used to supplement the analysis.

Chapter 3 discussed the utilization of simulations to obtain the efficiency of the electric drive train required in the technical and economic analysis. The main loss mechanisms in a wind energy conversion system based on a permanent magnet (PM) machine and a full power converter were described, and their modeling in a time domain simulator was discussed. Based on the calculated efficiencies, the properties of the turbine, and the wind statistics, the annual energy outputs of the compared configurations can be calculated. An add-on to a simulation package specifically focused on the efficiency analysis was developed. The feasibility of the simulation-based approach was tested with three case examples representing different use cases. The first one involved two alternative component selections (alternative IGBT modules). In the second case, the method was applied to the selection of the nominal power of the electric drive train when the properties of the turbine were fixed (a "partial" site-matching problem). In the third case, two high-level control principles were compared in the case of a turbine with three converters operating in parallel. Differences between the compared configurations were clearly attainable from the simulations.

Cases to which the proposed method could be applicable include

1. Component selection
    - Selection of alternative drive train components. For example, selection of different filter core materials.
    - Benefits of the simulation-based approach over analytical loss calculation include the possibility to take into account interactions between different components in a more straigthforward way. The result of the component change can be expressed as an income change, not merely an efficiency change. The feasibility of the change can also be evaluated based on the payback time difference, which describes the change in the risk associated with the component change. The effect of the change on the technical performance (e.g. fault ride-through) of the system can be checked using the same simulation.
    - In practice, the designer may not be able to select components totally freely, but there may nonetheless be alternatives.
    - Simulations are an essential tool in this case, mainly because the system needs to be considered as a whole (the total efficiency of the system is not generally the product of the efficiencies of the constituent components analyzed independently of the system).
    - Example in Case 1 (selection of different IGBT modules).
2. Site matching
    - Comparison of different wind energy conversion systems for a specific site.
    - Traditionally carried out assuming a constant electrical efficiency (unity, or some other constant value). Simulations not needed in a rough feasible/not feasible

analysis. When optimizing the drive train configuration (components, parameters, control algorithms), however, simulations are again very useful or even required.

- If the choice is to be made between a number of configurations with fixed, very different properties (different nominal powers, for example), the simulator may not be needed.
- Illustrated in Case 2, where two different power classes for the frequency converter and generator were considered. In this case, the simulator did not provide significant additional information compared with assuming the efficiency constant – except showing that assuming the efficiency constant in this case did not generate significant errors.

3. Siting (site selection)

   - Comparison of different sites for a specific wind energy conversion system.
   - Somewhat similar to site matching. However, only one candidate system exists, and, therefore, only one set of simulations is needed. The rough selection of the site can be made without the simulator (as is traditionally done), but, again, if the drive train parameters can be tuned, the simulator is required.
   - Although site matching was the main focus of Case 2, also siting was demonstrated, since the economic performance of the two compared configurations was calculated for multiple sites.

4. Control development

   - Comparison of different control methods.
   - Illustrated at a high level in Case 3, where the staircase-like utilization curve of the parallel-connected converters yielded superior performance, as could have been expected. Also, low-level control principles (generator converter control, network converter control) could be compared.
   - Simulations widely applied to the design and analysis of control methods. The performance of the control is evaluated based on traditional control theory figures (such as step response) as well as based on the performance of the system in abnormal situations (such as loss of network or voltage drop). The control methods could also be evaluated based on their economic performance using the methods discussed in this book. Simulations would be an essential tool in this kind of an analysis.

5. Converter configuration

   - Comparison of for example multilevel converters and two-level converters, or different parallelization schemes.
   - There are numerous schemes for the generator-converter combination in high-power wind energy conversion systems. Paralleled IGBT modules and paralleled low-voltage converters enable an increase of current while still using a low-voltage generator. A medium-voltage generator, on the other hand, can be used with low-voltage converters in series or using a medium-voltage converter. The study of these alternatives from a technical and economic point of view would be very interesting.

- Simulations would be a very useful tool, since interactions between the converter and the generator (as well as the possible filter) need to be taken into account.

The objective of this work was to assess the feasibility of utilizing a simulation-based approach to the technical and economic analysis and comparison of alternative wind turbine configurations. It was shown that time domain simulations are a useful tool not only in their current fields of application (analysis of technical performance), but also in the economic analysis. The work can be used to analyze problems related to some of the areas listed above, or other types of wind-power-related problems. Successful utilization of the method requires simulation models that accurately model the loss mechanisms of the specific components under consideration. These models could be verified using measurements of the actual configurations. This work is intended to serve as a basis for further work. The eventual application of the method as well as the development and verification of the required models is left to the those applying the method to analyze an actual problem.

Appendices

Appendix A

Loss Calculation over a Three-Phase Component

This appendix provides the derivation of an equation for the power loss over a non-balanced three-phase two-terminal component with no neutral wire. The equation takes into account the contribution of both differential-mode and common-mode currents. Figure A.1 illustrates a ”black box” model of a two-terminal three-phase device and the measurable voltages. Additionally, all phase currents are measured.

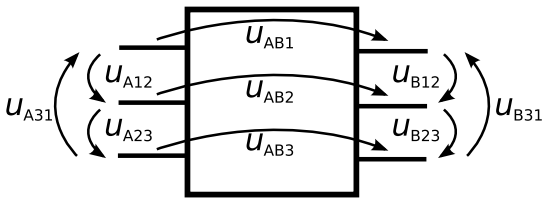

Fig. A.1. Measured voltages in a ”black box” three-phase device.

Internally, the black box can be modeled using a three-phase T equivalent circuit, as shown in Figure A.2. Instantaneous currents and internal voltages of the model are also presented in the Figure.

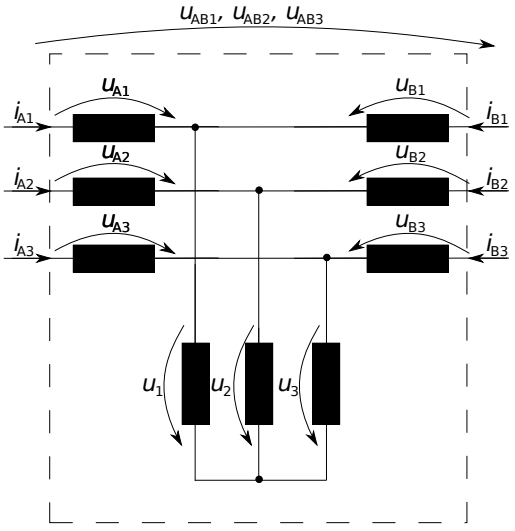

Fig. A.2. Model of the loss measurement from the terminals of a "black box" three-phase system with two terminals. Phase-to-phase voltages, phase currents, and voltages over the component (per phase) measured.

The sum of the currents entering the device must be zero at all instants of time. Hence,

$$i_{A1} + i_{A2} + i_{A3} + i_{B1} + i_{B2} + i_{B3} = 0. \tag{A.1}$$

The instantaneous power dissipation $p_{\text{loss}}(t)$ in the circuit is the sum of the power dissipations in the component impedances. Using voltages and currents, this can be written as

$$\begin{aligned} p_{\text{loss}} = & u_{A1} i_{A1} + u_{B1} i_{B1} + u_1 (i_{A1} + i_{B1}) \\ & + u_{A2} i_{A2} + u_{B2} i_{B2} + u_2 (i_{A2} + i_{B2}) \\ & + u_{A3} i_{A3} + u_{B3} i_{B3} + u_2 (i_{A3} + i_{B3}). \end{aligned} \tag{A.2}$$

All voltages in the equation are unknown. However, either voltages u_{Ax} or u_{Bx} (where $x = 1,2,3$) can be eliminated, since $u_{ABx} = u_{Ax} - u_{Bx}$. We choose to eliminate u_{Bx} by substituting $u_{Bx} = u_{Ax} - u_{ABx}$ in Equation A.2. Performing the substitution and rearranging the terms yields

$$\begin{aligned} p_{\text{loss}} = & (u_{A1} + u_1) i_{A1} + (u_{A1} - u_{AB1} + u_1) i_{B1} \\ & + (u_{A2} + u_2) i_{A2} + (u_{A2} - u_{AB2} + u_2) i_{B2} \\ & + (u_{A3} + u_3) i_{A3} + (u_{A3} - u_{AB3} + u_3) i_{B3}. \end{aligned} \tag{A.3}$$

One of the current terms can be eliminated using Equation A.1. We choose to substitute $i_{B3} = -i_{A1} - i_{A2} - i_{A3} - i_{B1} - i_{B2}$. This gives

$$\begin{aligned} p_{\text{loss}} = & (u_{A1} + u_1 - u_{A3} + u_{AB3} + u_3) i_{A1} + (u_{A1} - u_{AB1} + u_1 - u_{A3} + u_{AB3} + u_3) i_{B1} \\ & + (u_{A2} + u_2 - u_{A3} + u_{AB3} + u_3) i_{A2} + (u_{A2} - u_{AB2} + u_2 - u_{A3} + u_{AB3} + u_3) i_{B2} \\ & + u_{AB3} i_{A3}. \end{aligned} \tag{A.4}$$

The expression can be simplified using Kirchhoff's voltage law for selected loops. The loop equations are

$$-u_{\mathrm{A31}} = u_{\mathrm{A1}} + u_1 - u_3 - u_{\mathrm{A3}} \tag{A.5}$$

$$u_{\mathrm{A23}} = u_{\mathrm{A2}} + u_2 - u_3 - u_{\mathrm{A3}}. \tag{A.6}$$

Substituting these into Equation A.4 gives the expression

$$\begin{aligned} p_{\mathrm{loss}} =& (u_{\mathrm{AB3}} - u_{\mathrm{A31}})i_{\mathrm{A1}} + (u_{\mathrm{AB3}} - u_{\mathrm{AB1}} - u_{\mathrm{A31}})i_{\mathrm{B1}} \\ &+ (u_{\mathrm{AB3}} + u_{\mathrm{A23}})i_{\mathrm{A2}} + (u_{\mathrm{AB3}} - u_{\mathrm{AB2}} + u_{\mathrm{A23}})i_{\mathrm{B2}} \\ &+ u_{\mathrm{AB3}}i_{\mathrm{A3}}, \end{aligned} \tag{A.7}$$

which is Equation 3.9.

This form contains only quantities that can be measured outside the "black box". Other selections in the derivation of the equation would have resulted in a different but equivalent form.

Appendix B

Wind Distribution Graphs

This appendix presents the wind speed distribution graphs for the locations used in the example cases.

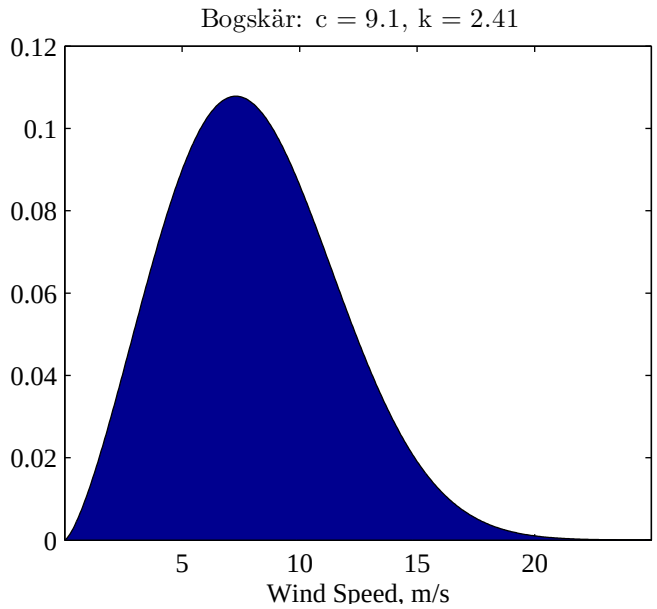

Fig. B.1. Bogskär, Finland.

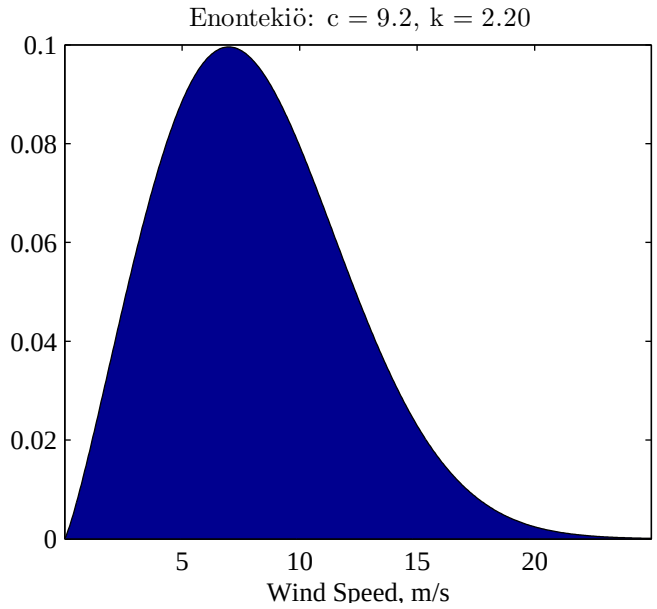

Fig. B.2. Enontekiö, Finland.

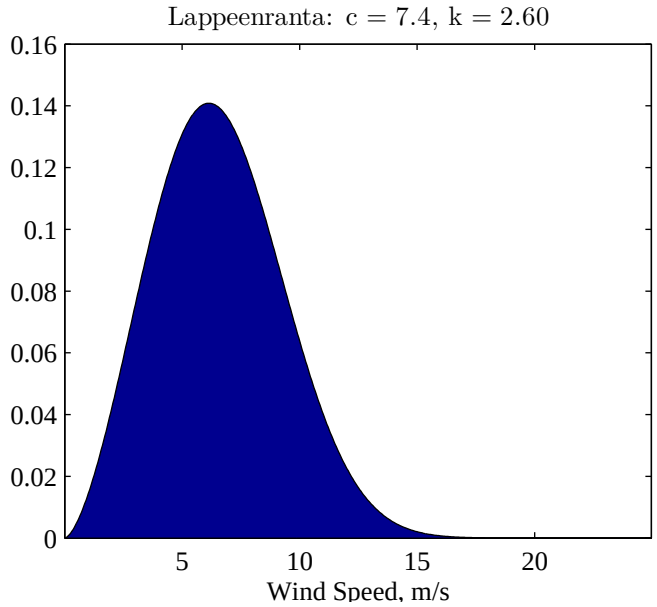

Fig. B.3. Lappeenranta, Finland.

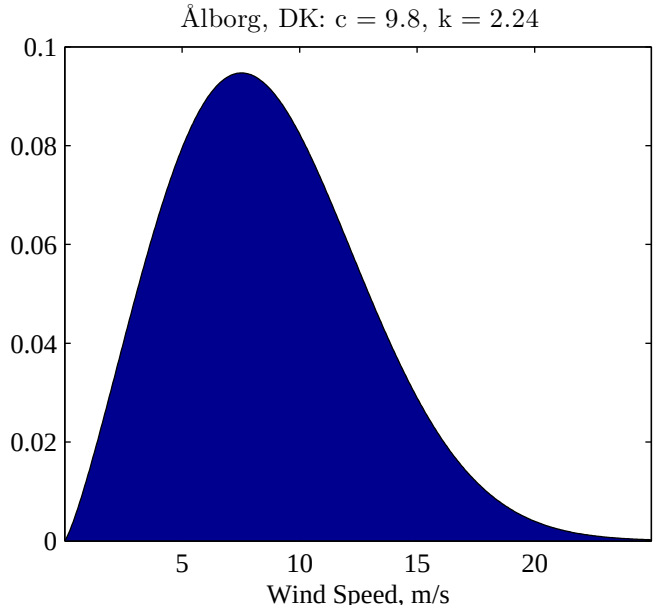

Fig. B.4. Ålborg, Denmark.

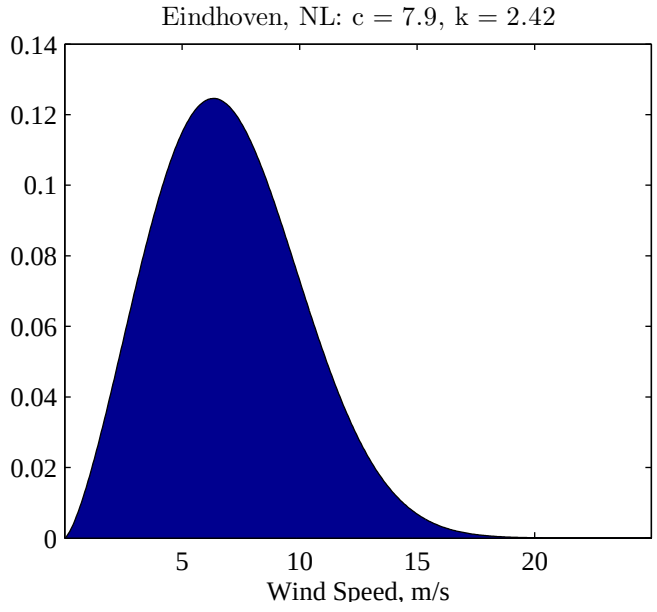

Fig. B.5. The Netherlands.

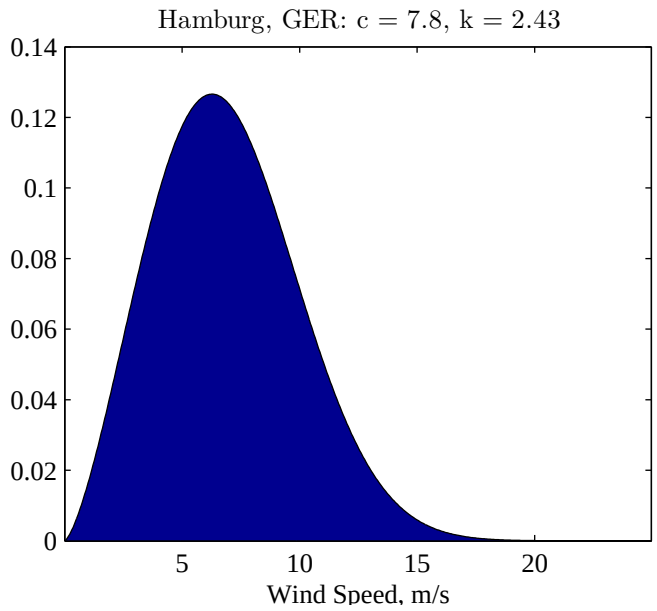

Fig. B.6. Hamburg, Germany.

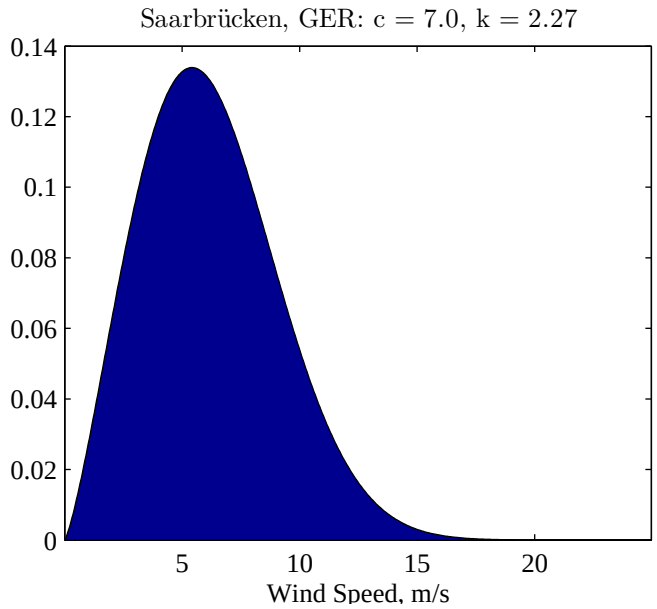

Fig. B.7. Saarbrücken, Germany.

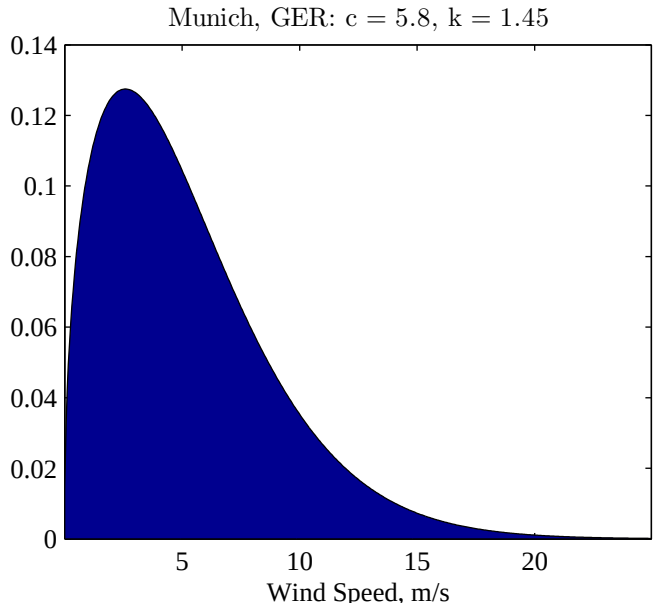

Fig. B.8. Munich, Germany.

References

Affärsverket Svenska Kraftnät (2005), "Affärsverket Svenska Kraftnäts föreskrifter och allmänna råd om driftsäkerhetsteknisk utformning av produktionsanläggningar," Online, http://www.svk.se/Global/07_Tekniska_krav/Pdf/Foreskrifter/SvKFS2005_2.pdf, accessed Mar 3 2009.

Aggarwal, S.K., Saini, L.M., and Kumar, A. (2009), "Electricity price forecasting in deregulated markets: A review and evaluation," *Electrical Power & Energy Systems*, vol. 31, no. 1, pp. 13–22.

Ahmed Shata, A.S. and Hanitsch, R. (2008), "Electricity generation and wind potential assessment at Hurghada, Egypt," *Renewable Energy*, vol. 33, no. 1, pp. 141–148.

Akhmatov, V., Knudsen, H., and Nielsen, A.H. (2000), "Advanced simulation of windmills in the electric power supply," *International Journal of Electrical Power and Energy Systems*, vol. 22, no. 6, pp. 421–434.

Akhmatov, V., Knudsen, H., Nielsen, A.H., Pedersen, J.K., and Poulsen, N.K. (2003), "Modelling and transient stability of large wind farms," *International Journal of Electrical Power and Energy Systems*, vol. 25, no. 2, pp. 123–144.

de Alegría, I.M., Andreu, J., Martín, J.L., Ibañez, P., Villate, J.L., and Camblong, H. (2007), "Connection requirements for wind farms: A survey on technical requirements and regulation," *Renewable and Sustainable Energy Reviews*, vol. 11, no. 8, pp. 1858–1872.

Archer, C.L. and Jacobson, M.Z. (2005), "Evaluation of global wind power," *Journal of Geophysical Research*, , no. 110.

Aspliden, C.I., Elliot, D.L., and Wendell, L.L. (1986), *Resource Assessment Methods, Siting and Performance Evaluation*, pp. 321–376, New Jersey: World Scientific.

Baroudi, J.A., Dinavahi, V., and Knight, A.M. (2007), "A review of power converter topologies for wind generators," *Renewable Energy*, vol. 32, no. 14, pp. 2369–2385.

Burton, T., Sharpe, D., Jenkins, N., and Bossanyi, E. (2001), *Wind Energy Handbook*, John Wiley & Sons Ltd.

Bywaters, G., John, V., Lynch, J., Mattila, P., Norton, G., Stowell, J., Salata, M., Labath, O., Chertok, A., and Hablanian, D. (2004), "Northern power systems WindPACT drive train

alternative design study report," National Renewable Energy Laboratory (NREL) Subcontractor Report NREL/SR-500-35524.

Carlin, P.W., Laxson, A.S., and Muljadi, E.B. (2001), "The history and state of the art of variable-speed wind turbine technology," Tech. Rep. NREL/TP-500-28607, National Renewable Energy Laboratory (NREL).

Carlin, P.W. (1997), "Analytical expressions for maximum wind turbine average power in a Rayleigh wind regime," in *Proceedings of the 16th American Society of Mechanical Engineers Wind Energy Symposium*, Reno, Nevada, USA.

Celik, A.N. (2003), "Energy output estimation for small-scale wind power generators using Weibull-representative wind data," *Journal of Wind Engineering and Industrial Aerodynamics*, vol. 91, no. 5, pp. 693–707.

Coelingh, J.P., van Wijk, A.J.M., and Holtslag, A.A.M. (1996), "Analysis of wind speed observations over the North Sea," *Journal of Wind Engineering and Industrial Aerodynamics*, vol. 61, no. 1, pp. 51–69.

Couture, T. and Gagnon, Y. (2010), "An analysis of feed-in tariff remuneration models: Implications for renewable energy investment," *Energy Policy*, vol. 38, no. 2, pp. 955–965.

Danish Renewable Energy Promotion Act 2008 (2008), "Lov om fremme af vedvarende energi," Online, http//www.retsinformation.dk, accessed 10 Nov 2009.

Dynex Semiconductor (a), "DIM1600FSM12-A single switch IGBT module datasheet," Online, www.dynexsemi.com, accessed Oct 1 2009.

Dynex Semiconductor (b), "DIM1800ESM12-A single switch IGBT module datasheet," Online, www.dynexsemi.com, accessed Oct 1 2009.

E.ON Netz GmbH (2006), "Grid code, high and extra high voltage," Online, http://www.eon-netz.com, accessed Mar 3 2009.

Finnish Wind Atlas 2009 (2009), "Suomen tuuliatlas (Finnish wind atlas)," Online, http://www.tuuliatlas.fi, accessed 11 Dec 2009.

Fleten, S.E., Maribu, K.M., and Wangensteen, I. (2007), "Optimal investment strategies in decentralized renewable power generation under uncertainty," *Energy*, vol. 32, no. 5, pp. 803–815.

Fouquet, D. and Johansson, T.B. (2008), "European renewable energy policy at crossroads – focus on electricity support mechanisms," *Energy Policy*, vol. 36, no. 11, pp. 4079–4092.

German Renewable Energy Act 2008 (2008), "Gesetz zur Neuregelung des Rechts der Erneuerbaren Energien im Strombereich und zur Änderung damit zusammenhängender Vorschriften," Bundesgesetzblatt, Jahrgang 2008, Teil I, Nr. 49.

Global Wind Energy Council (), "Global wind 2008 report," Online, http://www.gwec.net/fileadmin/documents/Global%20Wind%202008%20Report.pdf, accessed Oct 20 2009.

Gorban', A.N., Gorlov, A.M., and Silantyev, V.M. (2001), "Limits of the turbine efficiency for free fluid flow," *Journal of Energy Resources Technology*, vol. 123, pp. 311–317.

Grauers, A. (1996), "Design of direct-driven permanent-magnet generators for wind turbines," Doctoral thesis, Chalmers tekniska högskola, Gothenburg, Sweden.

Hanselman, D. (2003), *Brushless Permanent Magnet Motor Design*, Cranston, Rhode Island: The Writers' Collective, second edn.

Hansen, A.D. and Hansen, L.H. (2006), "Wind turbine concept market penetration over 10 years 1995 – 2004," *Wind Energy*, vol. 10, no. 1, pp. 81–97.

Hansen, L.H., Helle, L., Blaabjerg, F., Ritchie, E., Munk-Nielsen, S., Bindner, H., Sørensen, P., and Bak-Jensen, B. (2001), "Conceptual survey of generators and power electronics for wind turbines," Tech. Rep. Risø-R-1205(EN), Risø National Laboratory, Roskilde, Denmark.

Hoogwijk, M., de Vries, B., and Turkenburg, K. (2004), "Assessment of the global and regional geographical, technical and economic potential of onshore wind energy," *Energy Economics*, vol. 26, no. 5, pp. 889–919.

van der Hoven, I. (1956), "Power spectrum of horizontal wind speed in the frequency range from 0.0007 to 900 cycles per hour," *Journal of Meteorology*, vol. 14, no. 2, pp. 160–164.

Ibenholt, K. (2002), "Explaining learning curves for wind power," *Energy Policy*, vol. 30, no. 13, pp. 1181–1189.

IEC (1996), *IEC 60034-2: Rotating electrical machines — Part 2: Methods for determining losses and efficiency of rotating electrical machinery from tests (excluding machines for traction vehicles)*, Geneva, Switzerland.

IEC (2002), *IEC 61000-4-7: Electromagnetic Compatibility (EMC) — Part 4-7: Testing and measurement techniques — General guide on harmonics and interharmonics measurements and instrumentation, for power supply systems and equipment connected thereto*, Geneva, Switzerland: International electrotechnical commission, 2nd edn.

IEC (2005), *IEC 61400-12-1: Wind turbines — Part 12-1: Power performance measurements of electricity producing wind turbines*, Geneva, Switzerland: International electrotechnical commission, 1.0 edn.

IEC (2008), *IEC 61400-21: Wind turbines — Part 21: Measurement and assessment of power quality characteristics of grid connected wind turbines*, Geneva, Switzerland, 2.0 edn.

Ikonen, M., Laakkonen, O., and Kettunen, M. (), "Two-level and three-level converter comparison in wind power application," Online, http://www.elkraft.ntnu.no/smola2005/Topics/15.pdf, accessed Dec 2 2009.

Iov, F., Blaabjerg, F., Chen, Z., Hansen, A.D., and Sørensen, P. (2002), "A new simulation platform to model, optimize and design wind turbines," in *Proceedings of the IEEE 2002 28th Annual Conference of the Industrial Electronics Society (IECON 2002)*, Sevilla, Spain, Nov 5–8, 2002.

Iov, F., Hansen, A.D., Sørensen, P., and Blaabjerg, F. (2004), "Wind turbine blockset in Matlab/Simulink," Tech. rep., Institute of Energy Technology, Aalborg University, Denmark.

Johnson, G.L. (2001), *Wind Energy Systems*, public domain, electronic edn.

Jowder, F.A.L. (2009), "Wind power analysis and site matching of wind turbine generators in Kingdom of Bahrain," *Applied Energy*, vol. 86, no. 4, pp. 538–545.

Junginger, M., Faaij, A., and Turkenburg, W.C. (2005), "Global experience curves for wind farms," *Energy Policy*, vol. 33, no. 2, pp. 133–150.

Justus, C.G., Hargraves, W.R., Mikhail, A., and Graber, D. (1978), "Methods for estimating wind speed frequency distributions," *Journal of Applied Meteorology*, vol. 17, no. 3, pp. 350–353.

Kaldellis, J.K. and Gavras, T.J. (2000), "The economic viability of commercial wind plants in Greece – a complete sensitivity analysis," *Energy Policy*, vol. 28, no. 8, pp. 509–517.

Keller, C. and Tadros, Y. (1993), "Are paralleled IGBT modules or paralleled IGBT inverters the better choice?" in *Proceedings of the Fifth European Conference on Power Electronics and Applications, 1993*, vol. 5, pp. 1–6, Brighton, UK.

Kouro, S., Perez, M.A., Robles, H., and Rodríguez, J. (2008), "Switching loss analysis of modulation methods used in cascaded h-bridge multilevel converters," in *Proceedings of the 39th IEEE Power Electronics Specialists Conference (PESC08)*, pp. 4662–4668, Rhodes, Greece.

Kwon, S.D. (2010), "Uncertainty analysis of wind energy potential assessment," *Applied Energy*, vol. 87, no. 3, pp. 856–865.

de León, F. and Semlyen, A. (1994), "Complete transformer model for electromagnetic transients," *IEEE Transactions on Power Delivery*, vol. 9, no. 1, pp. 231–239.

Lewis, J.I. and Wiser, R.H. (2007), "Fostering a renewable energy technology industry: An international comparison of wind industry support mechanisms," *Energy Policy*, vol. 35, no. 3, pp. 1844–1857.

Li, H. and Chen, Z. (2007), "Design optimization and comparison of large direct-drive permanent magnet wind generator systems," in *Proceedings of the Intl. Conf. on Electrical Machines and Systems 2007*, Seoul, Korea, october 8–11, 2007.

Lindh, T., Tiainen, R., Ahola, J., Niemelä, M., and Särkimäki, V. (2008), "Performance of rotational speed controlled small-scale head-dependent hydroelectric power plant," in *Proceedings of the International Conference on Renewable Energies and Power Quality (ICREPQ'08)*, Santander, Spain, March 12–14, 2008.

Lund, T., Eek, J., Uski, S., and Perdana, A. (2005), "Dynamic fault simulation of wind turbines using commercial simulation tools," in *Fifth International Workshop on Large-Scale Integration of Wind Power and Transmission Networks for Offshore Wind Farms*.

Luukko, J., Haverinen, V., Ruuskanen, V., Lindh, T., Pöllänen, R., Kärkkäinen, V., and Tiainen, R. (2009a), "Simulation package for simulating wind power drives," in *EPE Wind Energy Chapter – 2nd Seminar*, Stockholm, Sweden, April 23–24, 2009.

Luukko, J., Haverinen, V., Ruuskanen, V., Lindh, T., Pöllänen, R., Kärkkäinen, V., Tiainen, R., Pääkkönen, M., and Pyrhönen, O. (2009b), "Simulation package for simulating wind power drives," in *Proceedings of the 13th European Conference on Power Electronics and Applications (EPE 2009)*, Barcelona, Spain.

Lysen, E.H. (1983), *Introduction to Wind Energy*, Amersfoort, Netherlands: Consultancy Services Wind Energy Developing Countries (CWD).

Manwell, J.F., McGowan, J.G., and Rogers, A.L. (2002), *Wind Energy Explained – Theory, Design and Application*, John Wiley & Sons Ltd.

Matevosyan, J., Ackermann, T., Bolik, S., and Söder, L. (2004), "Comparison of international regulations for connection of wind turbines to the network," in *Proceedings of the Nordic Wind Power Conference 2004*, Gothenburg, Sweden, March 1–2, 2004.

Mi, C., Slemon, G.R., and Bonert, R. (2003), "Modeling of iron losses of permanent-magnet synchronous motors," *IEEE Transactions on Industry Applications*, vol. 39, no. 3, pp. 734–742.

Neij, L. (1999), "Cost dynamics of wind power," *Energy*, vol. 24, no. 5, pp. 375–389.

Neij, L. (2008), "Cost development of future technologies for power generation – a study based on experience curves and complementary bottom-up assessments," *Energy Policy*, vol. 36, no. 6, pp. 2200–2211.

Polinder, H., van der Pijl, F.F.A., de Vilder, G.J., and Tavner, P.J. (2006), "Comparison of direct-drive and geared generator concepts for wind turbines," *IEEE Transactions on Energy Conversion*, vol. 23, no. 4, pp. 725–733.

Pyrhönen, J., Jokinen, T., and Hrabovcová, V. (2008), *Design of Rotating Electrical Machines*, John Wiley & Sons Ltd.

Ramírez, P. and Carta, J.A. (2005), "Influence of the data sampling interval in the estimation of the parameters of the Weibull wind speed probability density distribution: a case study," *Energy Conversion & Management*, vol. 46, no. 15–16, pp. 2419–2438.

Rehman, S., Halawani, T.O., and Mohandes, M. (2003), "Wind power cost assessment at twenty locations in the kingdom of Saudi Arabia," *Renewable Energy*, vol. 28, no. 4, pp. 573–583.

Rehman, S. and Ahmad, A. (2004), "Assessment of wind energy potential for coastal locations of the kingdom of Saudi Arabia," *Energy*, vol. 29, no. 8, pp. 1105–1115.

Reiche, D. and Bechberger, M. (2004), "Policy differences in the promotion of renewable energies in the EU member states," *Energy Policy*, vol. 32, no. 7, pp. 843–849.

REN21 (2008), "Renewables 2007 – global status report," Online, http://www.ren21.net/pdf/RE2007_Global_Status_Report.pdf, accessed Aug 27 2008.

Ringel, M. (2005), "Fostering the use of renewable energies in the European Union: the race between feed-in tariffs and green certificates," *Renewable Energy*, vol. 31, no. 1, pp. 1–17.

Seman, S. (2006), "Transient performance analysis of wind-power induction generators," Doctoral thesis, Helsinki University of Technology, Helsinki, Finland.

Seman, S., Iov, F., Niiranen, J., and Arkkio, A. (2006), "Comparison of simulators for variable-speed wind turbine transient analysis," *International Journal of Energy Research*, vol. 30, no. 9, pp. 713–728.

Skibinski, G., Kerkman, R., and Schlegel, D. (1999), "EMI emissions of modern PWM AC drives," *IEEE Industry Applications*, vol. 5, no. 6, pp. 1021–1029.

Slootweg, J.G., de Haan, W.H., Polinder, H., and Kling, W.L. (2003), "General model for representing variable speed wind turbines in power systems dynamics simulations," *IEEE Transactions on Power Systems*, vol. 18, no. 1, pp. 144–152.

Söder, L. and Ackermann, T. (2005), *Wind Power in Power Systems*, chap. 3, pp. 26–51, John Wiley & Sons.

Sørensen, B. (2007), *Renewable Energy Conversion, Transmission and Storage*, Academic Press.

Tammelin, B. (1991), *Suomen tuuliatlas (Finnish Wind Atlas)*, Helsinki, Finland: Finnish Meteorological Institute.

Tan, K., Yao, T.T., and Islam, S. (2005), "Effect of loss modeling on optimum operation of wind turbine energy conversion systems," in *Proceedings of 7th Intl. Power Engineering Conference (IPEC 2005)*, Singapore, Nov 29–Dec 2, 2005.

Tande, J.O. and Hunter, R. (1994), "IEA Wind recommended practices for wind turbine testing: 2. Estimation of cost of energy from wind energy conversion systems," 2nd edition, International Energy Agency.

Thiringer, T. (1996), "Measurements and modelling of low-frequency disturbances in induction machines," Doctoral thesis, Chalmers University of Technology, Gothenburg, Sweden.

Tiainen, R., Lindh, T., Ahola, J., Niemelä, M., and Särkimäki, V. (2008), "Energy price-based control strategy of a small-scale head-dependent hydroelectric power plant," in *Proceedings of the International Conference on Renewable Energies and Power Quality (ICREPQ'08)*, Santander, Spain, March 12–14, 2008.

Troen, I. and Petersen, E.L. (1989), *European Wind Atlas*, Roskilde, Denmark: Dept. of Meteorology and Wind Energy, Risø National Laboratory.

Tuller, S.E. and Brett, A.C. (1984), "The characteristics of wind velocity that favor the fitting of a weibull distribution in wind speed analysis," *Journal of Climate and Applied Meteorology*, vol. 23, no. 1, pp. 124–134.

Tumański, S. (2006), *Principles of Electrical Measurement*, CRC Press, Taylor & Francis Group, LLC.

Ucar, A. and Balo, F. (2009a), "Evaluation of wind energy potential and electricity generation at six locations in Turkey," *Applied Energy*, vol. 86, no. 10, pp. 1864–1872.

Ucar, A. and Balo, F. (2009b), "Investigation of wind characteristics and assessment of wind-generation potential in Uludağ-Bursa," *Applied Energy*, vol. 86, no. 3, pp. 333–339.

Uski, S., Lemström, B., Kiviluoma, J., Rissanen, S., and Antikainen, P. (2004), "Adjoint wind turbine modeling with ADAMS, Simulink and PSCAD/EMTDC," in *Proceedings of the Nordic Wind Power Conference*, Gothenburg, Sweden, Mar 1–2, 2004.

Versteegh, C.J.A. (2004), "Design of the Zephyros Z72 wind turbine with emphasis on the direct drive PM generator," in *Proceedings of the Nordic Workshop on Power and Industrial Electronics (NORPIE) 2004*, Trondheim, Norway.

Wijenayake, A.H. and Schmidt, P.B. (1997), "Modeling and analysis of permanent magnet synchronous motor by taking saturation and core loss into account," in *Proceedings of the 1997 Intl. Conf. on Power Electronics and Drive Systems*, Singapore, May 26–29, 1997.

WWEA (2008), "Wind turbines generate more than 1 % of the global electricity," Online, http://www.wwindea.org/home/images/stories/pr_statistics2007_210208_red.pdf, accessed Aug 27 2008.

Ye, Z., Boroyevich, D., and Lee, F.C. (2000), "Paralleling non-isolated multi-phase PWM converters," in *Conf. Record of the 2000 IEEE Industry Applications Conference*, vol. 4, pp. 2433–2439, Rome, Italy.

Ye, Z. (2000), "Modeling and control of parallel three-phase PWM converters," Doctoral thesis, Virginia Polytechnic Institute and State University, Blacksburg, Virginia, USA.

ACTA UNIVERSITATIS LAPPEENRANTAENSIS

348. UKKO, JUHANI. Managing through measurement: A framework for successful operative level performance measurement. 2009. Diss.

349. JUUTILAINEN, MATTI. Towards open access networks – prototyping with the Lappeenranta model. 2009. Diss.

350. LINTUKANGAS, KATRINA. Supplier relationship management capability in the firm´s global integration. 2009. Diss.

351. TAMPER, JUHA. Water circulations for effective bleaching of high-brightness mechanical pulps. 2009. Diss.

352. JAATINEN, AHTI. Performance improvement of centrifugal compressor stage with pinched geometry or vaned diffuser. 2009. Diss.

353. KOHONEN, JARNO. Advanced chemometric methods: applicability on industrial data. 2009. Diss.

354. DZHANKHOTOV, VALENTIN. Hybrid LC filter for power electronic drivers: theory and implementation. 2009. Diss.

355. ANI, ELISABETA-CRISTINA. Minimization of the experimental workload for the prediction of pollutants propagation in rivers. Mathematical modelling and knowledge re-use. 2009. Diss.

356. RÖYTTÄ, PEKKA. Study of a vapor-compression air-conditioning system for jetliners. 2009. Diss.

357. KÄRKI, TIMO. Factors affecting the usability of aspen (Populus tremula) wood dried at different temperature levels. 2009. Diss.

358. ALKKIOMÄKI, OLLI. Sensor fusion of proprioception, force and vision in estimation and robot control. 2009. Diss.

359. MATIKAINEN, MARKO. Development of beam and plate finite elements based on the absolute nodal coordinate formulation. 2009. Diss.

360. SIROLA, KATRI. Chelating adsorbents in purification of hydrometallurgical solutions. 2009. Diss.

361. HESAMPOUR, MEHRDAD. Treatment of oily wastewater by ultrafiltration: The effect of different operating and solution conditions. 2009. Diss.

362. SALKINOJA, HEIKKI. Optimizing of intelligence level in welding. 2009. Diss.

363. RÖNKKÖNEN, JANI. Continuous multimodal global optimization with differential evolution-based methods. 2009. Diss.

364. LINDQVIST, ANTTI. Engendering group support based foresight for capital intensive manufacturing industries – Case paper and steel industry scenarios by 2018. 2009. Diss.

365. POLESE, GIOVANNI. The detector control systems for the CMS resistive plate chamber at LHC. 2009. Diss.

366. KALENOVA, DIANA. Color and spectral image assessment using novel quality and fidelity techniques. 2009. Diss.

367. JALKALA, ANNE. Customer reference marketing in a business-to-business context. 2009. Diss.

368. HANNOLA, LEA. Challenges and means for the front end activities of software development. 2009. Diss.

369. PÄTÄRI, SATU. On value creation at an industrial intersection – Bioenergy in the forest and energy sectors. 2009. Diss.

370. HENTTONEN, KAISA. The effects of social networks on work-team effectiveness. 2009. Diss.

371. LASSILA, JUKKA. Strategic development of electricity distribution networks – Concept and methods. 2009. Diss.

372. PAAKKUNAINEN, MAARET. Sampling in chemical analysis. 2009. Diss.

373. LISUNOV, KONSTANTIN. Magnetic and transport properties of II-V diluted magnetic semiconductors doped with manganese and nickel. 2009. Diss.

374. JUSSILA, HANNE. Concentrated winding multiphase permanent magnet machine design and electromagnetic properties – Case axial flux machine. 2009. Diss.

375. AUVINEN, HARRI. Inversion and assimilation methods with applications in geophysical remote sensing. 2009. Diss.

376. KINDSIGO, MERIT. Wet oxidation of recalcitrant lignin waters: Experimental and kinetic studies. 2009. Diss.

377. PESSI, PEKKA. Novel robot solutions for carrying out field joint welding and machining in the assembly of the vacuum vessel of ITER. 2009. Diss.

378. STRÖM, JUHA-PEKKA. Active*du*/d*t* filtering for variable-speed AC drives. 2009. Diss.

379. NURMI, SIMO A. Computational and experimental investigation of the grooved roll in paper machine environment. 2009. Diss.

380. HÄKKINEN, ANTTI. The influence of crystallization conditions on the filtration characteristics of sulphathiazole suspensions. 2009. Diss.

381. SYRJÄ, PASI. Pienten osakeyhtiöiden verosuunnittelu – empiirinen tutkimus. 2010. Diss.

382. KERKKÄNEN, ANNASTIINA. Improving demand forecasting practices in the industrial context. 2010. Diss.

383. TAHVANAINEN, KAISA. Managing regulatory risks when outsourcing network-related services in the electricity distribution sector. 2010. Diss.

384. RITALA, PAAVO. Coopetitive advantage – How firms create and appropriate value by collaborating with their competitors. 2010. Diss.

385. RAUVANTO, IRINA. The intrinsic mechanisms of softwood fiber damage in brown stock fiber line unit operations. 2010. Diss.

386. NAUMANEN, VILLE. Multilevel converter modulation: implementation and analysis. 2010. Diss.

387. IKÄVALKO, MARKKU. Contextuality in SME ownership – Studies on owner-managers´ ownership behavior. 2010. Diss.

388. SALOJÄRVI, HANNA. Customer knowledge processing in key account management. 2010. Diss.

389. ITKONEN, TONI. Parallel-Operating Three-Phase Voltage Source Inverters – Circulating Current Modeling, Analysis and Mitigation. 2010. Diss.

390. EEROLA, TUOMAS. Computational visual quality of digitally printed images. 2010. Diss.